NATIONAL AND KAPODISTRIAN UNIVERSITY OF ATHENS

FACULTY OF SCIENCES

DEPARTMENT OF CHEMISTRY

POSTGRADUATE DEGREE
«ENVIRONMENTAL CHEMISTRY AND TECHNOLOGY»

MSc THESIS

Chemical Characterization of Fine Atmospheric Particulate Matter in the City of Athens. Identification of Sources.

VASILEIOS BAMPOURIS
ENVIRONMENTAL SCIENTIST

ATHENS
OCTOBER 2019

MSc THESIS

Chemical Characterization of Fine Atmospheric Particulate Matter in the City of Athens. Identification of Sources.

VASILEIOS BAMPOURIS

A.M.: 91506

SUPERVISOR:
Manos Dassenakis, Professor, NKUA

EXAMINATION COMMITTEE

Manos Dassenakis, Professor, NKUA
Nikolaos Mihalopoulos, Senior Researcher, National Observatory of Athens
Evangelos Bakeas, Associate Professor, NKUA

DATE OF EXAMINATION
14/10/2019

ΕΡΕΥΝΗΤΙΚΗ ΕΡΓΑΣΙΑ ΔΙΠΛΩΜΑΤΟΣ ΕΙΔΙΚΕΥΣΗΣ

Χημικός Χαρακτηρισμός Λεπτών Αιωρούμενων Σωματιδίων στην Πόλη της Αθήνας. Προσδιορισμός Πηγών Προέλευσης.

ΒΑΣΙΛΕΙΟΣ ΜΠΑΜΠΟΥΡΗΣ

Α.Μ.: 91506

ΕΠΙΒΛΕΠΩΝ ΚΑΘΗΓΗΤΗΣ:
Μάνος Δασενάκης, Καθηγητής, ΕΚΠΑ

ΤΡΙΜΕΛΗΣ ΕΞΕΤΑΣΤΙΚΗ ΕΠΙΤΡΟΠΗ

Μάνος Δασενάκης, Καθηγητής, ΕΚΠΑ
Νικόλαος Μιχαλόπουλος, Κύριος Ερευνητής, Εθνικό Αστεροσκοπείο Αθηνών
Ευάγγελος Μπακέας, Αναπληρωτής Καθηγητής, ΕΚΠΑ

ΗΜΕΡΟΜΗΝΙΑ ΕΞΕΤΑΣΗΣ
14/10/2019

ΠΕΡΙΛΗΨΗ

Στην παρούσα διατριβή ερευνάται η χημική σύσταση των λεπτών αιωρούμενων σωματιδίων στον αστικό ιστό της Αθήνας. Η συλλογή των δειγμάτων έγινε μέσω της τεχνικής PILS (Particle Into Liquid Sampler) και ο προσδιορισμός της χημικής σύστασης των σωματιδίων με τη βοήθεια της τεχνικής της Ιοντικής Χρωματογραφίας (Ion Chromatography-IC). Η περίοδος συλλογής των δειγμάτων είναι από 16/1/2017 μέχρι 1/11/2017 και πραγματοποιήθηκε συνεχόμενα κάθε 15 λεπτά. Τα κατιόντα που μετρήθηκαν είναι Na^{+}, K^{+}, NH_4^{+}, Mg^{+2} και Ca^{+2}, τα οποία χαρακτηρίζουν πηγές ανθρωπογενούς και φυσικής ρύπανσης. Παρουσιάζεται η διακύμανση της συγκέντρωσής τους καθόλη την περίοδο δειγματοληψίας. Επίσης, παρουσιάζεται η ωριαία, η μηναία και η εποχιακή διακύμανση. Ταυτόχρονα, συσχετίζονται οι συγκεντρώσεις κατιόντων μεταξύ τους, αλλά και του K^{+} με συγκεντρώσεις Black Carbon (BC) με σκοπό να προσδιοριστούν οι πηγές προέλευσής τους (στερεός φλοιός, θάλασσα, καύση βιομάζας, δευτερογενής παραγωγή αιωρούμενων σωματιδίων,χρήση ορυκτών καυσίμων κ.ά.).

Θεματική Περιοχή: Λεπτά Αιωρούμενα Σωματίδια

Λέξεις Κλειδιά: Τεχνική Συλλογής Αιωρούμενων Σωματιδίων PILS (Particles into Liquid Sampler), Ιοντική Χρωματογραφία, Κατιόντα Αιωρούμενων Σωματιδίων, Μαύρος Άνθρακας (Black Carbon-BC), Πηγές Προέλευσης Αιωρούμενων Σωματιδίων.

ABSTRACT

The research is focused on the chemical characterization of fine particulate matter in the urban area of Athens. The air samples were collected with a PILS (Particles Into Liquid Sampler) and the chemical composition of the particles were determined with the Ion Chromatography (IC) technique. The sampling period was from 16/1/2017 until 1/11/2017 and air samples were collected every 15 minutes almost uninterruptedly. The cations which were measured were Na^{+}, K^{+}, NH_4^{+}, Mg^{+2} and Ca^{+2}. The fluctuation of the concentration of the cations in every sample during the whole sampling period is displayed. Also, the hourly, diurnal, monthly and seasonal variation of the cations is displayed. At the same time, the concentrations of the cations are correlated and the concentration of K^{+} with Black Carbon (BC), in order to determine the sources of the particles (crust, sea salt, biomass combustion, secondary aerosol production, fossil fuel combustion etc).

Subject Area: Fine Particulate Matter

Keywords: PILS (Particles into Liquid Sampler), Ion Chromatography, Cations of Particulate Matter, Black Carbon, Sources of Particulate Matter.

To Franky

ACKNOWLEDGMENTS

I would like to thank the following people who contributed to the completion of this thesis.

Nikolaos Mihalopoulos, Manos Dassenakis, Despina Paraskevopoulou and Evangelos Bakeas.

I would especially like to thank Francesca Paraskou, Xristina Zogaki, Nelly Karapetsa and Aggeliki Bampouris.

CONTENTS

LIST OF FIGURES

LIST OF TABLES

PROLOGUE

In order to establish measures for environmental protection new analytical techniques have to be developed. These techniques have to be reliable, fast, they have to indicate high resolution, provide results in real time and be affordable.

Fine particulate matter is associated with cardiopulmonary and respiratory disease. Epidemiological studies, also, have related fine particles to mortality. Moreover, the impacts to ecosystems, visibility and climate are severe. This leads to the increase of scientific interest for the investigation of the chemical composition and the sources of these particles.

This research of the chemical characterization of the fine particulate matter was conducted at the centre of Athens. More specifically, at the area of Thissio is located the measurement station of the Institute of Environmental Research and Sustainable Development of the National Observatory of Athens.

1 INTRODUCTION

1.1 Atmospheric Pollution

1.1.1 General

The degradation of the atmospheric environment affects health and ecosystems. It is caused by the physical or chemical transformations of air which have hazardous impacts. More specifically, according to Environmental Protection Agency of the United States of America (EPA) air pollution can be defined as:

One or more chemicals or substances in high enough concentrations in the air to harm humans, other animals, vegetation, or materials. Such chemicals or physical conditions (such as excess heat or noise) are called air pollutants [1].

Throughout history the impacts of atmospheric pollution have been well documented [2]. Carbon and dust remains were found in lung tissue of the Late Neolithic Tyrolean Iceman (5,300 years old) [3]. Furthermore, it has been recorded that in the Mishnah Laws in Israel during the first and second centuries A.D. tanneries had to be located at least 30m away from the towns and only to the east side. This was due to the fact that the prevailing westerly winds transferred the emitted odors [4].

1.1.2 Sources of Air Pollution

The sources of air pollution depending on the origin are the following:

- Naturally occurring pollutants, over which man has either very little or no control, originate from forest fires, volcanic eruptions, organic materials emanating from plants, decaying vegetation, dust storms and salt from sea spray [5].
- Sources of air pollution from human activities. The major sources are the products of combustion released in ever-increasing quantities through the use of fossil fuels for domestic and industrial heating, power generation, transportation and other purposes [6].

1.1.3 Impacts of Air Pollution

Atmospheric pollution affects:

- Human health. More specifically, heart disease and stroke are the most common

reasons for premature death attributable to air pollution and are responsible for 80% of cases of premature death. Lung diseases and lung cancer follow [7]. Additionally, to causing premature death, air pollution increases the incidence of a wide range of diseases (e.g. respiratory, cardiovascular diseases and cancer), with both long and short-term health effects. Also, air pollution as a whole has recently been classified as carcinogenic [8]. Some of the most significant incidents of air pollution and the health effects on humans are presented in the following Table 1.

Table 1: The most significant incidents of air pollution and their health effects on humans

Location and Date	**Cause**	**Health Effects**
Meuse Valley, Belgium (1930)	Fog. Industrial plants, including coke ovens, blast furnaces, steel mills, power plants, glass factories, lime furnaces, zinc reduction plants, a sulfuric acid plant, and an artificial fertilizer plant [9].	Thousands of people were ill. 60 of them died and the number of deaths was considered as having been about 10.5 times the expected amount for an equivalent period of time and season under ordinary circumstances [5].
Donora, United States of America (1948)	Fog. It accumulated atmospheric pollution to abnormal levels of concentration, particularly in highly industrialized areas [5].	5.910 persons (42.7 % of the population) were affected by symptoms of illness. During that same period 17 deaths in the community, occurred which normally experienced an average of two deaths in an equivalent period of time [10-18].
London, United Kingdom (1952)	Sulfur oxides and the solid matter in coal smoke [5].	4,000 excess deaths in the Greater London Area, compared with a similar period in previous years [19].
Los Angeles, United States of America (late 1940's)	SO_x, NO_x, aldehydes, ketones, acids, chlorinated hydrocarbons,acrolein, chlorinated aldehydes, formyl compounds, ozonides and peroxides of hydrocarbons, O_3, nitro-olefins, peracylnitrites, organic free radicals, and carbon suboxide (C_3O_2)[5].	Eye irritation, and some irritation of the nose and throat, but the rates of occurrence of these subjective complaints have not been adequately recorded [5].
Poza Rica, Mexico (1950)	Hydrogen sulfide gas[20,21]. Caused by accidental mishandling of natural	Illness of 320 persons and 22 deaths[20,21].

	gas processing machinery [5].	
East coast of Prussia facing the Baltic Sea (1924-1927)	Arsine (AsH_3) gas [9, 23, 24]. A possible source of the gas was arsenic-containing iron pyrites present in processed material that was discarded from a nearby factory [5].	‘‘Haff disease’’. It was named by the name of the areas. 811 local fisherman, in all these years, who worked on the low-lying land along the lagoons had muscle cramps, haematuria and anaemia [9, 23, 24].

- **Ecosystems.** First of all, it may directly affect vegetation, as well as the quality of water and soil and the ecosystem services that they support. For example, ground-level O_3 damages agricultural crops, forests and plants by reducing their growth rates [25]. Other pollutants, such as nitrogen oxides (NO_x), SO_2 and NH_3 contribute to the acidification of soil, lakes and rivers, causing the loss of animal and plant life. In addition to causing acidification, NH_3 and NO_x emissions also disrupt land and water ecosystems by introducing excessive amounts of nutrient nitrogen. This leads to eutrophication that subsequently leads to changes in species diversity and to invasions of new species [26].

Furthermore, during major air pollution incidents illnesses and deaths of **animals** have been reported. For example, at the city if Donora of Pennsylvania (USA) in 1948 (Table 1) 229 dogs (15.5 %) were reported as having become ill and 10 canine deaths were attributed to the smog. At the same period 40% of the affected birds had died [27]. Other examples include the London (UK) smog incident in 1952 (Table 1) during which a number of prize cattle were reported as having been severely affected [28,29]. Additionally, an undetermined number of canaries, chickens, cattle, pigs, geese, ducks and dogs were exposed to the polluted atmosphere at Poza Rica (Mexico) in 1950 (Table 1). The reports of animal injury during this disaster disclosed that 100% of the canaries in the area had died. It was also estimated that 50% of the other exposed animals had died during the same period, too [27].

Plants are also severely affected by air pollution. Most of the air pollutants cause damages to plant tissues and affect their physiology. For example, SO_2 as a gas is absorbed into the mesophyll of the leaves through the stomata. Toxicity is largely due to the reducing properties of the gas. The limiting concentration that can be tolerated in the cells is about the same for many diverse species, including water plants. When this concentration is exceeded, the cells are first inactivated with or without plasmolysis, then

killed [30, 31]. Also, fluorides absorbed in the leaves are translocated towards the margins of broad leaves or the tips of leaf blades. By this means, marginal necrosis is caused [27]. Additionally, ozone causes lesions to the plants which are generally confined to the upper surface [32-34].

Figure 1.1: Effect of acid aerosol on leaves [35].

Figure 1.2: Spruce trees affected by acid rain in Norway [36].

At the same time, acid aerosol as droplets that settles on the leaves contains enough acid and perhaps other toxicants to injure the leaf [37, 38] (Figures 1.1 and 1.2).

- **Climate.** Several air pollutants are also climate forcers and have a potential impact on the planet's climate and global warming in the short term (i.e. decades). Tropospheric O_3, CO_2, CH_4 and Black Carbon (BC), a constituent of PM, are examples of air pollutants that are short lived climate forcers and that contribute directly to global warming [26].

On the other hand, analyses of meteorological data in heavily urbanized regions of China demonstrate significant downward trends in both sunshine duration (1% to 3% per decade) and max daily temperatures (0.2–0.6 °C per decade) [39-41]. The observed cooling trends are consistent with the predicted effects of elevated soot levels in fine PM [41] and are achieved despite a general warming observed for most of the globe over the same time period.

Additionally, high PM loadings that increase the number of effective cloud condensation nuclei can also influence precipitation levels. Satellite observations show significant rainfall suppression downwind of major cities [42].

Yet, another consequence of long-range transport involves impacts on urban areas due to sand, dust or smoke that originate beyond the cities. For example, dust and sand storms that originate in the dry regions of northern China (Figure 1.3) and Mongolia and blow across parts of China, the Korean peninsula, and Japan are now taking place nearly five times as often as in the 1950's [43,44]. The whole effect is expected to get intensified, since nearly 30% of China's land area is affected by desertification caused by over-farming, over-grazing, and deforestation [43].

Figure 1.1: Sandstorm in Beijing, China [45].

- **Economy and Society.** Air pollution can also damage materials and buildings.

The impact of air pollution on cultural heritage buildings is a serious concern because it can lead to the loss of parts of our history and culture. Damage includes corrosion, biodegradation and soiling [26].

The economic impacts due to air pollution are as follows:

(1) Losses due to direct or indirect effects of pollution:

(a) on human health

(b) on livestock

(c) on plants.

(2) Losses due to corrosion of various materials and of their protective covering.

(3) Losses due to maintenance costs, inside and outside houses and other buildings; to depreciation of objects or merchandise exposed to pollution.

(4) Losses due to unburnt residue in chimneys, motors, and various engines which contribute to the general pollution.

(5) Expenditure directly incurred by the adoption of technical measures for the suppression or reduction of smoke or emissions from factories.

(6) Increase in cost of electric power due to dust removal and other treatment of smoke

from power or nuclear stations.
(7) Various losses due indirectly to pollution: increased transport costs in periods of smog; wasted electricity due to premature twilight caused by smoke, etc.
(8) Expenditure in connection with the administrative organization of pollution control.
(9) Costs of medical, agricultural, chemical, and physicochemical research aimed at working out techniques for the measurement of pollution investigating the ways in which pollution affects persons, animals, plants, and materials; and studying appliances or installations for the reduction or suppression of various dusts and sources [46].

Additionally, air pollution is a factor which undermines the well-being of affected populations. It is inherent in all congested areas, and in all industrial undertakings unless these are provided with every possible facility for effectively combating the emissions Also, industry is certainly expanding rapidly and areas which were formerly free from pollution are now becoming exposed. As a result, there is an observed deterioration of the quality of life [46].

1.1.4 Air Pollution and Cities

About half of the world's population now lives in urban areas because of the opportunity for a better quality of life [43]. Approximately, 48% of the world's population in 2000 lived in urban areas, and the number of urban dwellers is expected to grow by 2% per year during the coming three decades [47]. These concentrations of people and activity are exerting increasing stress on the natural environment, with impacts at urban, regional and global levels [43].

Urbanization and industrialization have important consequences for the Earth's atmosphere [48]. The degradation of urban air quality is enhanced through complex topographic areas and unfavourable meteorological conditions [49].

Two heavy smog episodes in metropolitan areas led to the enhancement of scientific interest in atmospheric pollution. These two incidents of severe air pollution in urban space are the London smog in 1952 and the Los Angeles smog in the late 1940's. These episodes are significant because they represent the types of air pollution which appear in many cities all around the world.

1.1.5 London smog

In **London** in December of 1952 there were 4,000 excess deaths due to smog (Figure 1.5). The air pollutants have not been fully identified but there were high concentrations of SO_2 and particles (Figure 1.4). The dense fog that was created stayed in low altitude due to strong meteorological inversions. That fog and the smoke combined led to the term ‘‘smog’’ [50].

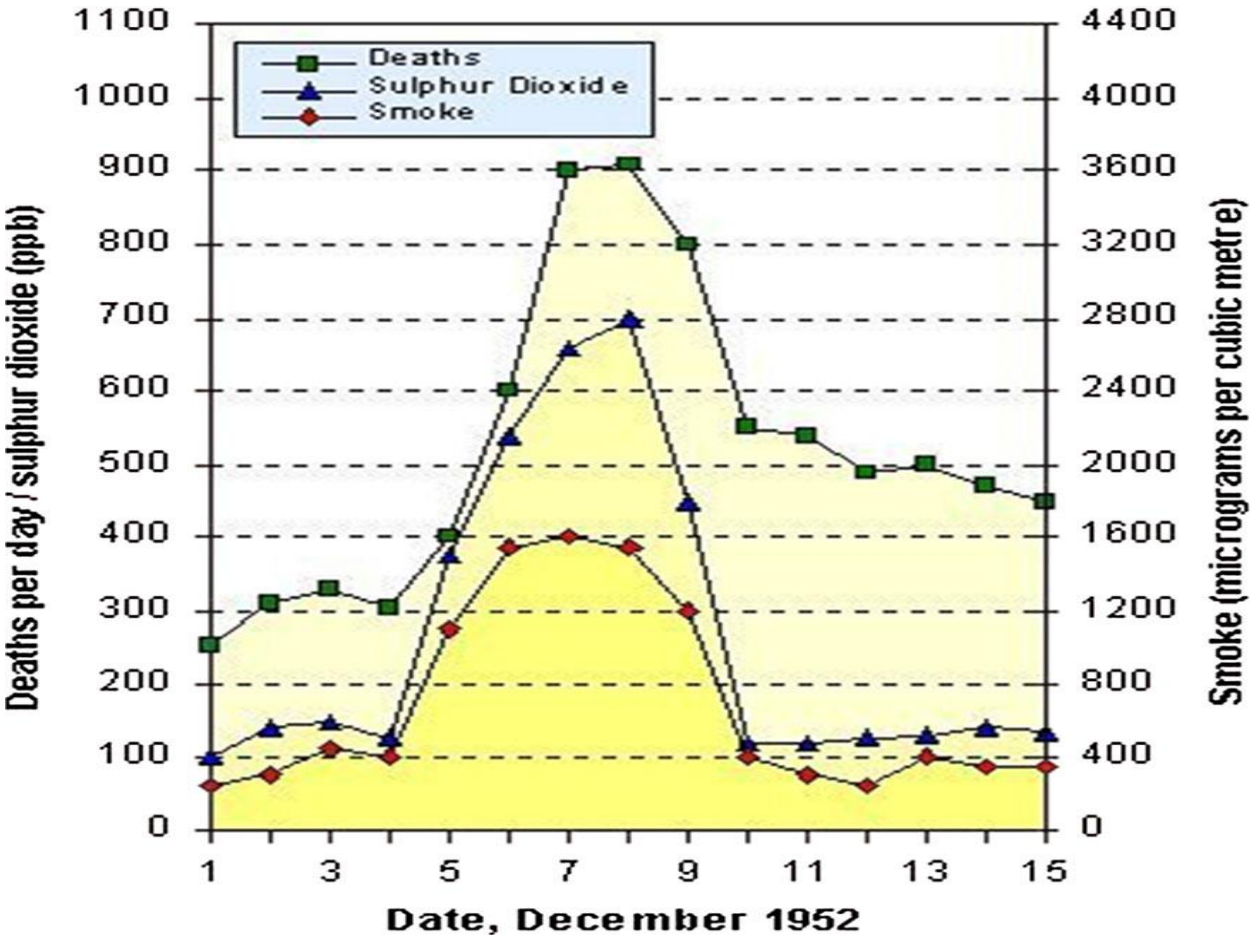

Figure 1.2: Concentrations of SO_2 and ‘‘smoke’’, as well as the death rate during the 1952 smog episode[50].

1.1.6 Los Angeles smog

In the late 1940’s strongly oxidizing, eye-watering and plant killing pollutants occurred during hot days with bright sunshine in the area of **Los Angeles** (Figure 1.6). This new type of smog was reported from the scientific community as the ‘‘Los Angeles smog’’ and its main pollutant is O_3. This pollutant is produced from Volatile Organic Compounds (VOC’s) and NO_x with the help of high voltage (hv) solar radiation. It is, therefore, called as secondary pollutant and has appeared in metropolitan areas with high temperatures such as Athens (Greece), Syndey (Australia), Rome (Italy), Mexico City (Mexico) etc.

VOC'S and NO_x concentrations mainly produced by traffic and industry are ''trapped'' in the troposphere by thermal inversions and irradiated by hv sunlight during transport to downwind regions [51-57].

Figure 1.5: Piccadilly Circus, London in the smog: On the weekend that began on Friday December 5 1952 [58].

Figure 1.6: Los Angeles in smog [59].

These two phenomena of atmospheric pollution are linked through their chemistry and ''construct'' the airborne toxic chemicals. Nowadays, in many urban areas air pollution is mainly formed by ozone and other oxidants rather than by SO_2, air particles and H_2SO_4[60].

1.2 Air Pollutants

An air pollutant is defined as: *Any substance in air that could, in high enough concentrations harm animals, humans, vegetation and/or materials. Such pollutants may be present as solid particles, liquid droplets or gases* [61,62].

They fall into two main groups: (1) those emitted from identifiable sources (primary pollutants) and (2) those formed in the atmosphere by interactions between two or more primary pollutants or by reaction with normal atmospheric constituents with or without photoactivation (secondary pollutants). Identified pollutants are categorized in to following groups according to chemical and physical characteristics: solids, sulfur compounds, volatile organic chemicals, nitrogen compounds, oxygen compounds, halogen compounds, radioactive compounds and odors [61,63].

Air pollutants can also be divided into the following three groups:

- ‘‘Criteria pollutants’’.
- Air toxics.
- Biological pollutants [64].

‘‘Criteria air pollutants’’ is a term used to describe those pollutants that have been regulated and are basic indicators of air quality. The regulations and standards are based on criteria related to animal and human health and/or environmental quality. An important feature of these pollutants is the fact that they have a wide distribution across a country. In most countries ‘‘criteria air pollutants’’ can be:

- Carbon monoxide (CO_2)
- Lead (Pb)
- Nitrogen dioxide (NO_2)
- Ozone (O_3)
- Particles
- Sulfur dioxide (SO_2) [64,65].

Air toxics are also referred to as ‘‘hazardous air pollutants’’. The Living Cities-Air Toxics Program of Australia defines air toxics as: *Gaseous, aerosol or particulate pollutants that are present in the air in low concentrations with characteristics such as toxicity or persistence so as to be a to human, plant or animal life* [66]. Additionally, EPA states that ‘‘hazardous air pollutants, also known as toxic air pollutants or air toxics, are those pollutants that are known or suspected to cause cancer or other serious health effects, such as reproductive effects or birth defects, or adverse environmental effects’’. EPA categorizes 187 chemical substances as air toxics [65]. Some of them are benzene (C_6H_6), toluene (C_7H_8), xylene (C_8H_{10}), perchloroethylene (C_2Cl_4) formaldehyde (CH_2O), methylene chloride (CH_2Cl_2) and polyaromatic hydrocarbons [26,64,65].

Biological air pollutants are another class of air pollutants. They are defined as: *Aerosols or particulate matter of microbial, plant or animal origin that is often used synonymously with organic dust* [67]. They arise from:

- microbial populations (e.g. mold, microorganisms in the tissues of animals, humans, soil and plant debris),

- droppings from rodents, insects and other pests,
- pollens,
- protein in urine from animals. When it dries, it can become airborne [64,68].

Many of these pollutants are small enough to be inhaled (some of them are smaller than 0.7µm) [69].

1.3 Atmospheric Particles

1.3.1 Definitions

Particle or particulate matter (PM) may be solid or liquid, with diameters between 0.002 and 100 µm [60].

Aerosols are defined as a combination of liquid or solid particles suspended in a gaseous or liquid medium [70]. The term ‘‘aerosol’’ refers to both the particles and the medium in which they reside [71]. Atmospheric aerosols consist of solid or liquid particles suspended in the atmosphere [72].

1.3.2 Physical Characteristics of Particulate Matter (PM)

The physical characteristics of atmospheric particles are:

1. **Size:** It is the fundamental characteristic that determines the transport of the particles. For spherical particles, the size is given by particle’s diameter (*Dp*). In the case of irregularly shaped particles, an equivalent diameter is used, defined by the diameter of a sphere of equal volume (Figure 1.7) [73].

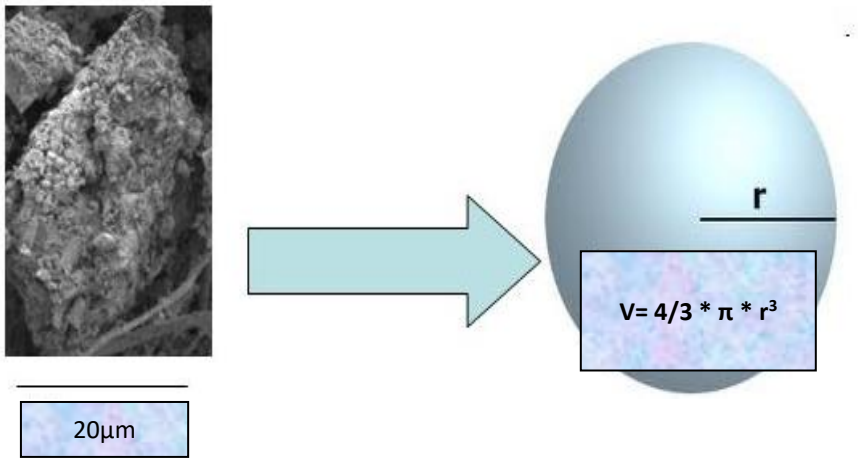

Figure 1.3: Determining diameter of irregularly shaped particles [74].

2. Shape: Liquid aerosol particles are nearly always spherical [72]. Surface tension helps to form them [73]. However, many particles in the atmosphere have quite irregular shapes for which geometrical radii and diameters are not meaningful [60]. In the development of the theory of aerosol properties it is usually necessary to assume that the particles have a shape of a sphere. Using equivalent diameters and correction factors helps applying these theories to non spherical particles [75]. The shape of a particle affects its aerodynamic and diffusive behavior, thus, it is one of the important factors determining particle transport and deposition (Figure 1.8) [73].

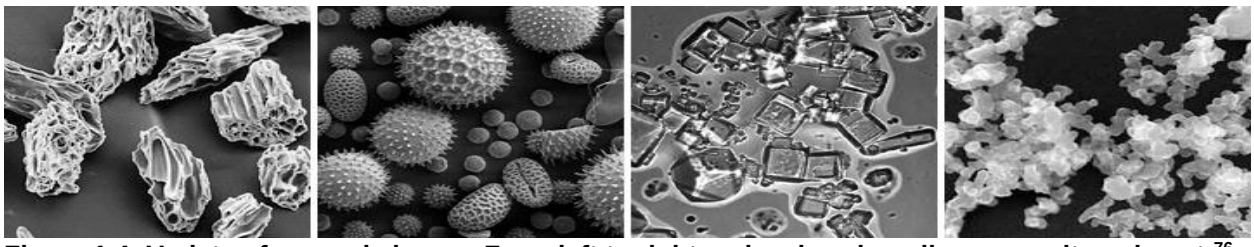

Figure 1.4: Variety of aerosol shapes. From left to right: volcanic ash, pollen, sea salt, and soot [76].

3. Density: Particle density (ρ) is defined as the mass per unit volume of the particle itself not of the aerosol (the ‘‘density’’ of which is called concentration). It is usually expressed in kg/m^3 [g/cm^3] [75]. The density of a particle plays an important role in its transport and deposition. Due to the fact that density is an intensive property, the density of a particle remains the same as that of the original material unless the particle undergoes surface oxidation or hydration [73]. When particles agglomerate to form larger particles, the bulk density is defined as the mass of the component particles making the agglomerate divided by the total volume occupied, which includes particle volume and inter-particle void volume. As a result, the bulk density of an agglomerate of particles is not an intensive property because it depends on how the constituent particles are arranged in the agglomerate [77].

1.3.3 Transformational Processes of Particulate Matter (PM)

The above-mentioned characteristics are important in the following transformational physical processes of particulate matter:

- **Condensation** which is the process of converting a material from a gaseous or vapour phase to a liquid or solid phase [78].
- **Evaporation** which is the process by which a liquid substance is converted to a gas or vapour [79].
- **Nucleation** is the localized emergence of a distinct thermodynamic phase at the

nanoscale that macroscopically grows in size with the attachment of growth units [80].

- **Hygroscopicity** is described as the ability of growth in particle diameter which occurs as the result of association with water vapor [81].
- **Coagulation** is a process in which particles collide with one another and adhere to form a larger particle. In the case of solid particles, this process is called agglomeration. It is an inter-particle phenomenon. The other processes involve mass transfer between a particle and the surrounding gas molecules [73].

1.3.4 Size Distribution of Particulate Matter (PM)

According to size, air particles are categorized into four categories (Figures 1.9 and 1.10):

1. **Coarse particles** (PM_{10}) with a diameter from 2.5 μm to 10μm [82-84].
2. **Fine particles** ($PM_{2.5}$ or PM_1) with a diameter smaller than 2.5 μm [85-87].
3. **Ultrafine particles** with a diameter smaller than 0.1 μm [88-90].
4. **Nanoparticles** with a diameter smaller than 50nm [91-93].

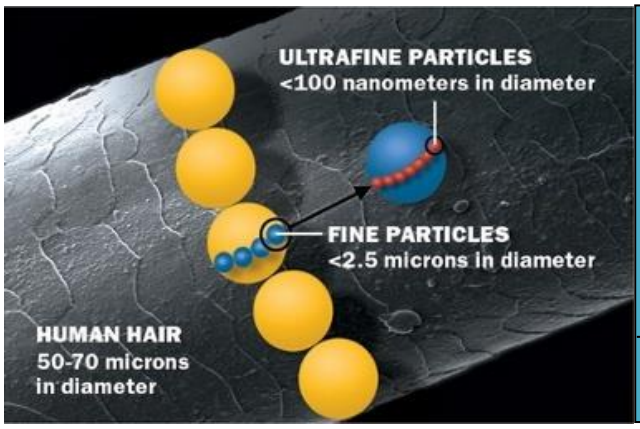

Figure 1.9: Fine and ultrafine particles' size compared to the width of a human hair [94].

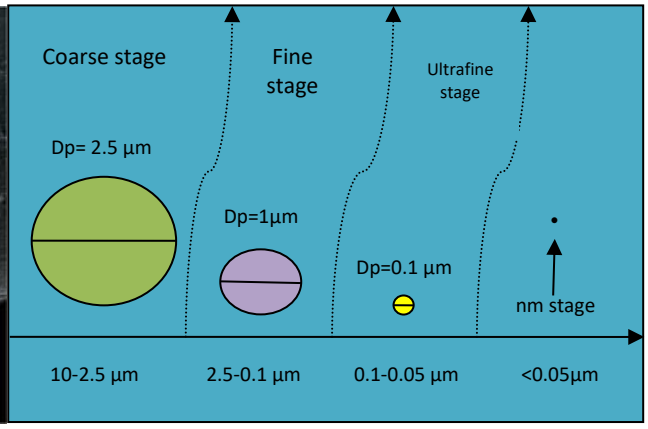

Figure 1.10: Size distribution of PM. The faded arrows indicate that the categorization based on size is not absolute.

Atmospheric particles may be either directly emitted into the atmosphere or formed there by chemical reactions; we refer to these as **primary** and **secondary** particles, respectively[60].The sources of primary particles are both anthropogenic and natural (dust, sea salt, soot, biological processes, etc.) [95,96].

1.3.5 Chemical Composition of Particulate Matter (PM)

The **chemical composition** of each particle range is being strongly dependent on their sources and their formation mechanism [97-99]. Particulate matter can consist both of organic and inorganic parts. More specifically:

- A large part (~50%) of this submicrometer aerosol mass in the troposphere consists of **organic material** [100,101]. Additionally, organic material significantly contributes (20–50%) to the total fine aerosol mass at continental mid-latitudes [102,103]. A major pathway for secondary organic aerosol is the atmospheric oxidation of precursor organic species [104,105]. Water-soluble organic carbon (WSOC) is considered a major component of carbonaceous aerosol as it serves as a proxy for secondary organic aerosols due to its highly oxidized and soluble nature [106].
- A predominant fraction of atmospheric aerosols consists in water soluble **inorganic matter** (WSIM). WSIM is emitted directly in the particulate form, principally as sea salt from the action of wind on the ocean surface (primary sources) [107]. Some of the characteristic ions that indicate fresh sea salt source are Na^+ and Cl^- [108,109]. Additionally, there is a secondary production of WSIM from gas to particle conversion (sulphate, nitrate and ammonia are considered the major secondary inorganic compounds in aerosols) [110].

1.3.6 Impacts of Particulate Matter (PM)

The impacts of PM in the natural and anthropogenic environment are associated with many effects on human health, visibility, as well as on the climate.

First of all, there is a range of effects on **human health**. For mortality, research has indicated many decades ago, that long term and repeated exposure to PM has been associated with increased population-based mortality rates [111-116]. More recent research indicates that there is association between fine particulate air pollution and cardiopulmonary and lung cancer mortality [117]. Additionally, exposure to $PM_{2.5}$ was estimated to cause 4.2 million premature deaths worldwide per year in 2016. This exposure causes cardiovascular, respiratory disease, and cancer [118]. Also, epidemiological evidence indicates that the development and progression of chronic obstructive pulmonary disease is associated with particulate matter [119-122].

Furthermore, atmospheric particulate matter results in reduced **visibility** [123]. In urban areas PM_{10} has received wide attention due to its association with visibility reduction [124-129]. Also, frequent regional haze pollution occurrence with high $PM_{2.5}$ concentrations and low visibility has become one of major environmental land public health issues in China [130]. Many studies have been recently conducted to investigate the precursors and characteristics of haze [131]. As a result, sources, formation pathways and nature of haze

are found to be significantly variable from region to region upon local specificities, meteorological conditions, and pollution characteristics [132]. In contrast, despite recently observed strong pollution over Northeast China corresponding to proximately 2-3 times of the historical severe haze episodes [133], little studies were conducted over the captioned region [132].

In terms of **climate change** atmospheric aerosols scatter and absorb solar radiation and thus, modify the radiation balance of the Earth [134]. Scattering of radiation has direct effects on climate, altering the amount of solar radiation reaching the earth's surface [60]. On the other hand, PM and specifically black carbon, sulfate, nitrate, ammonium, formate, acetate, and oxalate, absorb the infrared radiation emitted by the Earth's surface. This absorption of solar radiation generally results in positive radiative forcing [135,136] and leads to an increase of the energy which is converted to heat. Therefore, there is a contribution to the warming of the troposphere. Subsequently, as this energy does not reach the surface and heats the atmosphere directly, changes in the lapse rate may occur and this can contribute to global change by altering atmospheric circulation patterns [137,138]. An indirect impact of PM to climate change is that aerosols can also act as cloud condensation nuclei leading to change of the microphysical and radiative properties and hence the lifetime of clouds [72].

1.4 Fine Particulate Matter

1.4.1 General characteristics

Water soluble ions are one of the major components of atmospheric aerosols and there have been many studies that focus on their size distribution [139]. When it comes to particulate matter's toxicity, size is an important factor. More specifically, fine particulate matter PM_1 (Dp<1μm) and especially the one which is enriched with toxicants can penetrate deeper in the lungs and it is among the pollutants highlighted for adverse health effects [140,141].

In order to research PM's toxicity, campaigns have been carried out all around the world recording the particle concentration levels and investigating their composition [139,141]. But still there is uncertainty whether the toxicity of particles is better defined by chemical composition or size [142].

Particles below 1 μm arise mostly from anthropogenic sources, e.g. fuel combustion, industrial processes, and non-industrial fugitive sources[99]. Most primary particles maintain in their core non-volatile elements characteristic of their source (EC, metal oxides, etc.) but for fine aerosols these components usually represent a small fraction of the particle mass[143].

Fine PM in urban spaces arise predominantly from the gas-to-particle conversion processes within the atmosphere or they consist of secondary anthropogenic combustion products. Also, recent studies in European cities [144-147], even next to major roadways, indicate that most of the fine PM is secondary, mainly originating from vehicular traffic and energy production [148-150].

PM_1 measurements are important because they provide a better estimation of anthropogenic particles than $PM_{2.5}$ [151]. However, there is no regulation concerning PM_1 [152].

1.4.2 Impacts

Fine particles can remain in the atmosphere for several weeks and can be transported further by atmospheric circulation. Therefore, fine particles greatly impact the environment [153].

These particles are able to absorb more toxic substances than coarse particles and can enter the human body by deposition in the lungs through respiration, resulting in various respiratory and cardiovascular diseases [154]. Also, fine particles, which are respirable, are more deleterious than coarse ones, because they are not removed in the respiratory tract. Thus, they can penetrate the lungs and reach the alveoli [155]. In recent years, the problem of fine particles in urban areas has attracted increased concern, since the evidence from epidemiology and toxicology studies[156-158] has suggested statistically significant association between morbidity and ambient fine-particle concentrations [85]. Also, some epidemiological studies have confirmed a significant correlation between fine particles and mortality [159].

Fine PM as well as sulfur oxide related air pollution are associated with all cause lung cancer and cardiopulmonary mortality. More specifically, each 10μg/m^3 elevation of fine PM air pollution has been associated with a 4%, 6% and 8% increased risk of all cause, cardiopulmonary and lung cancer mortality, respectively. Additionally, long term exposure to combustion related fine particulate air pollution is an important environmental risk factor for these two diseases [160]. Thus, it is very important to research the concentration and sources of PM_1 but much less is known and even less has been done [161].

1.5 '' Tracer '' elements

1.5.1 General

For global aerosol emission, sea salt and mineral dust account for 36% and 42% respectively [99]. In order to define the origin of the particles the elemental part of PM can be used as a ''tracer'' [162]. In this thesis, we focused on the measurement of cations in the atmosphere and more specifically Ca^{+2}, Na^{+1}, Mg^{+2},NH_4^{+1} and K^{+1} as well as Black Carbon (BC) in order to determine the particles' sources.

1.5.2 Earth and ''Tracer'' Elements

Some of the above-mentioned cations are part of the **terrestrial dust** (Figure 1.11). The particles originated from this source are in the size range ~ > 10 /μm in diameter and is primarily composed of crustal elements, including silicon, aluminum, iron, sodium, potassium, calcium, and magnesium [60] .Inorganically driven processes such as weathering, cation exchanges, and soil leaching are often considerably more important in **base cation cycles** (Ca, K, Mg, Na), while organic processes such as heterotrophic immobilization and oxidation are typically less important [163].

Figure 1.5: Terrestrial dust is a main source of ‘‘tracer’’ elements in the atmosphere [164].

A part of the base cations available to the environment come from rock weathering. Base cations are emitted to the atmosphere as particles via natural processes such as soil erosion as well as from a number of anthropogenic activities. These activities include combustion of fuels such as coal and wood, different industrial processes, materials handling and storage, agricultural practices etc.

Emissions occur as particles of different size distributions and composition. For several types of emissions, the magnitude and character is not very well known [165]. There are generally little emission data available for base cations. The introduction of H^+, whether by atmospheric deposition or by internal processes, will directly impact the fluxes of Ca, K, and Mg via cation exchange or weathering processes. Thus, soil leaching is often of major importance in cation cycles, and many forest ecosystems show a net loss of base cations[166].

1.5.3 Sea and ‘‘Tracer’’ Elements

Particles are, also, generated at the surface of the ocean by the bursting of bubbles followed by wave breaking which is strongly wind speed dependent and some of these are carried inland (Figure 1.12) [60,167].

Figure 1.6: Creation of sea generated air particles with the help of the wind [168].

While the main production mechanism of sea salt (ss) particles is bubble bursting, the ss aerosol loadings in the marine boundary layer are governed by a number of factors, including production, entrainment, transport, mixing height, as well as removal by precipitation and dry deposition [167].

The chemical composition of **sea-generated particles** includes the elements found in seawater (primarily chlorine, sodium, sulfur, magnesium, potassium, and calcium) and organic materials, perhaps including microorganisms.

As for size distribution, more than 50% tend to be >3μm in diameter but recent studies suggest that there are also a number of particles produced in the submicron size range as well [60]. More specifically for different particle sizes:

1. Under the clean air and high wind conditions, sea salt accounts for approximately 75% of the total number concentration of particle sizes larger than 0.1 μm (fine and coarse particles) [169].
2. The size distribution of sea salt shows a peak at 2.5-4.1 μm (coarse particles) in diameter in the North Pacific [170].
3. Submicron sea salt plays an important role in determining the aerosol optical properties in remote ocean regions because of its high concentration relative to other chemical components [171].

4. Mean sea-salt mass fractions in the fine particle range (D <1μm) comprises 7-53% of all fine particle mass concentration over the Pacific Ocean covered from 60ºN to 70ºS [172].

1.6 Cations in the Atmosphere

1.6.1 Potassium in the Atmosphere

Potassium (K) is transferred in the atmospheric environment from natural and anthropogenic sources. First of all in plants, it is the abundant cation in the cells. Specifically, in leaves it is the second most abundant nutrient after nitrogen (N) [173]. Leaching from leaves (also mentioned as foliar) is of major importance in K cycling, often exceeding litterfall in importance. This is because K stays primarily in ionic form within plant tissue, playing a major role in osmoregulation of stomatal opening and closing [192]. Leaf wetness has an unusual composition because so much can be exuded as guttation through the stomata of plants such as high concentrations of dissolved CO_2 and plant delivered cations such as potassium [174].

Also, in the earth's crust K is estimated at 2.59% out of all the elements that are used as ''tracers'' of the chemical composition of PM [162] and in sea water the concentration is $3.8x10^2$ mgL^{-1} [175].

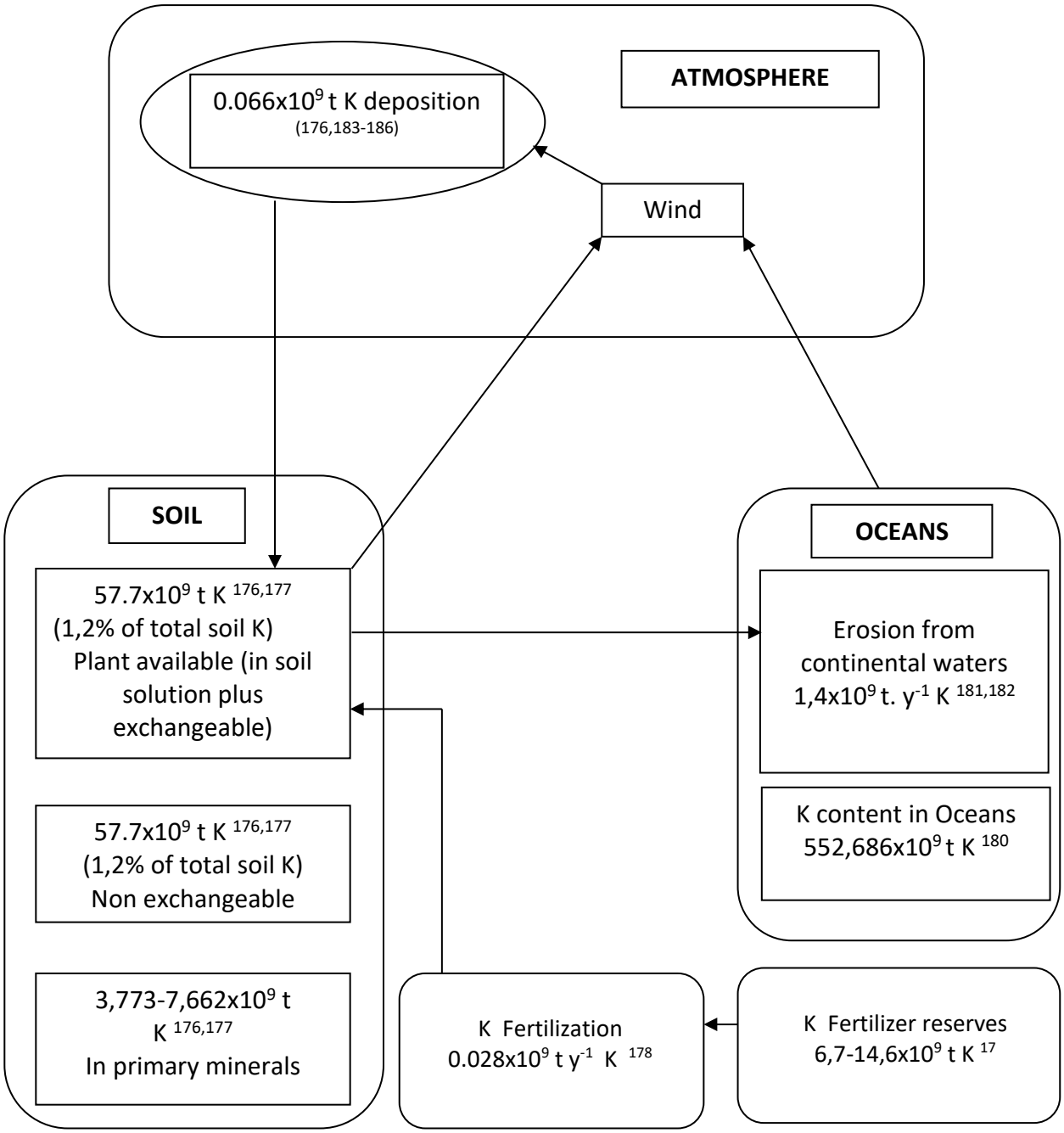

Figure 1.7: The K circle among soils, atmosphere and oceans [173,187].

Through wind potassium is transferred to the atmosphere from soil and oceans. Approximately 57.7 x 10^9 t of K (1-2% of total soil K) is in the appropriate composition to be transferred to atmosphere. There is no estimation of the amount which is in particulate form but approximately 0,006 x 10^9 t return to soil through atmospheric deposition (Figure 1.13) [176-187].

Finally, atmospheric K is transferred in the atmosphere through soot. The ratio of excess potassium to soot carbon in the fine fraction of aerosols is proposed as an indicator of the

relative contributions of biomass and fossil-fuel burning to soot carbon aerosols (Figure 1.14-1.15).

Figure 1.8: Biomass burning releases Potassium and Black Carbon in the atmosphere [188].

Figure 1.9: Fossil fuel burning is a source of Potasium and Black Carbon in the atmosphere[189].

The ratio of soot carbon to fine carbon suggests that most of the particulate organic carbon over the Atlantic is of continental origin [190]. Additionally, during biomass combustion KCl is the main potassium compound released into the gas phase. KCl may however be sulfated during combustion [191]. KCl has, also, been found to inhibit the formation of NO [192].

1.6.2 Sodium in the Atmosphere

A substantial amount of particulate sodium exists in the atmosphere because emission sources of sodium are widely spread on the Earth's surface. Most of the atmospheric sodium is derived from seawater and terrestrial substances [99]. In earth's crust Na is estimated as 2.83% out of all the elements that are used as ''tracers'' of the chemical composition of PM [162] and in sea water the concentration is $1.05x10^{4} mgL^{-1}$ (chlorine's concentration is estimated at $1.9x10^{4}$ mgL^{-1}) [175].

It is often believed that all of fine sodium is derived from sea salt (mainly NaCl salts) [193]. Genuine sea-salts are in the form of a mixture of NaCl and $MgCl_2$ entrained during their passage over sea [194]. In calculating the amount of chlorine loss, sodium is used as a tracer of sea salt [195]. Chlorine loss is due to heterogeneous reaction of sea salt with acid gases such as SO_2, NO_2, N_2O_5, HNO_3, H_2SO_4, and $ClONO_2$. This reaction is an important formation process of particulate sulfate and nitrate in the marine air [195-198].

Simultaneously, concentrations of non-sea-salt (nss) substances such as nss-sulfate or nss-calcium are calculated on the basis of average seawater composition [193]. If we ignore the contribution of nss-sodium, it is possible that the amount of chlorine loss will be overestimated [199]. The accurate calculation of non-sea-salt, or excess, concentrations of chemical constituents is essential for quantifying the influence of natural terrestrial, non-sea-salt marine, and anthropogenic sources on marine aerosol and precipitation chemistry [200].

1.6.3 Magnesium in the Atmosphere

References species such as Na^{+} or Mg^{+2} are commonly used to estimate the sea-salt fraction [200-203].

In sea water, magnesium's concentration is estimated at 1.35 x103 mgL^{-1} (sodium' s concentration is 1.05x104mgL^{-1}) [175]. In the earth's crust Mg is estimated as 2.83% out of all the elements that are used as ''tracers'' of the chemical composition of PM [162].

Additionally, the use of lubricating oil [204] and fossil fuel increases the concentration of Al, Mn, Mg and Fe nanoparticles and other potential toxic elements [205].

In plants Mg is intermediate between K and Ca in terms of its tendency to return from plant foliage compared to litterfall and compared to foliar leaching. Like Ca it becomes part of permanent plant tissue and it plays a critical role in photosynthesis within chloroplasts [163].

1.6.4 Calcium in the Atmosphere

It is clear from observations of the composition of precipitation and the PM that Ca is the most important in terms of mass [206].The content of Ca in the Earth' s crust is 3.63% [207] whereas in sea water calcium's concentration is estimated at $4x10^{2}$ mgL^{-1}.

Natural sources include:

1) Soils from arid regions [208] and the transfer in the atmosphere is mainly committed with wind erosion.
2) Biomass combustion

3) Volcanic eruptions [209] and

4) Sea salt [210].

Various anthropogenic sources have also been identified and they include:

1) Unpaved roads (they are important in North America) [211] as are some open sources such as quarrying [211,212].

2) Construction and general urban activities have been found to be a strong local influence on the Ca content of urban precipitation composition [213,214].

3) Agricultural tilling and wind-blown soil dust are likely to be an important source [209].

4) Industrial sources of Ca have also been considered an important source in Europe as a result of declining Ca in precipitation and air [215, 216]. In 1995 it was estimated that industry emitted 1.4 Mt y^{-1} of Ca [217] whereas, a study two years later showed a decline in this number at 0.75-0.8 Mt y^{-1} [216].

Calcium's most soluble minerals are $CaCO_3$ and $CaSO_4$ and they consist the main body of PM that is released in primary form. Calcium does not have any significant atmospheric chemistry that will change its transport and deposition properties (wet or dry) [209].

Finally, in plants Ca is unique among the macronutrients in that it continues to accumulate in foliage up to the time of senescence, and thus litterfall return of Ca usually exceeds foliar Ca content at maximum leaf biomass [218]. This is because Ca is a major component of permanent plant tissues, such as pectates in cell walls, and has a tendency to precipitate as oxalates [163].

1.6.5 Ammonium in the atmosphere

Ammonium (NH_4^+) is part of secondary produced PM. Secondary aerosols are formed through heterogeneous condensation. Low-vapor-pressure products are scavenged onto preexisting particles. If the concentration of particles is sufficiently high, this dominates over the formation of new nuclei via homogeneous nucleation [219,220].

Both natural and anthropogenic sources contribute to the emissions and precursors of secondary aerosols (SO_2, NO_x, NH_3, VOC_s and intermediate volatile organic compounds-IVOCs). The major source of SO_2 and NO_x is the combustion of fossil fuel that contain

sulphur. HNO_3 is formed in the atmosphere from NO_x. Its ability to form secondary particles is depended on the availability of NH_3 in a gaseous phase. The final product is NH_4NO_3 and the chemical reaction is bidirectional. NH_3 is emitted mainly from agriculture [221,222].

1.6.6 Black Carbon in the Atmosphere

Black carbon (BC) or elemental carbon (EC) is a distinct type of carbonaceous particulate matter mainly emitted from the incomplete combustion of fossil fuels, biofuels, biomass burning and from the weathering of graphite carbon from fossils (Figure 1.14-1.15) [223].

The two main forms of BC are char and soot. Char is produced at lower temperatures than soot and has assize range of 1-100 μm which is larger than that of soot [224].In the range of nanoparticles soot is of great importance due to its high magnitude toxicity and very small size [225]. Very small size particles can penetrate deep into the respiratory track and cause health problems [226].

As for the physical properties of BC nanoparticles they present high sorption and are strongly related to other potential toxic elements from this process. This happens because the BC nanoparticles have large surface to volume ratio and large number of nanopores[227]. Due to its large surface area it is involved in a variety of heterogeneous activates [228]. A decrease in particle size increases potential toxic concentration (Niu et al., 2010), and BC's concentration [230].

Black carbon is the dominant insoluble light-absorbing particulate species, both in the atmosphere and after deposition on snow and ice [223]. Because of its long range transport, it affects:

1. The snow's albedo through its decrease [231] and also the atmospheric circulation patterns. This leads to acceleration of the snowmelt and glacier retreat in the Arctic and across the mid-latitudes of the Northern hemisphere [232] (Figure 1.16). Many studies indicate that the efficacy of BC in snow is much greater than the efficacy of carbon dioxide or other anthropogenic forcers owing to a sequence of positive feedback mechanisms [231,233-242].

Figure 1.10: Black carbon decreases snow's and ice's albedo [243].

2. Solar radiation balance as it behaves like absorbent particulate matter [244]. BC is originally emitted together with organic compounds in chain-like fractal aggregates. Through condensation with vapour and other gas-phase species, these particles collapse into denser particle clusters (Bond et al., 2013). This coating that is created changes the morphology and also the hydroscopic and optical properties of the corresponding particles. The BC particles become more spherical and through deposition they can be removed from the atmosphere. But, they can also absorb solar radiation. The non-absorbing material in the particle can refract light towards the absorbing BC core, increasing the absorbed solar radiation (Ackerman and Toon, 1981). The coating of BC has been estimated to enhance its absorption by 50–200%, depending on the relative sizes of the BC core and the coating [232].

3. Clouds, as it contributes to the number of cloud condensation nuclei and therefore affects cloud cover and lifetime. Also, it acts as ice nuclei changing ice or mixed-phase clouds. Finally, absorbing aerosols perturb the temperature gradient in the atmosphere affecting atmospheric motions and cloud distributions [246].

1.7 Atmospheric Pollution and Athens

The Greater Athens Area (G.A.A.) is considered to be a typical Mediterranean area. Its climate is characterized by hot and dry summers as well as by wet and mild winters and most of the rainfall occurs during the cold days. Atmospheric stability is mainly neutral however, in the late autumn, winter and early spring the frequency of stable conditions increases and in the summer unstable conditions prevail [247, 248]. Atmospheric circulation is important for the air quality of the basin [249]. Especially the local scale circulation, being

generated by the landscape variability and complicated land water distribution greatly influences the air pollutants dispersion [250].

In Athens, several measures have been implemented since the 1980's in an effort to improve the existing air quality conditions. To name a few: old vehicles retirement plan, regular pollution controls of private vehicles, improvement of public transportation (metro, subway, bus routes),integration of catalytic anti-pollution technologies, the odd-even traffic regulation system, reduction of sulphur in heavy fuels and of benzene in gasoline, introduction of natural gas. As a result of the abatement practices, the level of most pollutants has exhibited a gradual decrease in the last decades [251]. In particular, sulphur dioxide, carbon monoxide, nitrogen oxides have been steadily declining since the 1990's, and a similar decline is present in PM_{10} concentrations but only during the last decade. From 2008 onwards, the reduction of pollutants was significantly accelerated because of the economic recession in Greece [252].

On the other hand, the economic crisis has also had a negative impact on Athens' air quality. The first strong evidence of negative impacts was observed during the winter of 2012-2013 during which a shift to wood burning (as the major fuel source for domestic heating) resulted in intense "smog" events [253]. The use of old and low efficiency domestic heaters, non-optimal handling of the equipment, as well as elaborated wooden or plastic material as heating fuel also rises significant concerns regarding public health. Wood burning holds a significant role in the emission of gases (e.g. CO) and particulate matter rich in soot and fine carbonaceous particles. The majority of these emissions such as polycyclic aromatic hydrocarbons (PAHs) etc., are considered to be toxic [254-258]. At the same time, due to the economic crisis, since 2011 elemental carbon (EC) has presented a net decrease which comes as a result of reduction in traffic and industrial activity during summertime whereas an increase has been observed in the wintertime as a result of wood burning [259]. Finally, smog events over Athens can also be amplified by local factors such as topography and meteorological patterns that favor the accumulation of local emissions [260].

2 STUDY AREA

2.1 Sampling Site

For the purpose of this study air samples were taken from the National Observatory of Athens (NOA) station in Thissio (38° 0.00′ N, 23° 43.48′ E, 110 m a.s.l.). This station is located on the top of a hill in the center of Athens and is mostly surrounded by a pedestrian zone and populated neighborhoods. To the S–SE sector it adjoins with the Filopappou and Acropolis Hills (Figure 2.1) [261]. The district of Thissio is located within the historical center of Athens and is part of the urban area of Athens, therefore, it is reflecting the average population of the city.

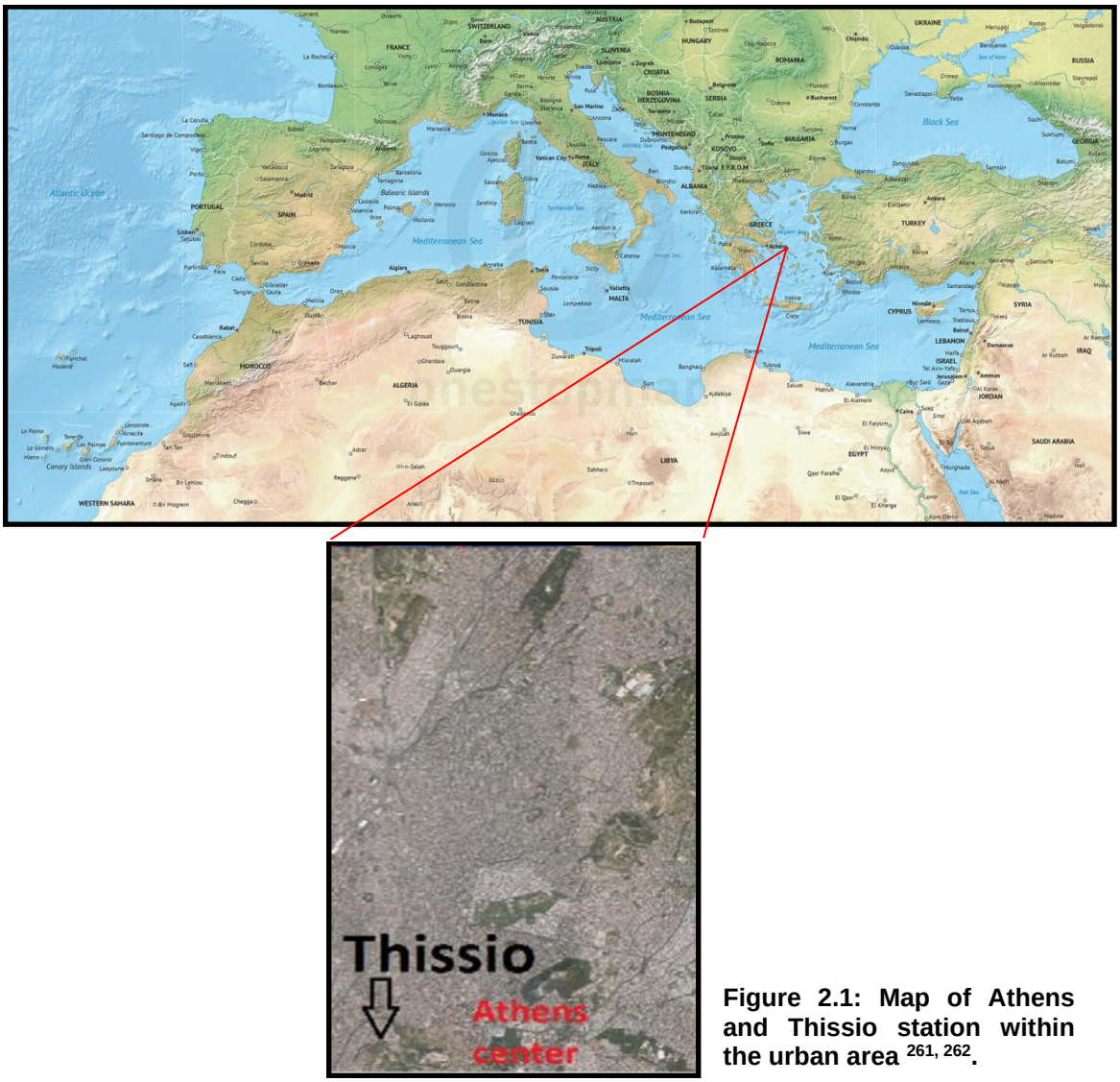

Figure 2.1: Map of Athens and Thissio station within the urban area [261, 262].

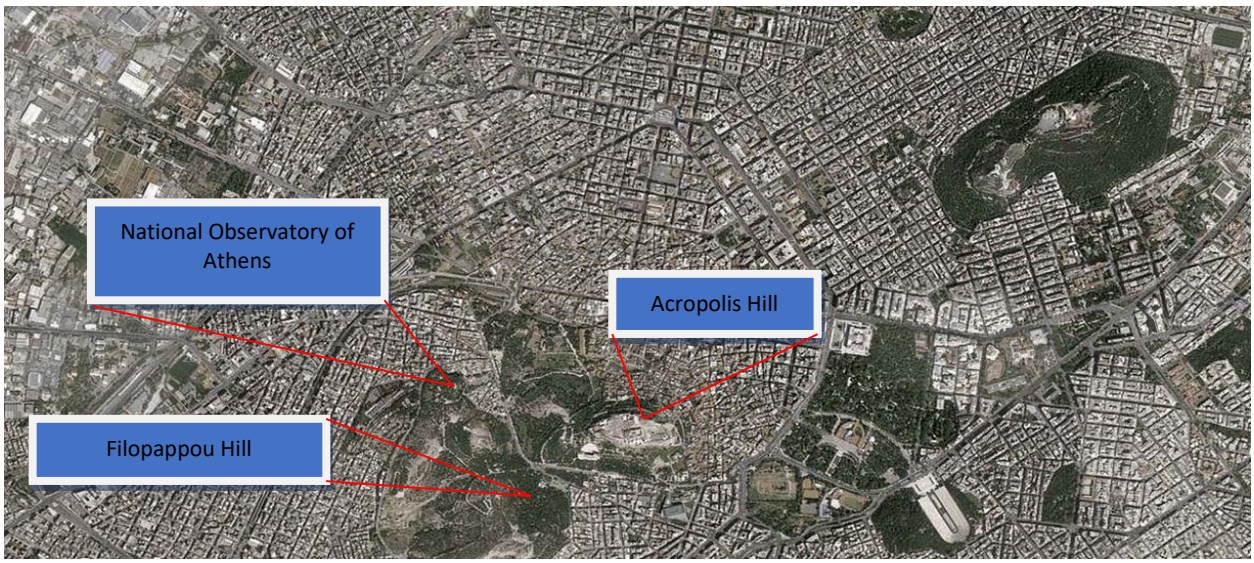

Figure 2.2: Map of the National Observatory and the Hills surrounding it [263].

Figure 2.3: National Observatory of Athens [264].

2.2 Characteristics of the Athens's Basin

The greater area of Athens gathers about 40% of Greece's total population in a basin on the west coast of the Attica peninsula [251]. It is surrounded by the mountains Parnes, Penteli and Hymettus and all three of them are over 1000m high. They mainly surround the North and East boundaries of the area [265].

2.2.1 Attica Winds

In terms of the wind profile, the prevailing axis is northeast/southwest and the ventilation takes place in northeasterly directions [266]. During the warmer part of the year, the mean

wind pattern in the atmospheric boundary layer is a persistent northeasterly flow of relatively high constancy. The area is also exposed to the summer monsoon circulation of the Eastern Mediterranean (Figure 2.4). Finally, a system of semi persistent summer northerly winds called ‘‘Etesians’’ favor good ventilation of the basin prohibiting pollution episodes (Figure 2.5) [251].

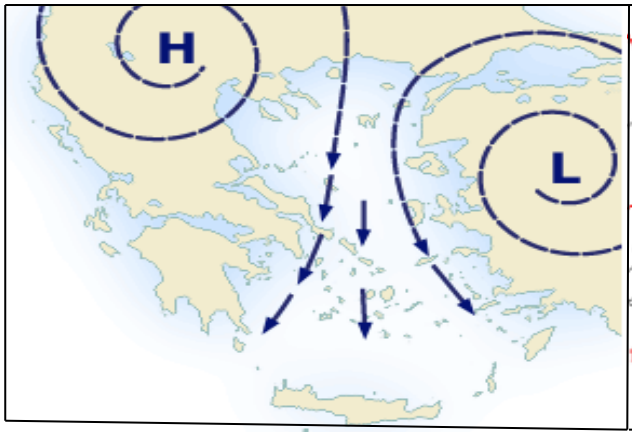

Figure 2.4: Monsoon circulation of the Eastern Mediterranean [267].

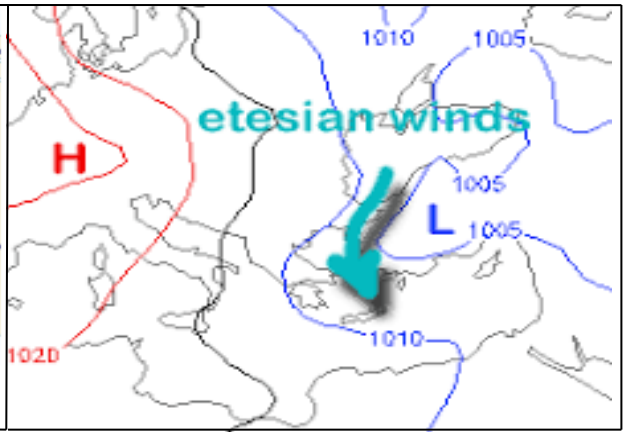

Figure 2.5: Etesian winds [268].

2.2.2 Attica Breezes

In terms of the breezes’ profiles, the area is subject to sea and land breeze local circulation phenomena, favored during the weakening of the synoptic wind [269]. This profile appears along the axis of the basin (NE to SW) and anabatic/katabatic winds flow from the surrounding mountains. Under these circumstances the ventilation of the basin is poor the boundary layer is shallow and the air pollution potential increases [266]. The sea breeze system from the Saronic Gulf, located to the south of Greater Athens Area sweeps primary pollution from the city center, combined with O_3 titration and favors pollutant accumulation to the northern suburbs where significant episodes are encountered. Air pollution episodes may occur in Athens during all seasons of the year but most of these episodes are associated with the development of sea-breeze [270].

3 METHODS AND MATERIALS

3.1 Sampling

For this research 21,478 atmospheric samples were measured during a period of 10 months almost uninterruptedly. From 16/1/2017 until 1/11/2017 the cationic composition of fine aerosol particulate matter (PM_1) was recorded at a time resolution of 15 min. The technique that has been used to analyze the samples and calculate the concentration of the particles, included a Particle-into-Liquid Sampler (PILS) coupled with Ion Chromatography (IC).

3.2 Particle into Liquid Sampler Technique (PILS)

The specific technique is based on the collection of ambient particulate matter into a small stream of high purity water. Thereby, a solution is produced containing the particulate matter which is sampled at a certain moment of time. This is accomplished by mixing an ambient aerosol sample flow (5-17 l min^{-1}) with a smaller turbulent flow of 100°C steam (~1.5 l min^{-1}) (Figure 3.1-3.2).

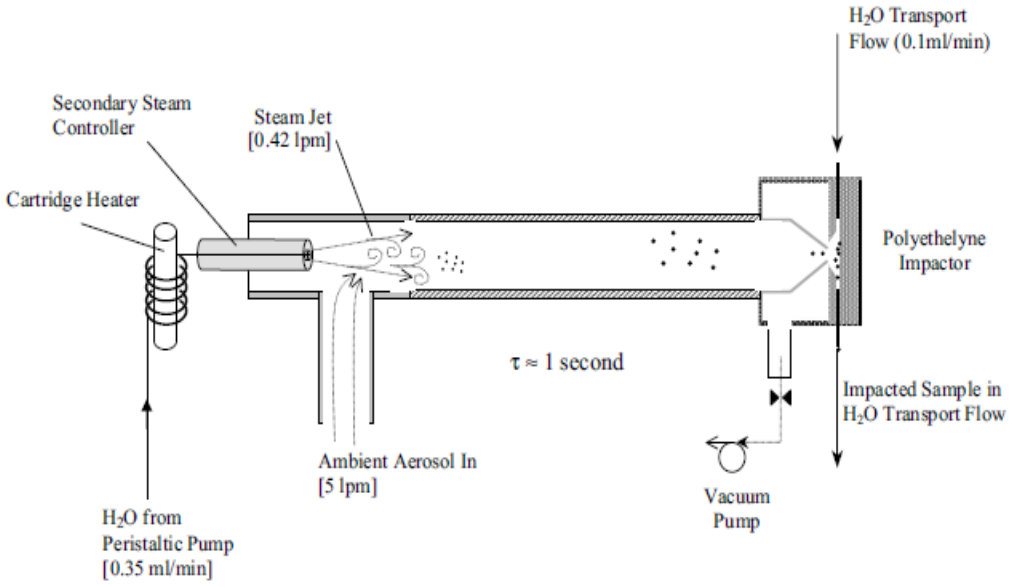

Figure 3.1: Intermediate 5 $lmin^{-1}$ PILS design [271].

Subsequently, rapid adiabatic cooling of the warmer turbulent steam by the cooler ambient sample provides a high supersaturation of water vapor. In this environment, the aerosol particles grow into droplets (Dp >1 μm) large enough to be collected by an impactor (Figure 3.2).

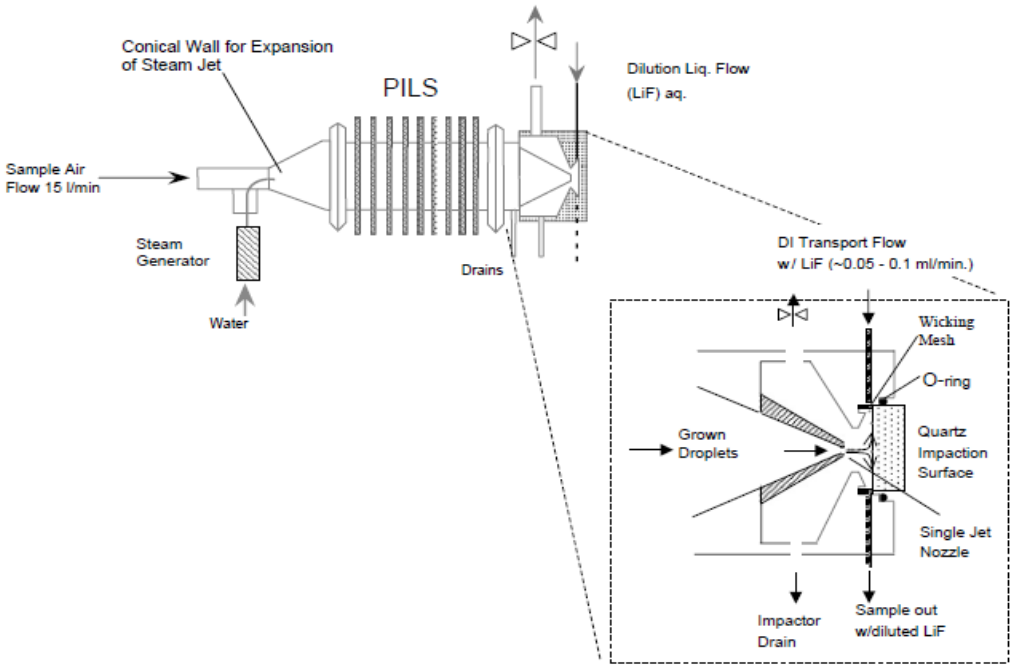

Figure 3.2: Schematic of a 15 lmin^{-1} PILS design [271] .

The droplets are collected to produce a continuous liquid flow for online analysis of the particles in solution. Any technique capable of continuous online analysis of the liquid sample can record the changing aerosol composition. Since ambient gases that are, also, present in the aerosol sample might contribute to the particle phase measurement, it is necessary to place denuders inline, upstream of the PILS to remove gas phase species.

Figure 3.3: PILS and IC of our research

3.3 Ion Chromatography (IC)

Real-time measurements of cations in the submicron mode (PM_1) were conducted by means of a Particle-Into-Liquid-Sampler (PILS - Metrohm ADI 2081) coupled with an Ion Chromatograph (Ion Chromatography System, Dionex). The principle of PILS operation is described in details by Orsini et al. (2003) [271]. Cations were determined using a Dionex ICS-1500 ion chromatography system equipped with an Ion Pac CS12A 4mm (10-32) column and an Ion Pac AG12A 4mm (10-32) guard column, under isocratic elution of 20 mM MSA (methanesulfonic acid), at a flow rate of 1.0 $mLmin^{-1}$.The PILS sample ambient air flow rate was 16.7±0.4 Lmin-1 and a cyclone was used to provide PM cut size of PM_1. The ion chromatograph was set for quantitative determination of sodium (Na^+), ammonium (NH_4^+), potassium (K^+), calcium (Ca^{+2}) and magnesium (Mg^{+2}) at a time resolution of 15 minutes. The detection limit was calculated at 1 ppb for Na^+, NH_4^+ and 2 ppb for K^+, Mg^{+2} and Ca^{+2}. Also, nss-K^+ concentrations were calculated using the Na^+ concentrations and the Na^+/K^+ ratio in seawater [272]. All reported concentrations were blank corrected.

3.4 Data Analysis with Chromeleon

The data from the ion analysis were collected through the system of Chromeleon ver. 6.80 (Figure). Identification and quantification of the studied cations took place, according to the retention time and the integration of each peak area, respectively

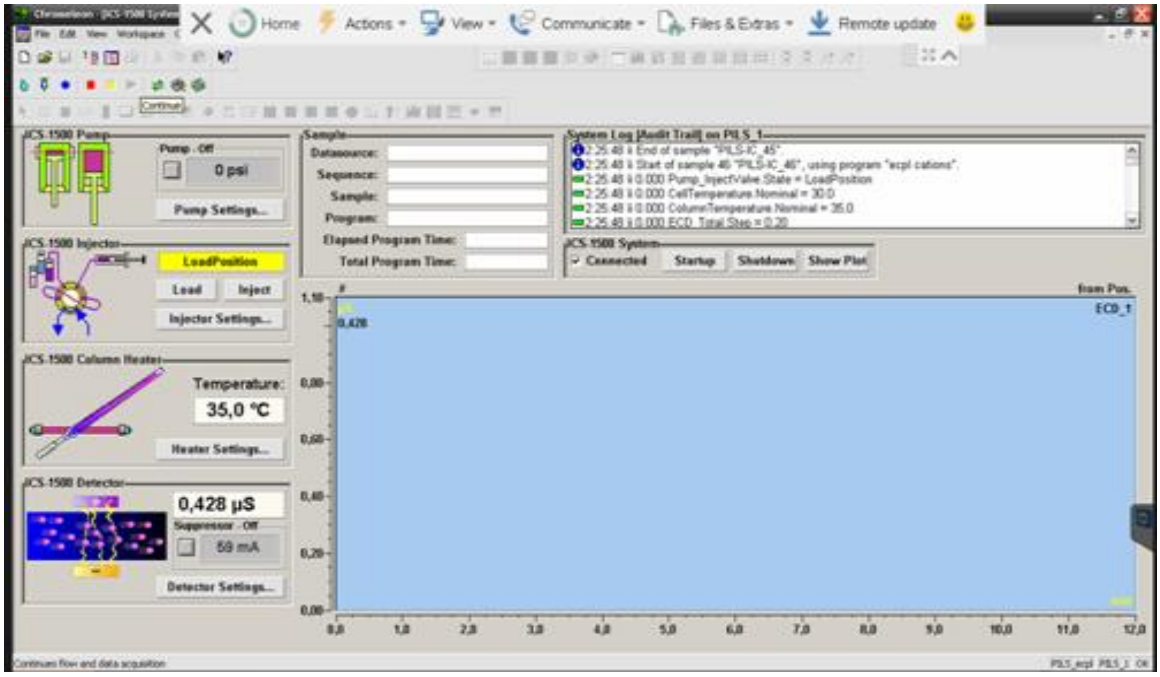

Figure 3.4: Chromeleon Control Panel of the IC

The cations have retention time in a characteristic interval, which is presented in the following Table 3.1.

Table 2: Retention time intervals of the cations

Cations	Retention Time Interval (min)
Sodium	2.97 - 3.17
Ammonium	3.48 - 3.68
Potassium	3.893 - 4.893
Magnesium	7.543 - 8.343
Calcium	9.43 - 10.55

In the following Figure 3.5, the chromatograph representative of an atmospheric sample is presented. In Figure 3.5, the peaks of every cation are distinguished. Axis (x) represents the retention time (in min) and axis (y) represents the detector's signal (in μS).

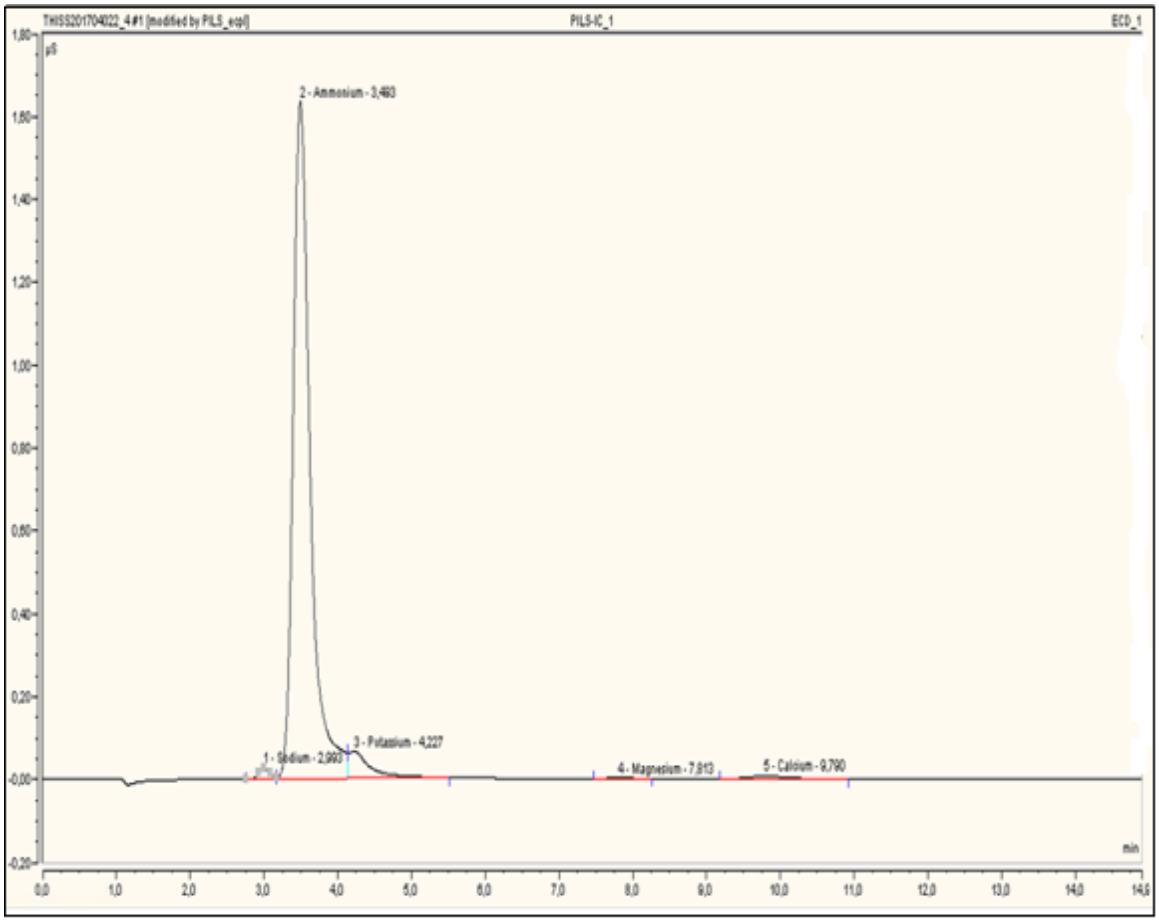

Figure 3.5: Chromatograph from the analysis

Integrating the peaks through Chromeleon's tools, the areas (in μS*min) were measured (Figure 3.6).

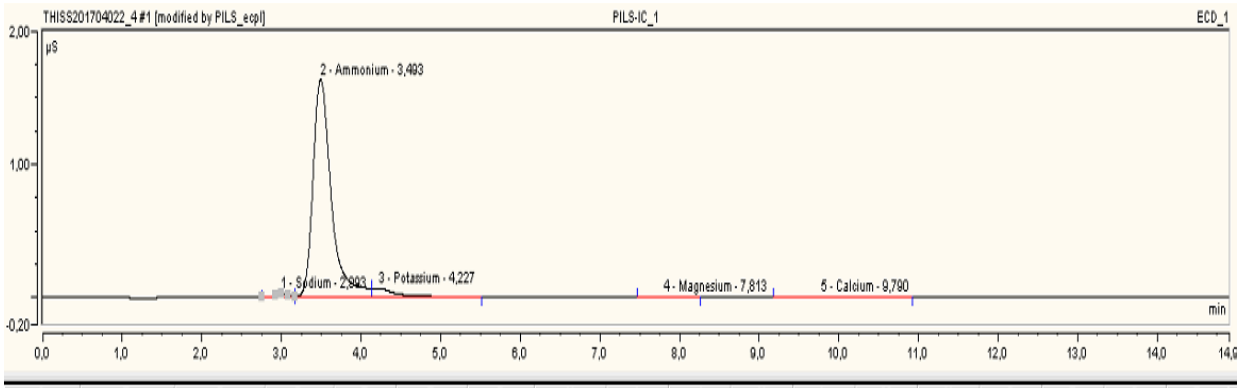

Sample No.	Sample Name	Time	Comment	Area µS*min Sodium ECD 1	Area µS*min Ammonium ECD 1	Area µS*min Potassium ECD 1	Area µS*min Magnesium ECD 1	Area µS*min Calcium ECD 1
1	PILS-IC 1	25/04/17 06:00		0,005	0,440	0,023	0,001	0,004
2	PILS-IC_2	25/04/17 06:15		0,005	0,466	0,031	0,001	0,004
3	PILS-IC_3	25/04/17 06:30		0,005	0,473	0,033	0,001	0,004
4	PILS-IC_4	25/04/17 06:45		0,005	0,467	0,031	0,001	0,004
5	PILS-IC_5	25/04/17 07:00		0,005	0,472	0,044	0,001	0,004
6	PILS-IC_6	25/04/17 07:15		0,005	0,474	0,055	0,001	0,004
7	PILS-IC_7	25/04/17 07:30		0,005	0,491	0,052	0,001	0,004
8	PILS-IC_8	25/04/17 07:45		0,005	0,514	0,046	0,001	0,004
9	PILS-IC_9	25/04/17 08:00		0,005	0,537	0,038	0,001	0,005

Figure 3.6: Creation of the areas of every cation through integration

3.5 Calibration and Concentration's Measurement

All data are quantified by comparing the sample peaks in the chromatograms to those produced from standard solutions that include known concentrations of every studied cation. The range of the applied standard solutions concentration was about 25-250 ppb. The applied reagents were NaCl, KCl, NH_4Cl, $MgSO_4$ and $CaCl_2$ dissolved in nanopure water, in order to detect Na^+, K^+, NH_4^+, Mg^{+2}, Ca^{+2}, respectively. Conversion of the samples' peak area (µS*min) into concentration, was achieved through the line regression equation acquired by the applied calibration curves. In the following Figures 3.7-3.11 are presented the calibration curves of the 5 measured cations.

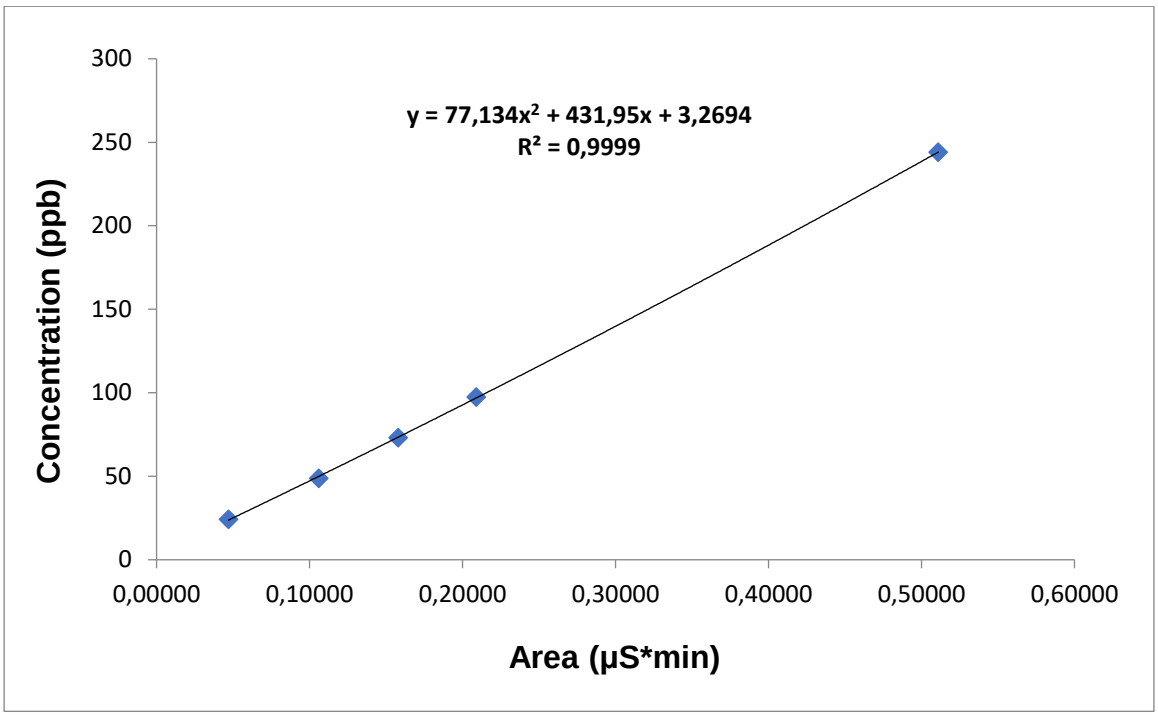

Figure 3.7: Calibration curve of NH_4^+

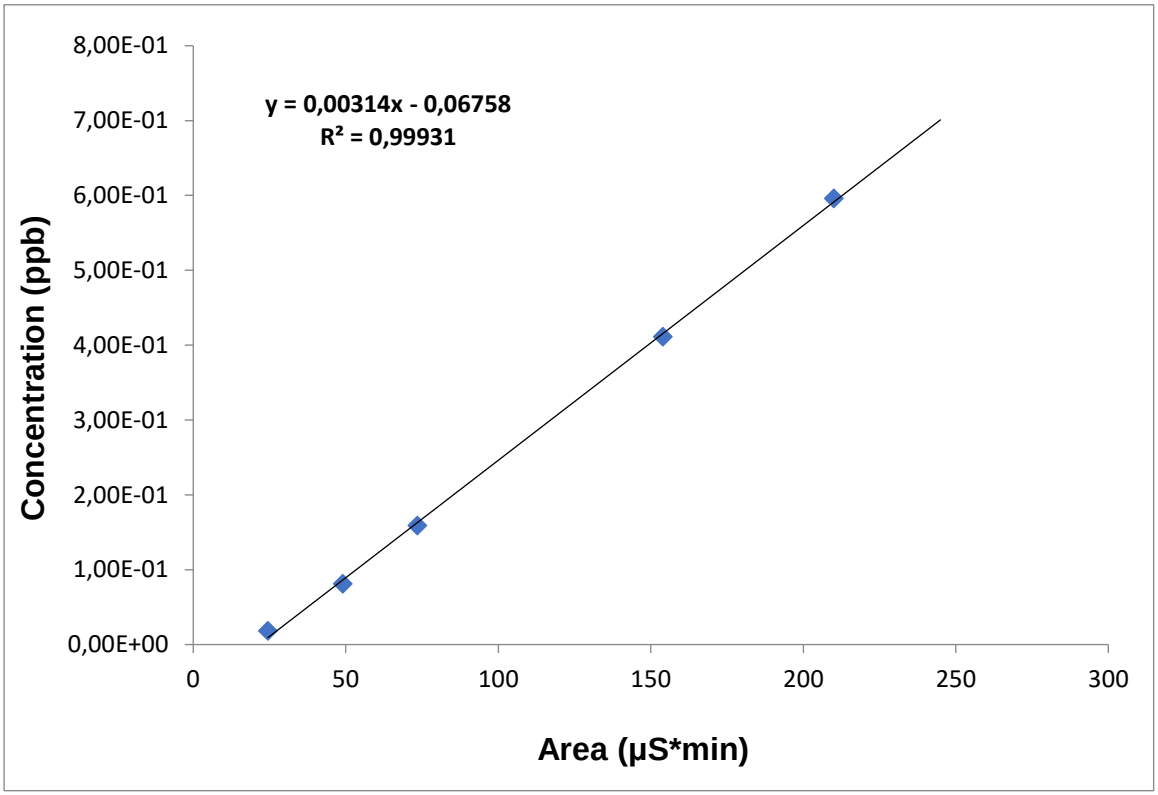

Figure 3.8: Calibration curve of Mg^{+2}

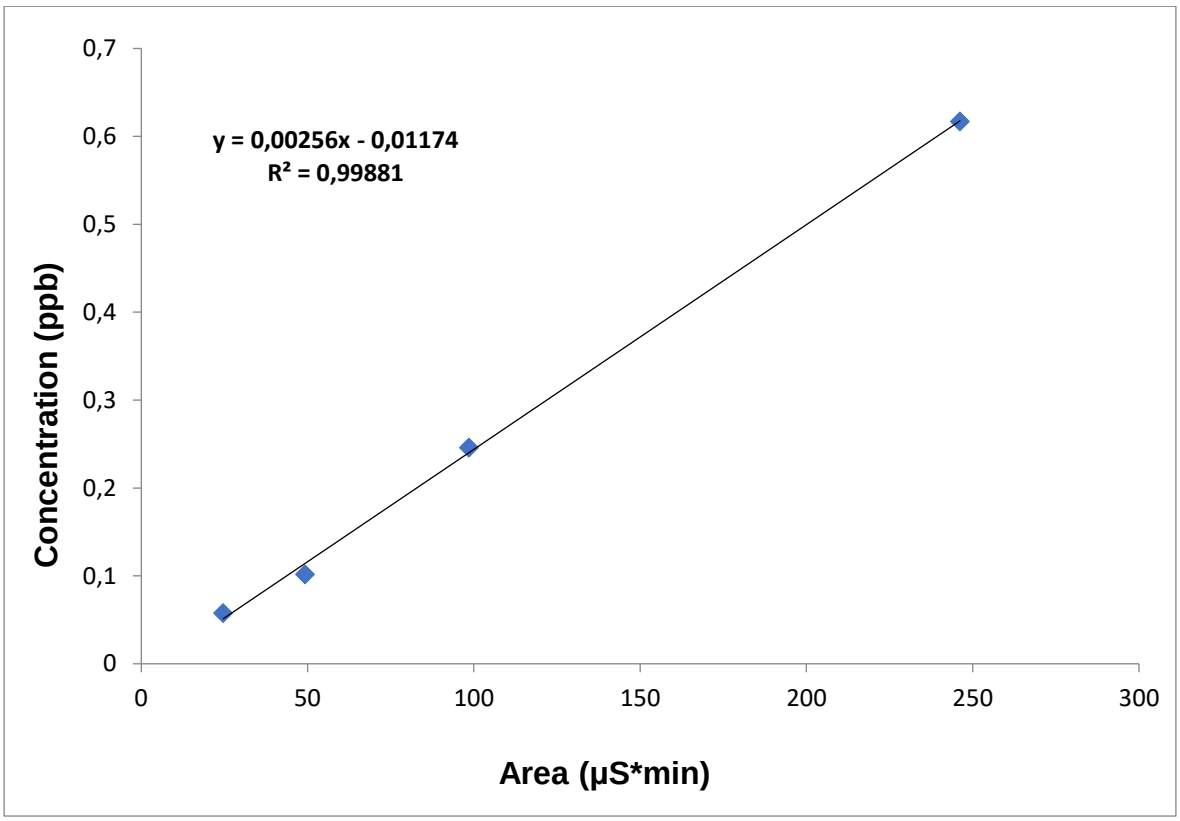

Figure 3.9: Calibration curve of Ca^{+2}

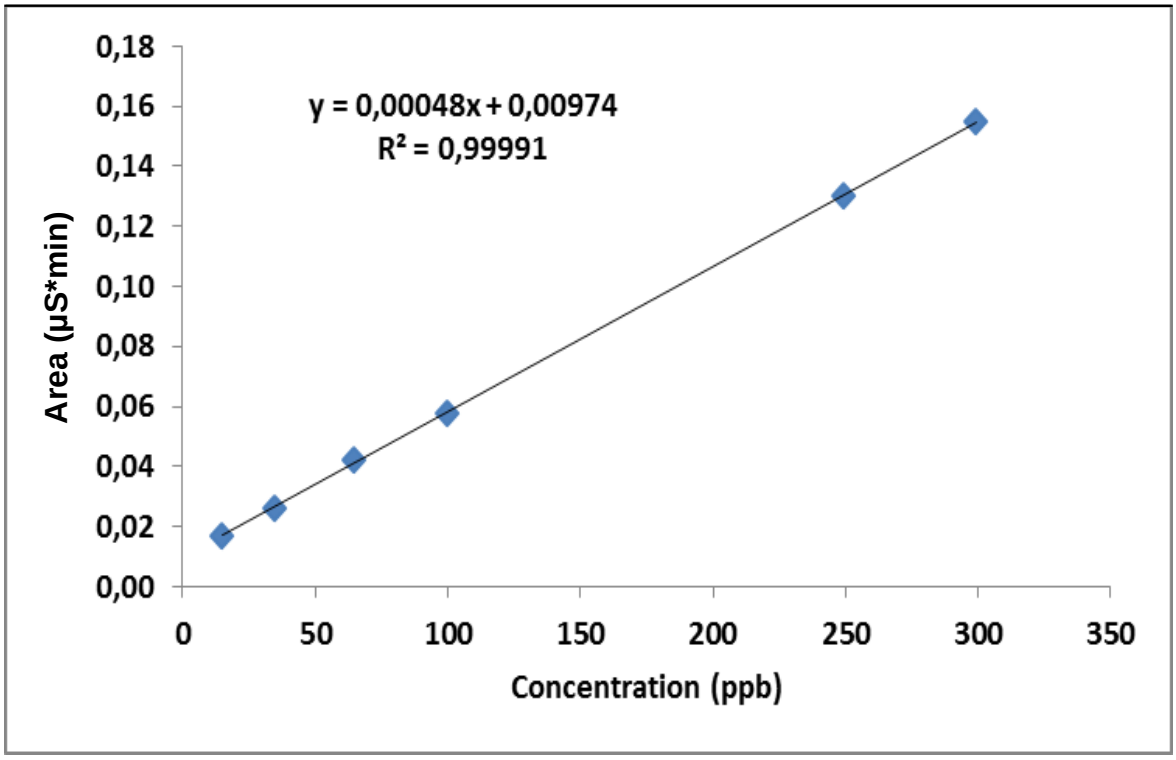

Figure 3.10: Calibration curve of K^{+}

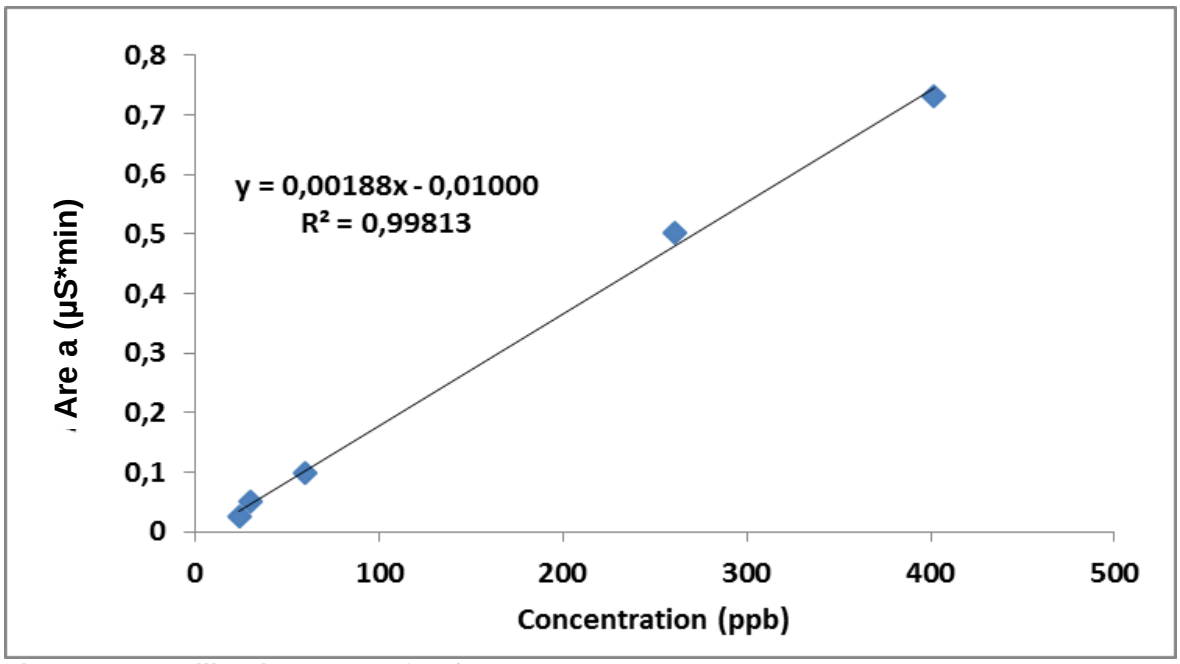

Figure 3.11: Calibration curve of Na^+

4 RESULTS AND DISCUSSION

4.1 Data Series of the Studied Chemical Substances for the Sampling Period

4.1.1 Data Series of Sodium

In the Figure 4.1 below is indicated the distribution of Sodium's concentration for the whole sampling period.

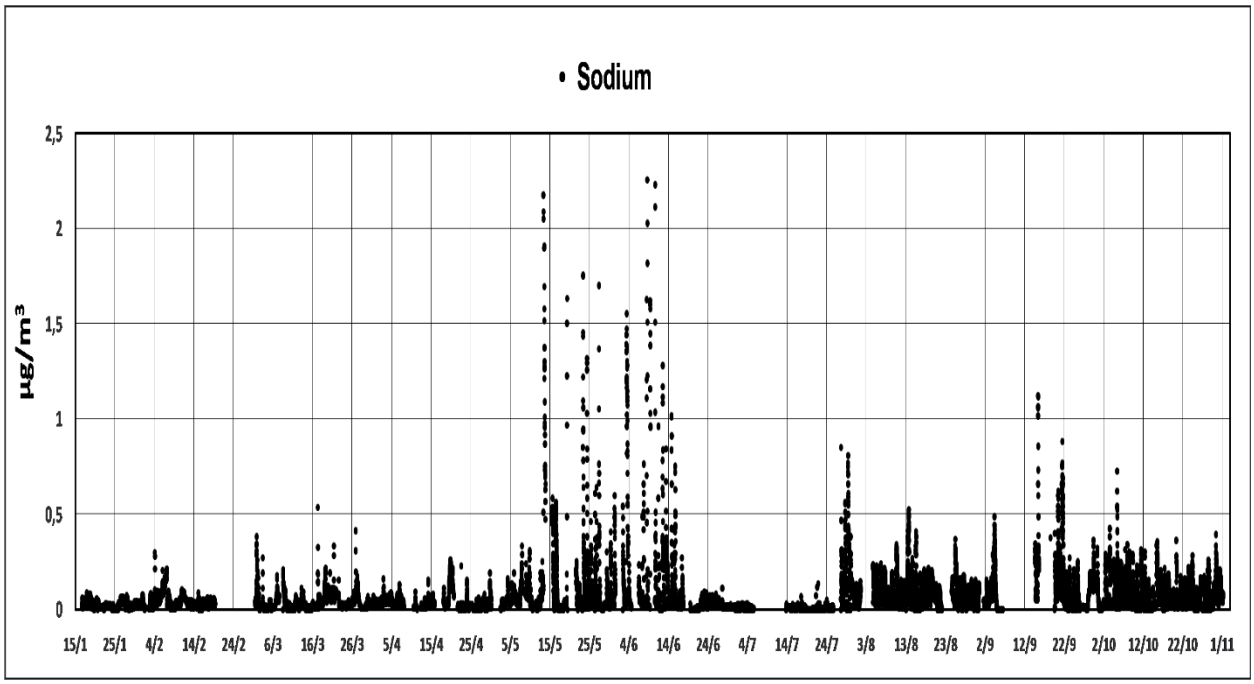

Figure 4.5: The data series of Sodium for the whole sampling period.

The concentration varies from 0 to 2.26 μg/m^3 with an average of 0.06 ± 0.12 μg / m^3.

The current results are comparable to those presented in the reported bibliography. In a two year research at Finolakia station, a remote area in Crete, the average concentration was 0.050±0.102 μg/m^3 (Koulouri et al., 2008) [275]. Also, in the research of Theodosi et al. (2011) the annual average concentration was approximately:

-0.8 μg/m^3 at the station of Goudi (in the GAA).

-0.7 μg/m^3 at Lykovrissi (a suburb of Athens).

-0.1 μg/m^3 at Finokalia station [276] (Table 4.1).

The values were derived from a chart at the paper of Theodosi et. al., 2017 that is why they are not precise.

Table 4.1: Comparison of our results with other studies in the greater area.

Results from our research					Other researches in the greater area		
Cation	**Average ($\mu g/m^3$)**	**Standard Deviation ($\mu g/m^3$)**	**Minimum ($\mu g/m^3$)**	**Maximum ($\mu g/m^3$)**	**Average ($\mu g/m^3$) (1)**	**Average ($\mu g/m^3$) (2)**	**Average ($\mu g/m^3$) (3)**
Na^{+2}	0.06	0.12	0	2.26	0.050± 0.102	0.8 (urban area) 0.7 (suburban area) 0.1 (remote station)	-
NH_4^+	1.88	1.12	0	7.74	1.45±0.73	0.9 (urban area) 0.9 (suburban area) 1.4 (remote station)	1.29 (urban area-GAA) 1.15 (Aegina) **For the same months of 2017 (our research): 2.13±1.26**
K^+	0.19	0.20	0	2.44	0.12±0.09	0.8 (urban area) 0.6 (suburban area) 0.2 (remote station)	0.34 (GAA) 0.47 (Aegina) **For the same months of 2017 (our research): 1.19± 0.21**
Mg^{+2}	0.01	0.02	0	0.20	0.005±0.017	0.5 (urban area) 0.5 (suburban area) 0.3 (remote station)	0.05 (GAA) 0.06 (Aegina) **For the same months of 2017 (our research): 0.004±0.012**

Ca^{+2}	0.16	0.25	0	2.79	0.074±0.220	0.4 (urban area) 0.3 (suburban area) 0.3 (remote station)	0.70 (GAA) 0.74 (Aegina) **For the same months of 2017 (our research): 0.107±0.177**

(1) Koulouri et al., 2008 [275].
(2) Theodosi et al., 2011 [276].
(3) Pateraki et al., 2012 [248]. (Time period of the research: 29th February until 2nd May and from 4th June until 5th August 2008.

4.1.2 Data Series of Ammonium

For the whole sampling period the NH_4^+ concentration varies from 0 to 7.74 μg/m^3 with an average of 1.88 ± 1.12 μg / m^3 (Figure 4.2). These results are comparable to others of the current bibliography. From Koulouri et al., (2008) the average concentration of NH_4^+ was 1.45 ± 0.73 μg / m^3 [275]. Additionally, the average concentration in GAA from 29th February until 2nd May and from 4th June until 5th August 2008 was 1.29 μg/m^3 in GAA and 1.15 μg / m^3 in Aegina station (an island very close to GAA) (Pateraki et al., 2012)[248]. For the same months of 2017, our research indicated an average of 2.13 ± 1.26 μg / m^3. Also, in the research of Theodosi et al. (2011) the annual average concentration was approximately:

-0.9 μg/m^3 at Goudi.

-0.9 μg/m^3 at Lykovrissi.

-1.4 μg/m^3 at Finokalia station [276] (Table 4.1).

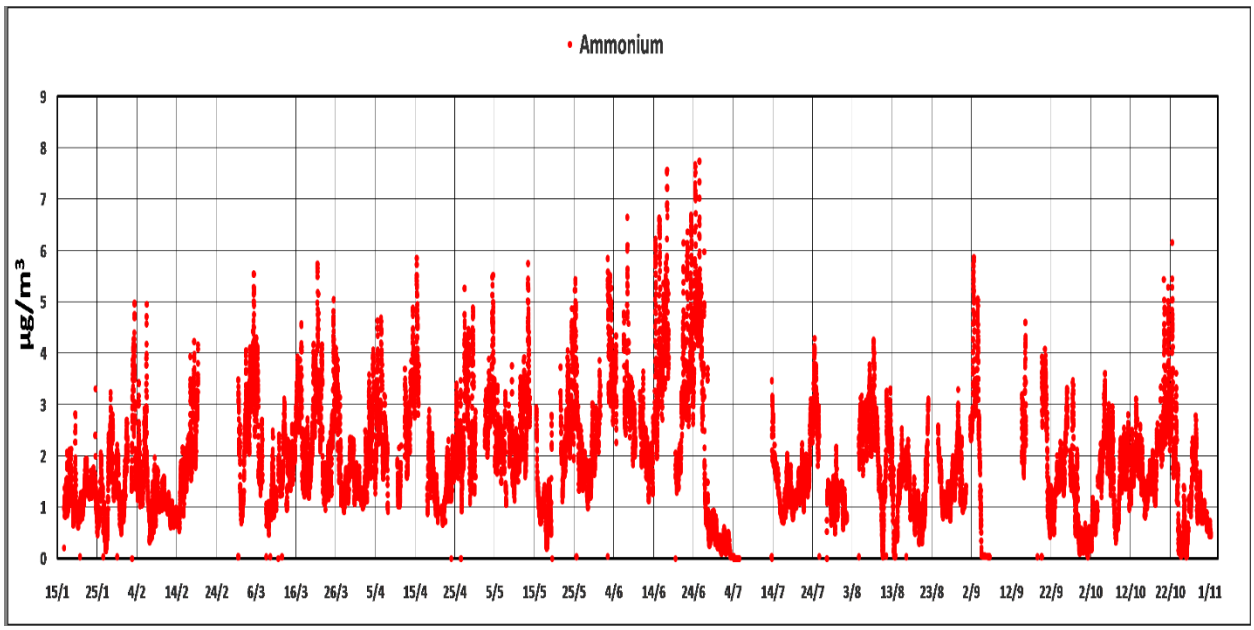

Figure 4.6: The data series of Ammonium for the whole sampling period.

It is shown that the lowest concentrations are presented during winter and they do not exceed the value of 5 µg / m^3.

4.1.3 Data Series of Potassium

In Figure 4.3 that presents the concentrations of potassium for the whole sampling period, it is observed that the potassium has a different variability compared to sodium and ammonium.

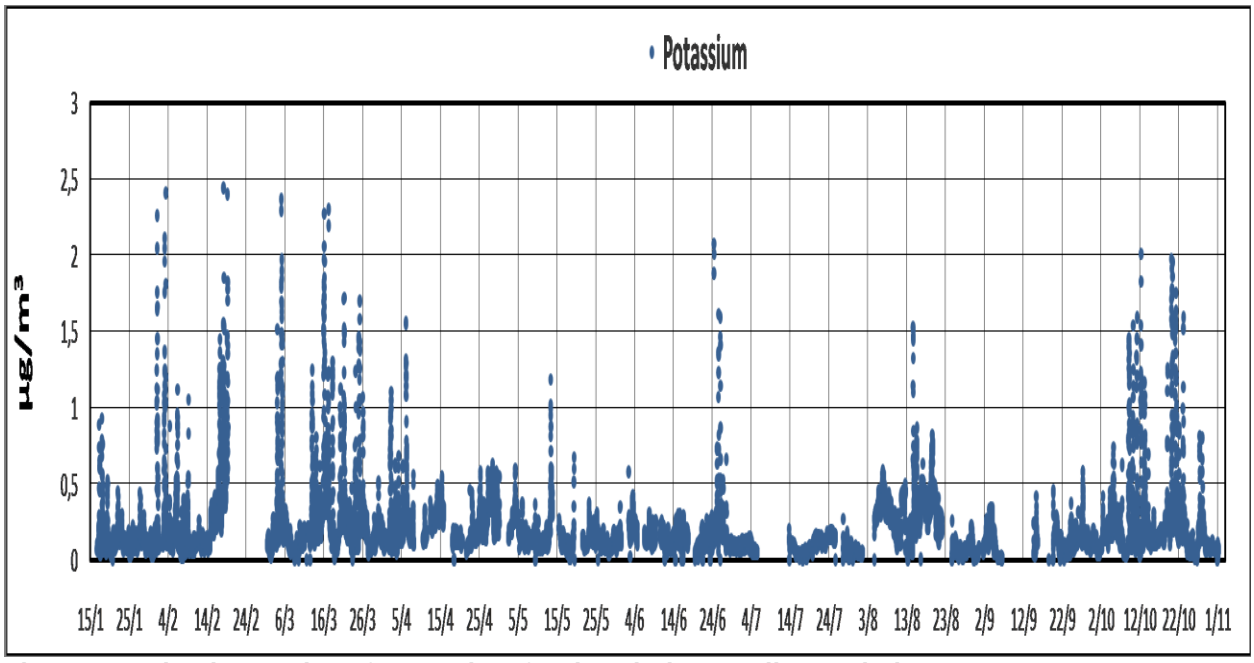

Figure 4.7: The data series of Potassium for the whole sampling period.

For the whole sampling period the K^+ concentration varies from 0 to 2.44 μg/m^3 with an average of 0.19± 0.20 μg/m^3. Again, from Koulouri et al., (2008) the average rate was 0.12 ± 0.09 μg/m^3 [275].

For the time period mentioned at Pateraki et. al., (2012), the average concentrations were 0.34 in GAA and 0.47 μg/m^3 at Aegina. For the same months of 2017, our research indicated an average of 1.19 ± 0.21 μg /m^3 [248] (Table 4.1).

Moreover, in the research of Theodosi et al., (2017) the annual average concentration was approximately:

-0.8 μg/m^3 at Goudi.

-0.6 μg/m^3 at Lykovrissi.

-0.2 μg/m^3 at Finokalia station [276] (Table 4.1).

From the Figure 4.3 the concentration variability of winter is the same, as the one presented by Fourtziou et al., (2017) [253].

4.1.4 Data Series of Magnesium

For magnesium the concentrations vary from 0 to 0.20 μg/m^3 and the average concentration is 0.01±0.02 μg / m^3 (Figure 4.4).

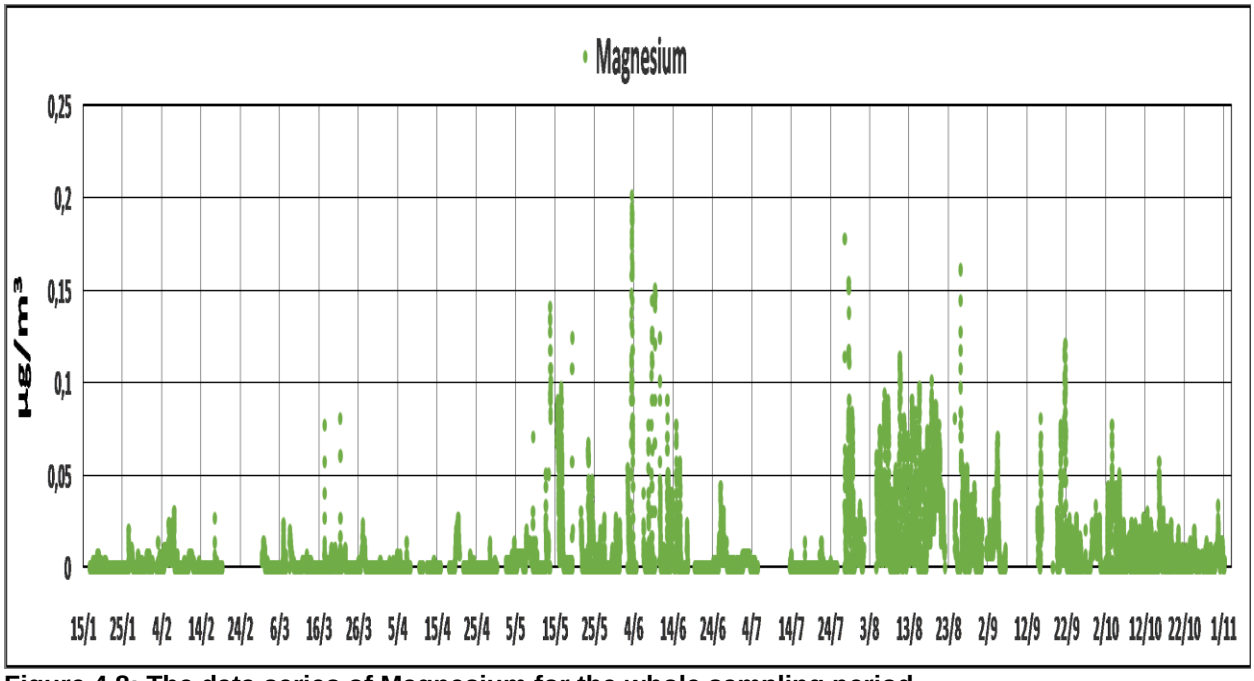

Figure 4.8: The data series of Magnesium for the whole sampling period.

Comparing these results to other researches, Koulouri et. al. ,(2008), indicated an average of 0.005±0.017 μg/m^3 [275].

For the time period mentioned at Pateraki et. al. (2012), the average concentrations were 0.05 in GAA and 0.06 μg/m^3 at Aegina [248]. For the same months of 2017, our research indicates an average of 0.004 ± 0.012 μg /m^3 (Table 4.1).

Additionally, in the research of Theodosi et al., (2011), the annual average concentration was approximately:

-0.5 μg/m^3 at Goudi.

-0.5 μg/m^3 at Lykovrissi.

-0.3 μg/m^3 at Finokalia station [276] (Table 4.1).

From Figure 4.4 it appears that magnesium indicates the lowest concentrations of all measured cations in this research. The profile from 15/1 until 19/2 is the same as the one presented by Fourtziou et al., (2017), with the same peaks around 25/1 and 4/2 [253].

4.1.5 Data Series of Calcium

In the following Figure 4.5 the trend of calcium concentrations is presented for the whole sampling period. The values range from 0 to 2.79 μg / m^3 and the average concentration is 0.16 ± 0.25 μg / m^3.

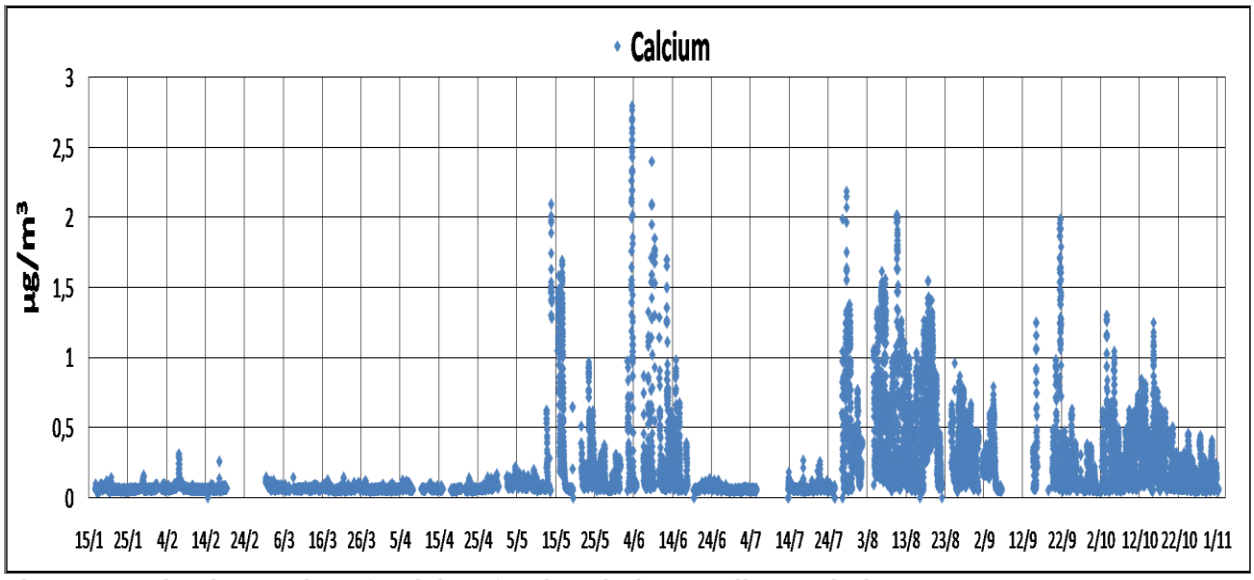

Figure 4.9: The data series of Calcium for the whole sampling period.

The result from the investigation of Koulouri et. al., (2008), indicates an average of 0.074 ± 0.220 μg / m^3 [275].

For the time period mentioned at Pateraki et. al., (2012), the average concentrations were 0.70 μg/m^3 in GAA and 0.74 μg/m^3 at Aegina [248]. For the same months of 2017, our research indicates an average of 0.107±0.177 μg/m^3 (Table 4.1).

Moreover, in the research of Theodosi et al., (2011), the annual average concentration was approximately:

-0.4 μg/m^3 at Goudi.

-0.3 μg/m^3 at Lykovrissi.

-0.3 μg/m^3 at Finokalia station [276] (Table 4.1).

The variation of the specific cation is the same as the one described for magnesium in the previous part of the current research. For the period 15/1 until 19/2 the variation of the trend is the same as the one described by Fourtziou et. al., (2017), with the peaks appearing at the same dates [253].

4.1.6 Data Series of Black Carbon

For Black Carbon the measurements are held on an hourly basis and for the whole sampling period are presented in the next Figure 4.6. The concentration varies from 0,09 to 16.26 μg / m^3 and the average value is 1.69±1.71 μg / m^3. The data appear to have wide dispersion, because the standard deviation is higher than the average value.

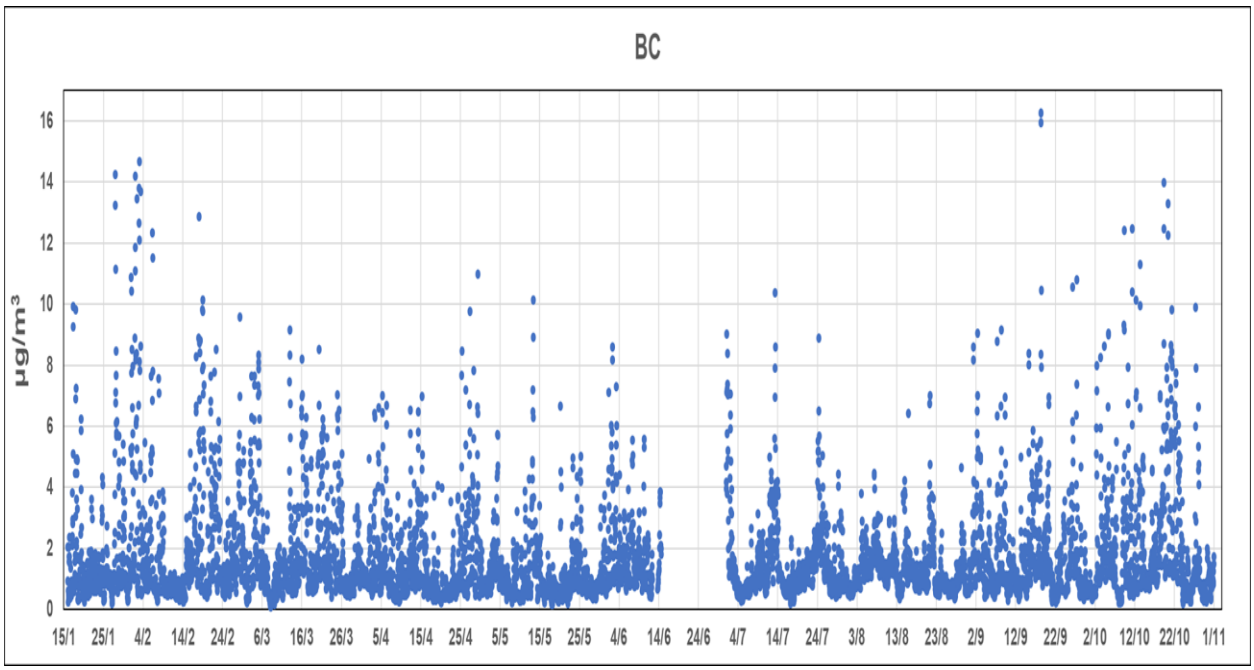

Figure 4.10: The hourly measurements of Black Carbon for the whole sampling period.

From the Figure 4.6 and the Figure 4.5 of the variation of potassium (chapter 4.1.3) is indicated that approximately, the two variations are the same. During the winter months there is an increase compared to the spring. Also, during the summer months there is a small increase compared to spring months and then from the end of the summer until the end of the sampling period the concentration gradually increases.

4.2 Correlations Between the Studied Chemical Substances during the Whole Sampling Period

In the following Table 4.2 the statistical analysis of the correlation of the measured chemical substances is presented for the whole sampling period.

Table 4.2: Statistical analysis of the correlations which can provide information for the sources of PM_1.

Statistical analysis ↓	Correlations during the whole sampling period					
	Correlations that indicate crustal sources			Correlations that indicate marine sources		Correlation that indicates combustion sources
	Mg^{+2} - Ca^{+2}	Mg^{+2} - K^{+}	Ca^{+2} - K^{+}	Mg^{+2} - Na^{+}	Ca^{+2} - Na^{+}	K^{+} - BC
R^2	0,88	0,01	0,01	0,51	0,40	0,35
R	0,08	0,02	0,20	0,08	0,09	1,35
P	0	6,83E-27	3,6E-30	0	2,68E-56	1,10E-136
n	21.349	21.352	21.447	21.353	21.446	4.995

In the Table 4.2 (R^2) stands for the correlation coefficient, (R) for the standard deviation, (P) for the probability value and (n) for the number of samples. It is indicated that all the correlations are statistically significant as P<0,001.

The correlation of K^+ with BC has the lower number of samples (n) compared to the other correlations because the measurements of BC are held on an hourly basis.

The correlation with the highest coefficient is the one of Mg^{+2} with Ca^{+2} (R^2=0,88). This correlation nominates the influence of crustal sources at the fine particles' chemical composition (Figure 4.7).

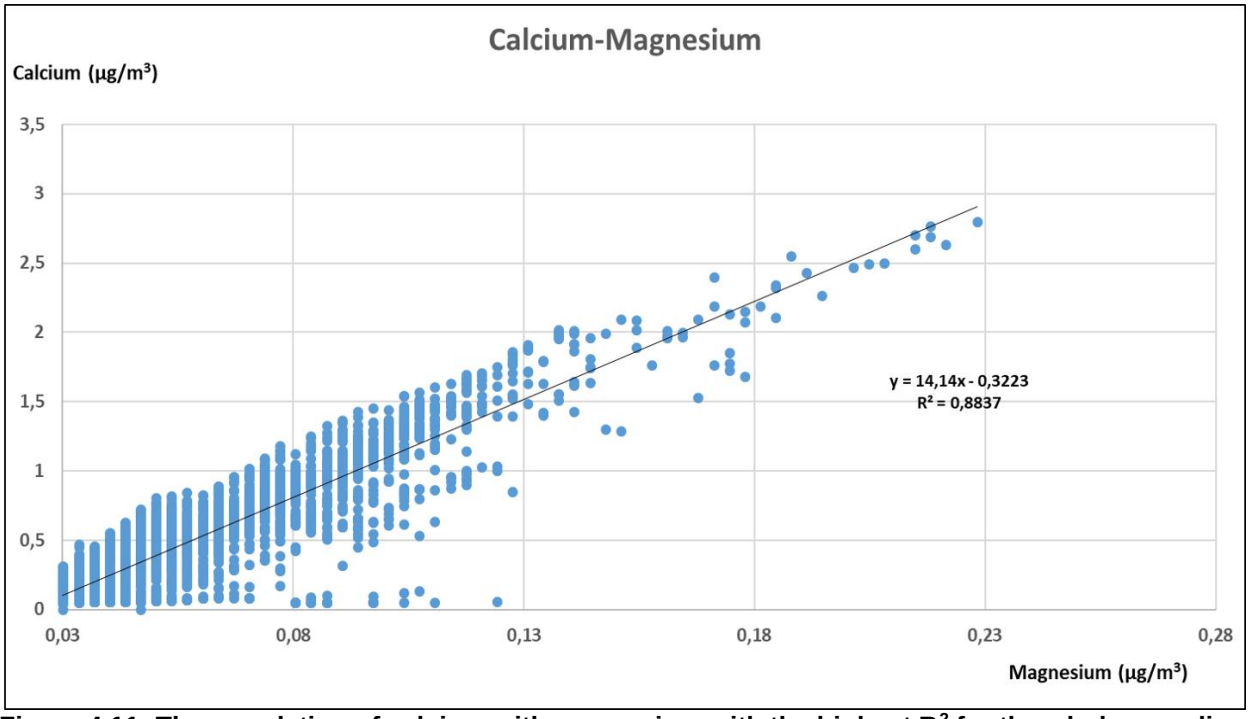

Figure 4.11: The correlation of calcium with magnesium with the highest R^2 for the whole sampling period.

Also, the effect of marine sources is displayed through the correlations of Mg^{+2} with Na^+ and of Ca^{+2} with Na^+ which are the main components of sea salt. From the Table 4.2 is indicated that the correlation of Mg^{+2} with Na^+ has the second highest R^2=0,51 among all the correlations and that of Ca^{+2} with Na^+ has a correlation coefficient of R^2=0,40.

The impact of the combustion sources is displayed through the correlation of K^+ with BC with R^2=0,35 but the standard deviation is the highest of all the researched correlations (R=1,35).

4.3 Diurnal Variation of the Studied Chemical Substances during the Whole Sampling Period

4.3.1 Diurnal variation of Sodium

In the following Figure 4.8 the diurnal variation of Sodium for the whole sampling period is presented. It has to be indicated that for all the diurnal variations the median values are used.

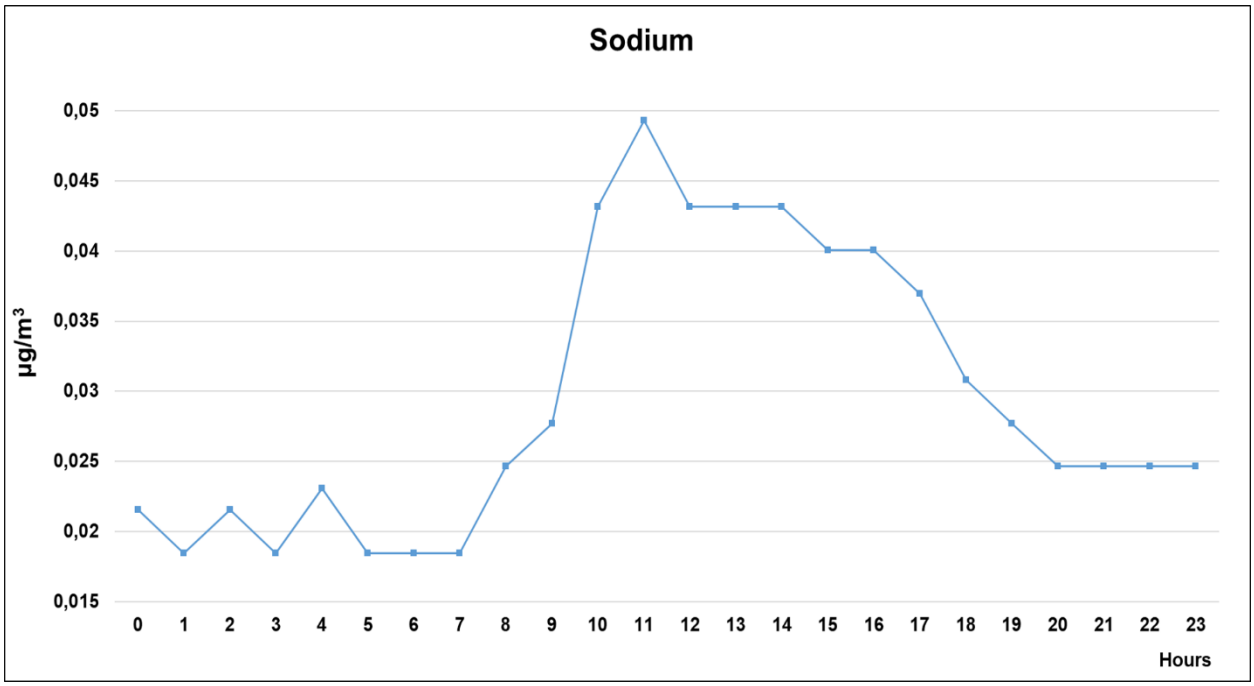

Figure 4.12: Diurnal variation of Sodium for the whole sampling period

During the early morning hours (0:00-07:00) the concentration is relatively stable. Then there is a significant increase from 07:00 until 11:00 and the concentration gradually decreases from 11:00 until 20:00. Finally, from 20:00 until 23:00 the concentration is stable. The increase from 07:00 until 11:00 is probably attributed to sea breezes and/or crustal sources. In order to deduce more accurate results, it has to be further investigated with meteorological conditions.

4.3.2 Diurnal variation of Ammonium

In the next Figure 4.9 the diurnal variation of Ammonium is displayed.

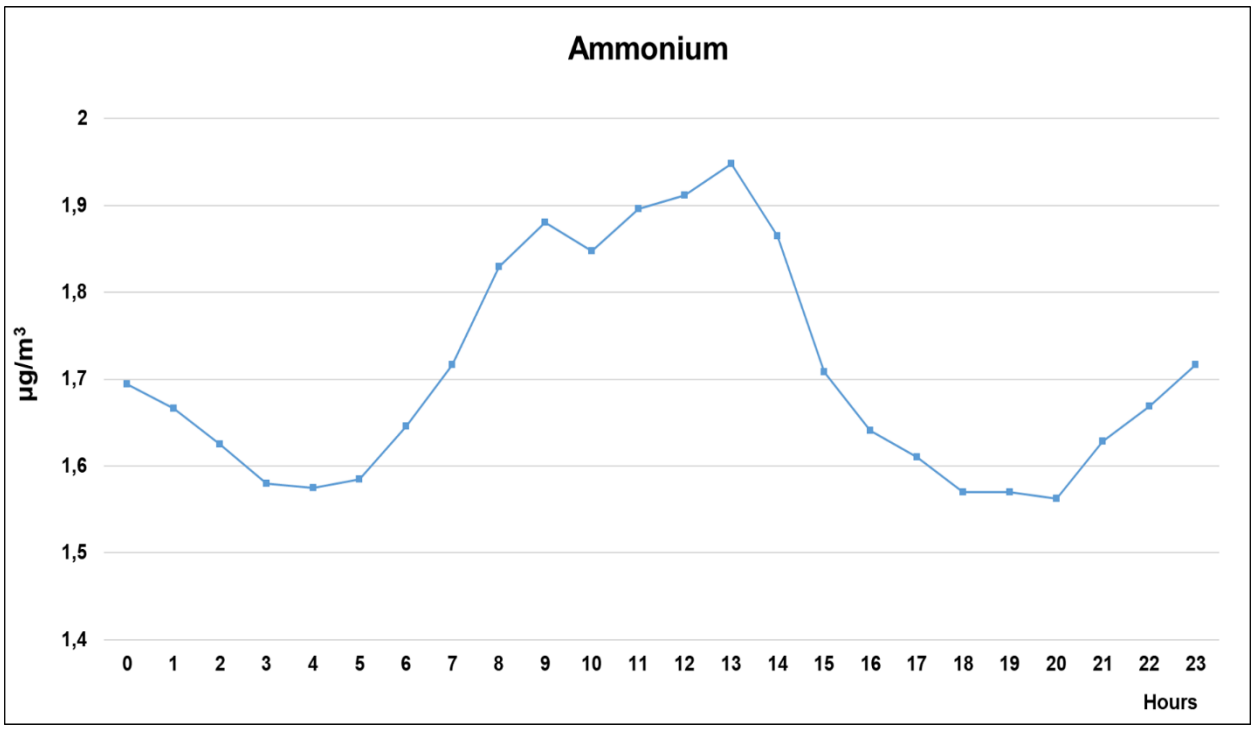

Figure 4.13: Diurnal variation of Ammonium for the whole sampling period

The concentration indicates higher values during day hours due to ammonium's secondary photochemical behavior. The high ammonium concentration during these hours which indicate higher temperature, is likely to exist because ammonium nitrate is semi-volatile and so it is difficult to condensate [219-222,273,274,277] (reaction 2).

$$NH_{3\,(g)} + HNO_{3\,(g)} \longleftrightarrow NH_4NO_{3\,(s)} \quad (1)$$

$$NH_4NO_{3\,(s)} \longrightarrow NH_4^+{}_{(aq)} + NO_3^-{}_{(aq)} \quad (2)$$

$$NH_3 + H_2SO_4 \longrightarrow NH_4HSO_4 + NH_3 \longrightarrow (NH4)_2SO_4 \longrightarrow 2\,NH_4^+ + SO_4^{-2} \quad (3)_{\,221,222}$$

The concentration increases from 20:00 until 00:00. In order to explain this increase it has to be considered that the reactions (1) and (2) take place at low temperatures and at Relative Humidity (RH) above the deliquescence. As the temperature falls and the humidity rises the dissociation constant (K) of the reaction (2) increases. As $K = [NH_4^+][NO_3^-] / [NH_4NO_3]$, then if it decreases then probably the $[NH_4^+]$ increases [221,222]. Also, probably due to thermal and/or meteorological inversions NH_4NO_3 stays at low altitudes. So with higher concentrations of NH_4NO_3 near the ground it is possible to dissociate at NH_4^+ and NO_3^-. Also, NH_4^+ is probably produced from the dissociation of $(NH4)_2SO_4$

(reaction 3). For better understanding and explanation of the diurnal variation of ammonium, meteorological conditions and the concentrations of NO_3^- and SO_4^{-2} have to be considered.

4.3.3 Diurnal variation of Potassium

As for Potassium's diurnal variation (Figure 4.10) the concentration indicates stability at the following time intervals:

- From 01:00 until 03:00.
- From 09:00 until 16:00.
- From 21:00 until 23:00.

From 01:00 until 03:00 and from 21:00 until 00:00 the high concentrations of potassium can be probably attributed to fossil fuel combustion for heating. Also, from 09:00 until 15:00 the high concentrations can be probably attributed to fossil fuel combustion for transportation and other human activities.

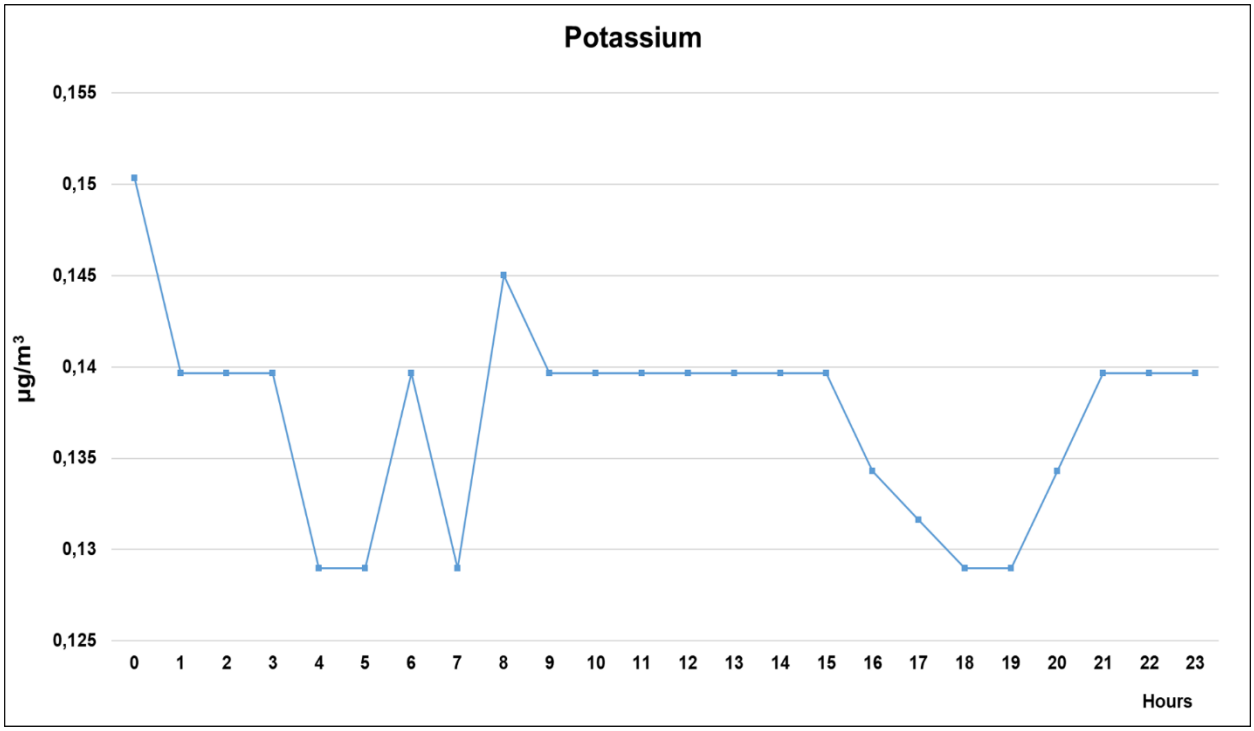

Figure 4.14: Diurnal variation of Potassium for the whole sampling period

A better understanding of potassium's variation during the hours of the day and night and the possible sources, can be derived from the seasonal diurnal variation.
In the following Figure 4.11 the diurnal variation of potassium during the four seasons is presented.

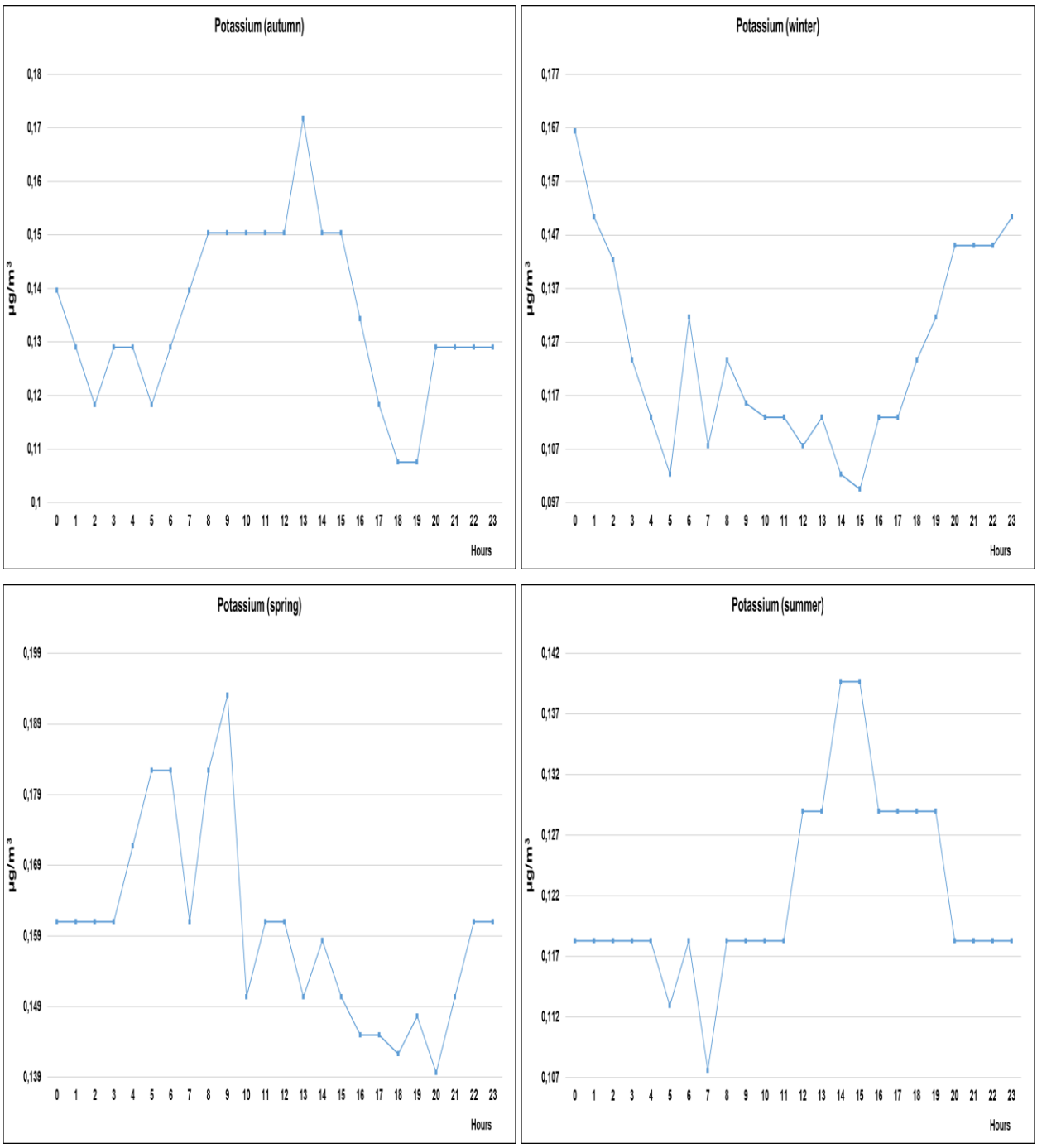

Figure 4.15: Diurnal variation of Potassium for every season

From Figure 4.10 is indicated that during winter there is an increase of potassium's concentration from 15:00 until 00:00. This increase is probably due to combustion of fossil fuel for heating. Also, during autumn there is an increase from 05:00 until 13:00 probably due to heating and traffic. During the same period the increase from 19:00 until 00:00 is attributed probably due to heating. Moreover, during spring there is an increase from 20:00 until 06:00 probably due to a combination of heating and traffic. Finally. during summer an increase is presented from 07:00 until 15:00 probably due to transportation.

4.3.4 Diurnal variation of Magnesium

In the Figure 4.12 the diurnal variation of Magnesium for the whole sampling period is presented.

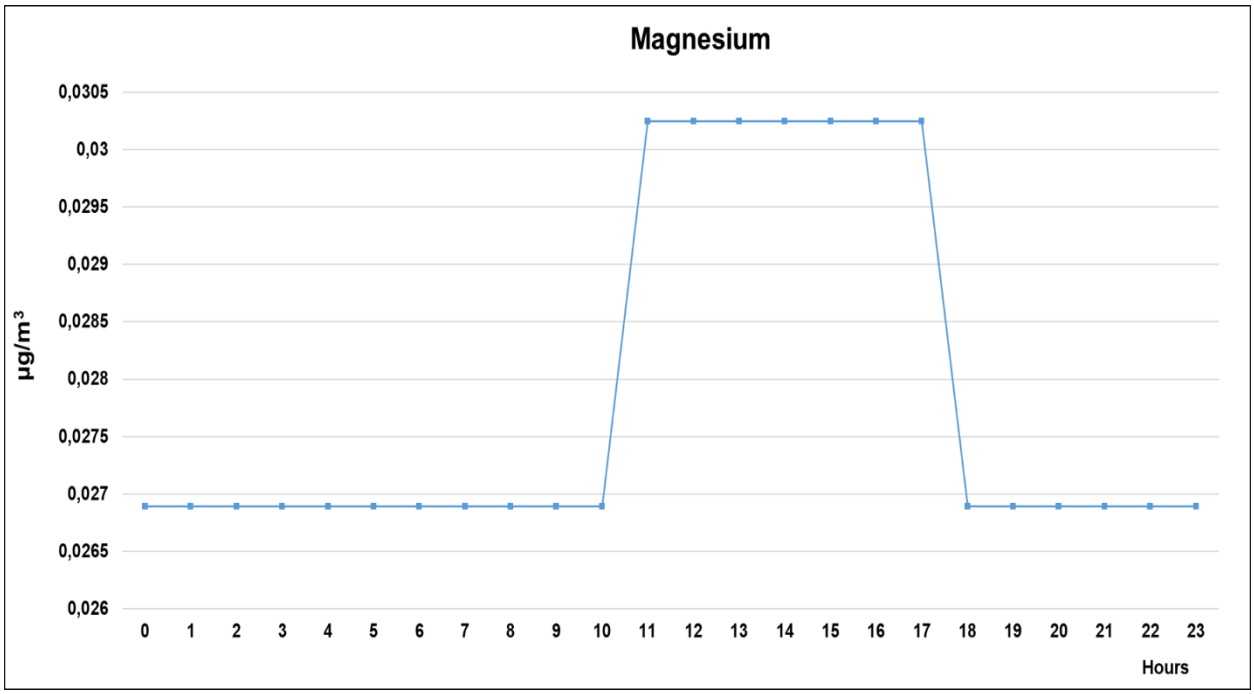

Figure 4.16: Diurnal variation of Magnesium for the whole sampling period

Magnesium indicates the same concentration from 18:00 until 10:00. The increased concentration from 11:00 until 17:00 occurs probably due crustal sources and other human activities that produce dust in the urban area.

4.3.5 Diurnal variation of Calcium

From the next Figure 4.13 is indicated an increase of Calcium's concentration from 07:00 until 12:00. Then the concentration is stable from 12:00 until 14:00 and it increases again from 14:00 until 15:00. At 15:00 calcium displays the highest concentration. The increase of calcium's concentration is probably due to urban produced dust from constructions[213,214].

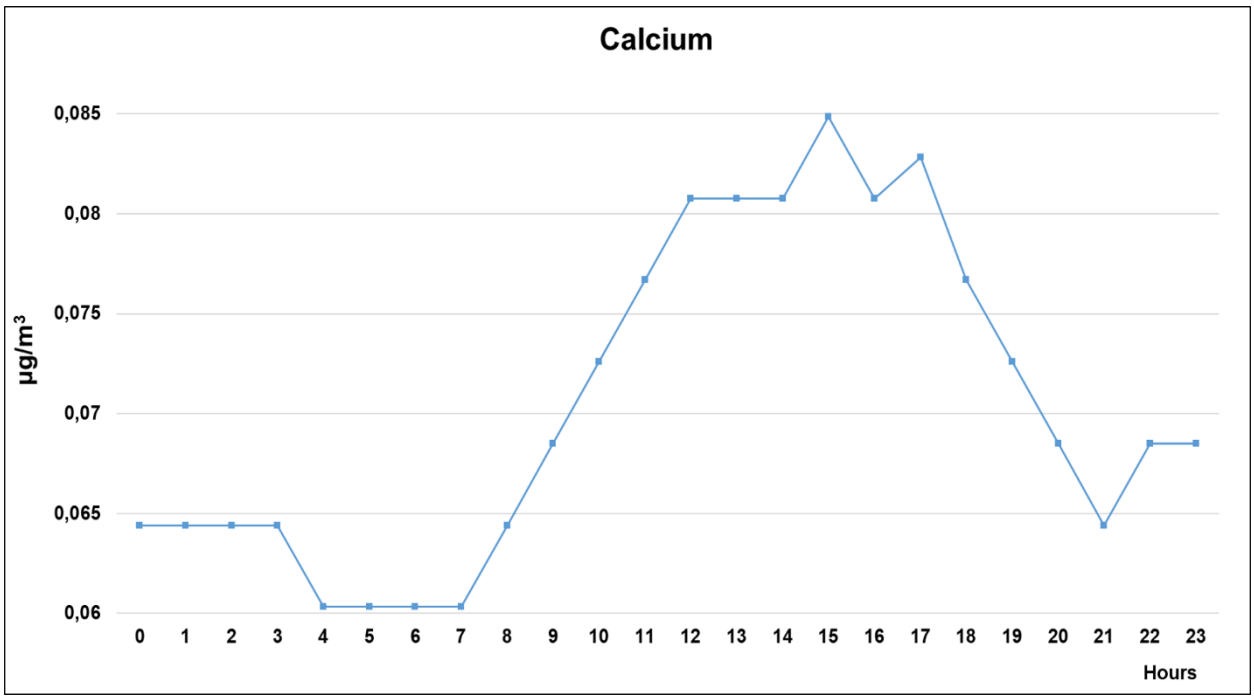

Figure 4.17: Diurnal variation of Calcium for the whole sampling period

4.3.6 Diurnal variation of Black Carbon

In the following Figure 4.14 the diurnal variation of Black Carbon for the whole sampling period is displayed.

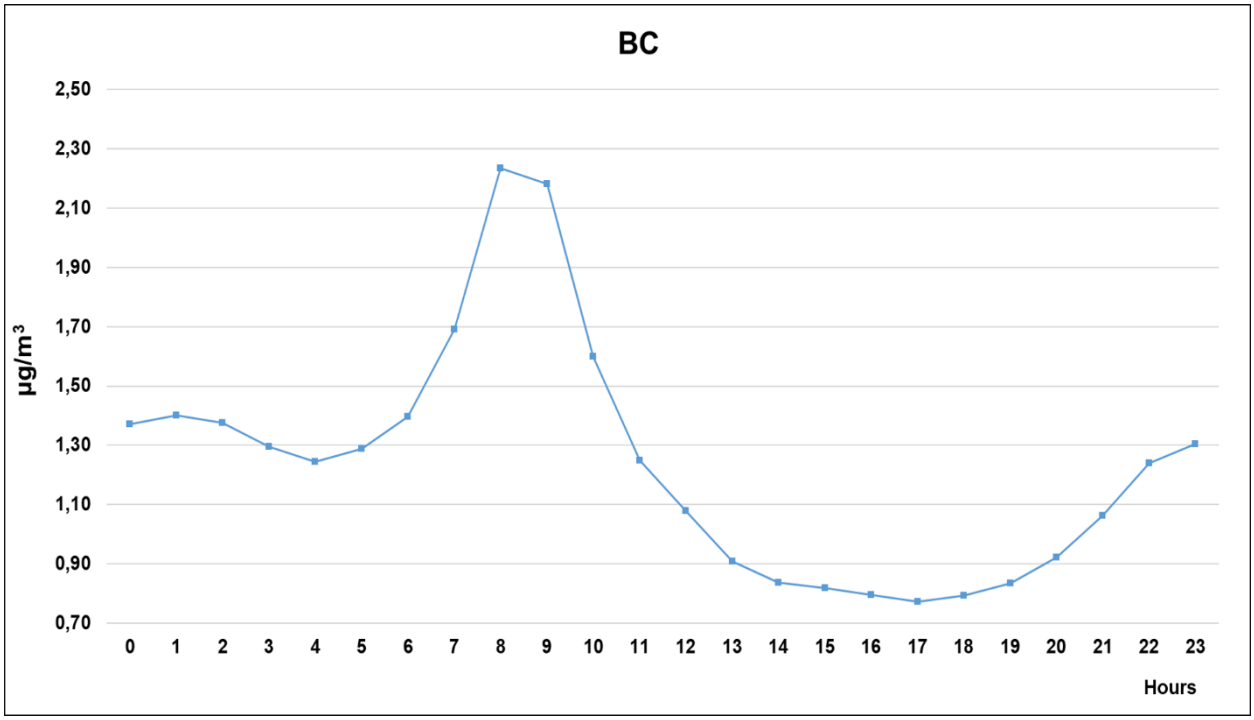

Figure 4.18: Diurnal variation of Black Carbon for the whole sampling period

An increase of Black Carbon's concentration from 17:00 until 01:00 is indicated. Also, potassium indicates an increase from 19:00 until 00:00 (Figure 4.10). This increase during these hours for these two ''tracers'' can be attributed to fossil fuel combustion for heating.

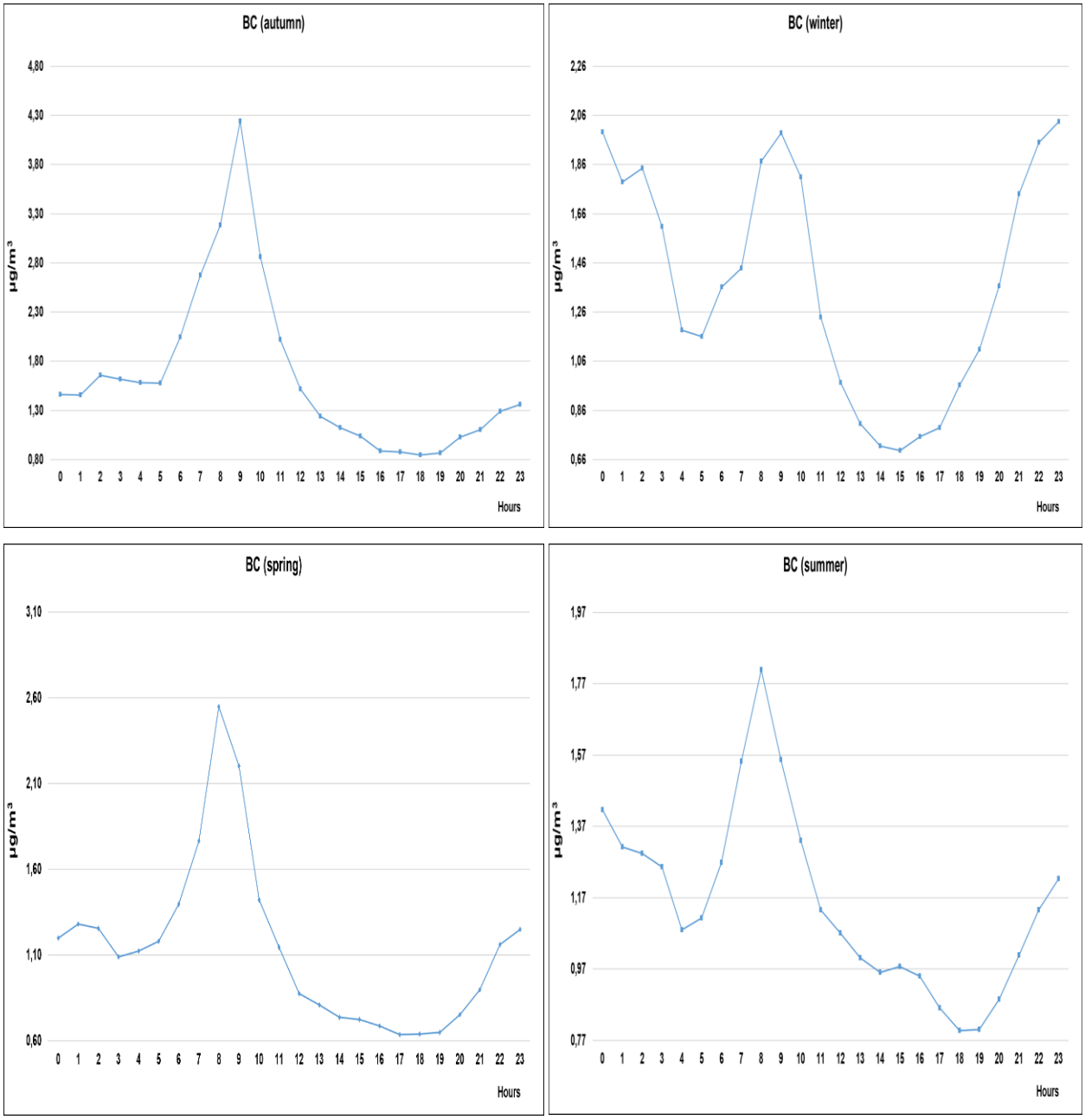

Figure 4.19: Diurnal variation of Black Carbon for every season

Also, from the Figure 4.15 during autumn is indicated an increase of Black Carbon's concentration from 05:00 until 09:00 probably due to heating and traffic. During the same season an increase is presented from 19:00 until 00:00 probably due to heating and during the same hours an increase is presented for potassium too (Figure 4.11). During winter there is an increase from 15:00 until 00:00 probably due to heating and a simultaneous increase of potassium is indicated too (Figure 4.10). Furthermore, during

spring an increase is displayed from 19:00 until 08:00 probably due to traffic and heating and an increase is presented approximately during the same hours for potassium too (Figure 4.10). Finally, during summer there is an increase from 18:00 until 00:00 and from 05:00 until 08:00 probably due to traffic.

4.4 Monthly Variation

4.4.1 Monthly variation of Sodium

The Figure 4.16 shows the monthly variation of sodium's concentration. The highest average value appears during May. Also, a high value is indicated during September.These high values are probably due to the sea breezes that prevail during these months [266, 270].

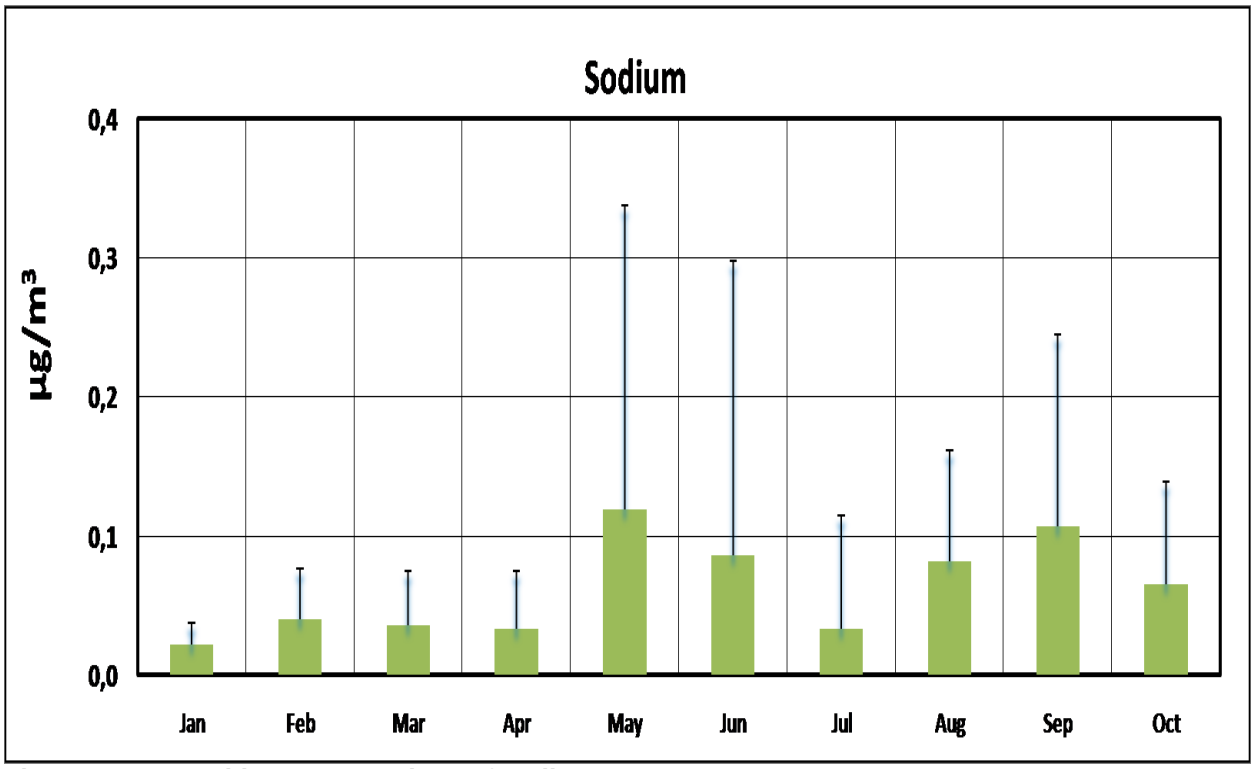

Figure 4.20: Monthly average values of sodium

4.4.2 Monthly variation of Ammonium

The next Figure 4.17 presents the average monthly values of ammonium. It appears that the higher concentrations are observed during summer and spring and can be attributed to intense photochemistry [219, 220, 273, 274, 277]. The low values during July need to be further investigated with meteorological conditions, as well.

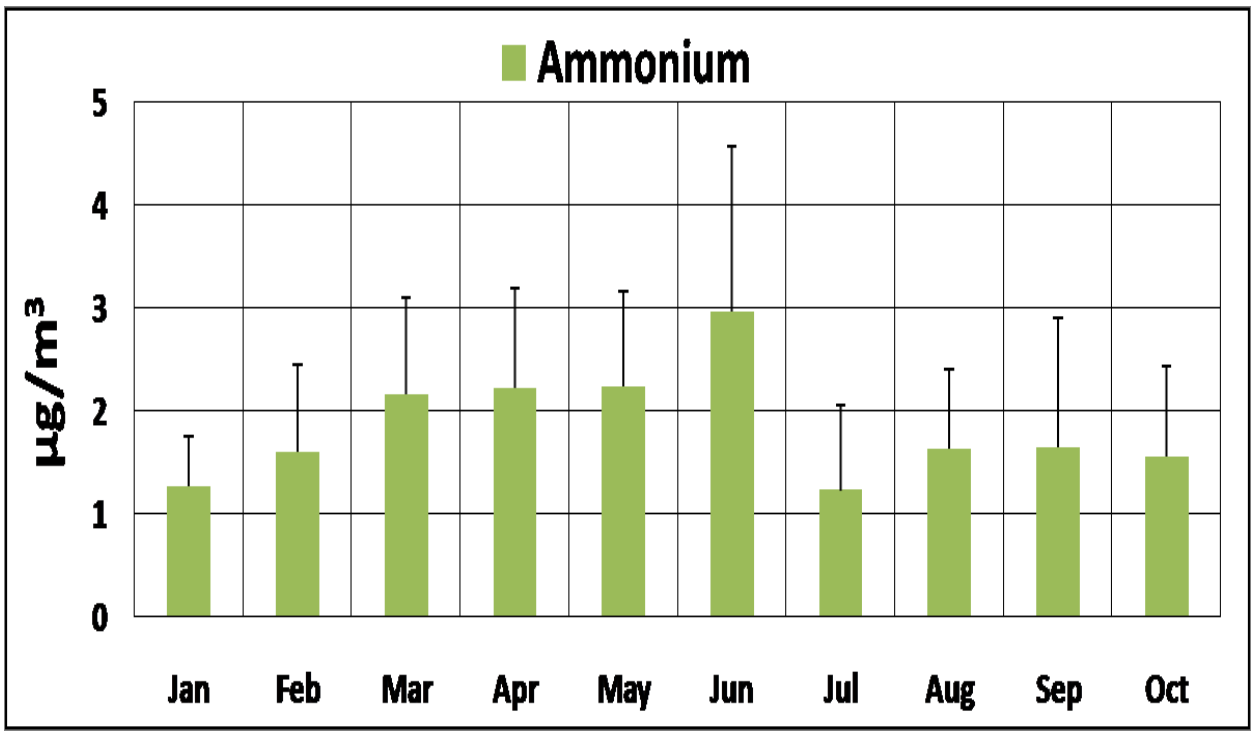

Figure 4.21: Monthly average values of ammonium

The monthly variation of ammonium is in agreement with the variations presented by Sciare et al., (2008) [273] and Koulouri et al., (2008) [275].

4.4.3 Monthly Variation of Potassium

Potassium's average monthly concentrations are displayed in the next Figure 4.18.

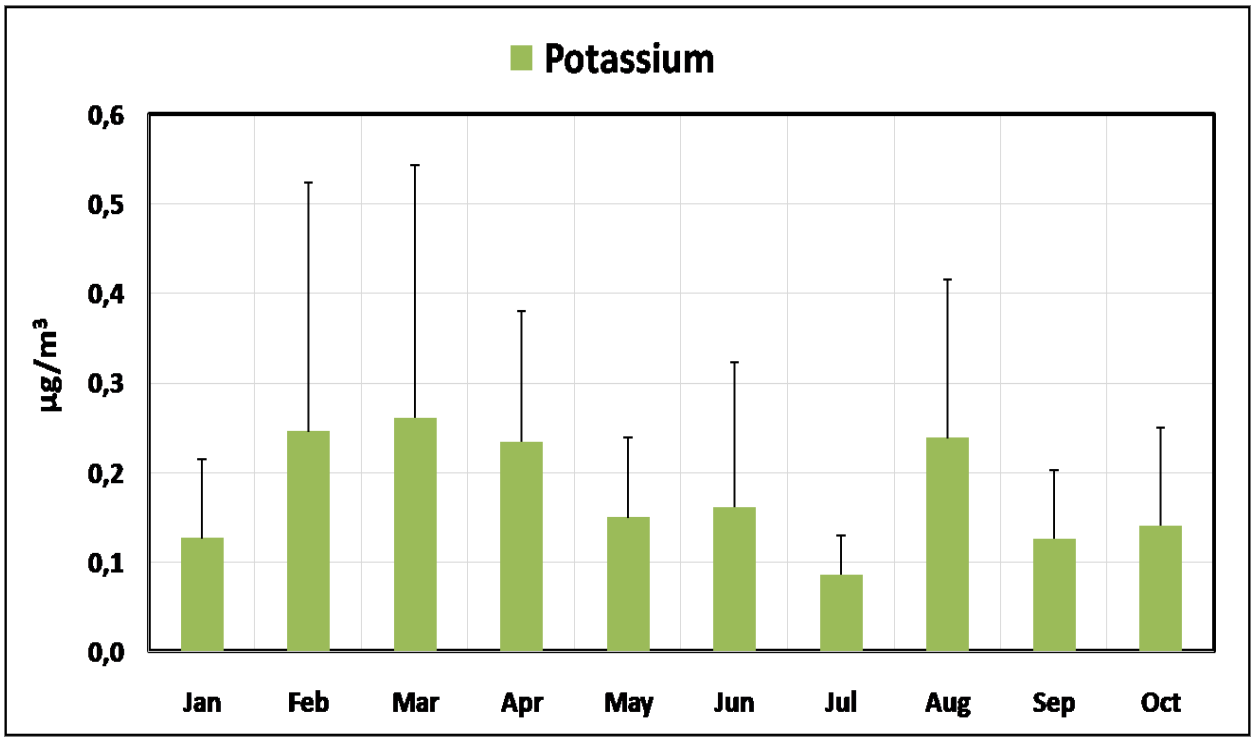

Figure 4.22: Monthly average values of potassium

The variability is the opposite compared to that od sodium and ammonium. Higher values are observed during winter and August, probably due to biomass and fossil fuel combustion [248, 276]. The current monthly variation is similar to that presented by Theodosi et al., (2011) [276].

4.4.4 Monthly Variation of Magnesium

The monthly average values for Mg^{+2} are presented in the following Figure 4.19. The highest value is displayed during August but with the highest standard deviation. The lowest value appears in January and April. The high concentrations during August and September can be attributed to Sahara dust transportation. Moving to the end of the summer the high Mg^{+2} in the atmosphere is probably due to recirculation of the dust and low precipitation [278-282].

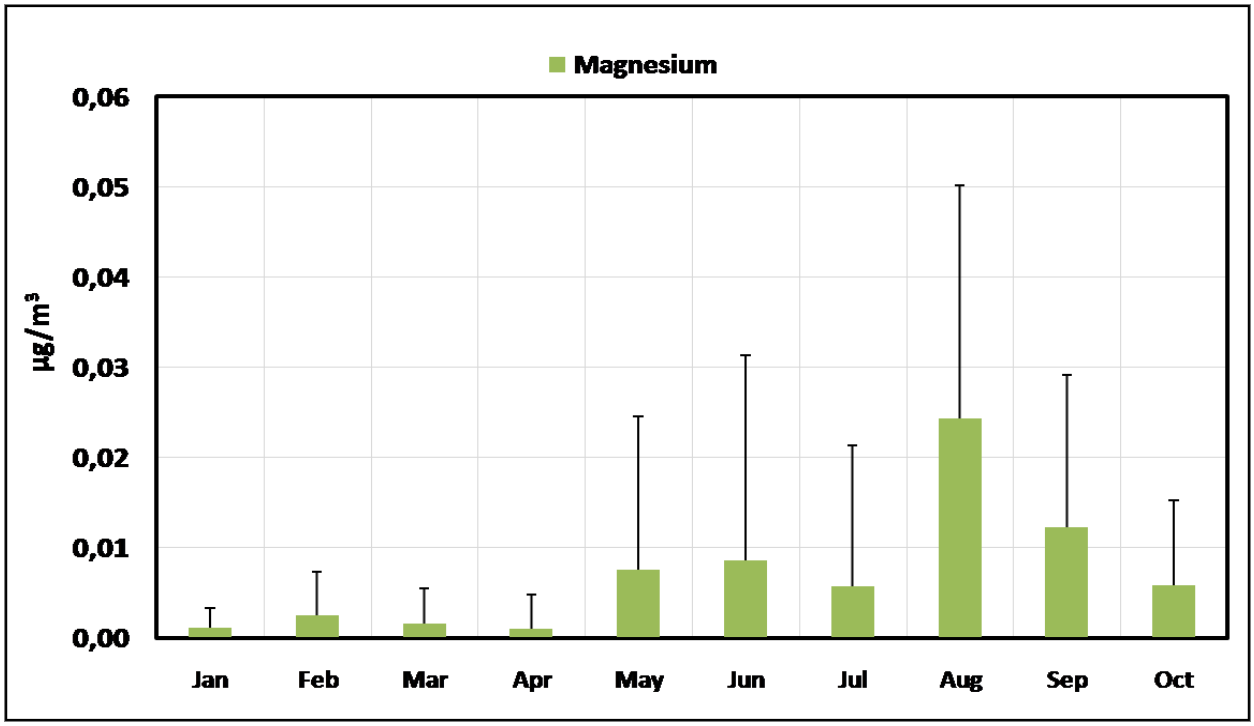

Figure 4.23: Monthly average values of magnesium

4.4.5 Monthly Variation of Calcium

The monthly average values of calcium are presented in the following Figure 4.20.

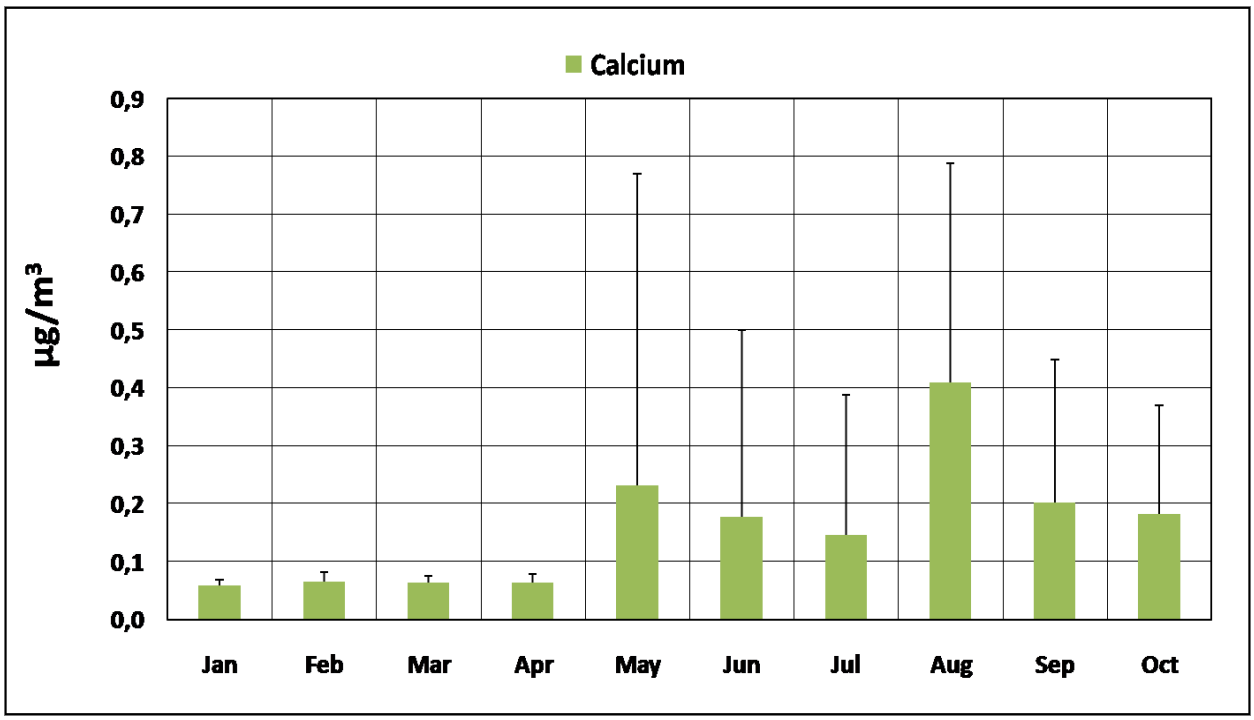

Figure 4.24: Monthly average values of calcium

The monthly variaion of calcium is approximately the same as magnesium's. From January until April the concentrations are stable and the lowest of the whole sampling period. This variability is the same as magnesium's. The stability during the winter period is in relevance with the results of Fourtziou et al., (2017) [253]. The only difference is that in the results of Fourtziou et. al. there were dust events in 21st January and 12th February that increased the concentration of Ca^{+2}. Next, there is a big increase in May (increase of 0,53 μg / m^3), which is the highest for the whole sampling period. Then during June and July the concentration decreases but it doesn't decline to the very low winter values. In August the concentration reaches 0,41 μg/m^3, which is the highest value of the whole sampling period. Finally, the concentration decreases during September and October and it is, approximately, the same as the concentration of June. The high concentrations of calcium during August and May can be attributed to Sahara dust transportation. Moving to the end of summer the concentration of calcium is still high due to recirculation of the dust and low precipitation [278-282].

4.4.6 Monthly Variation of Black Carbon

In the following Figure 4.21 the monthly variation of Black Carbon is displayed.

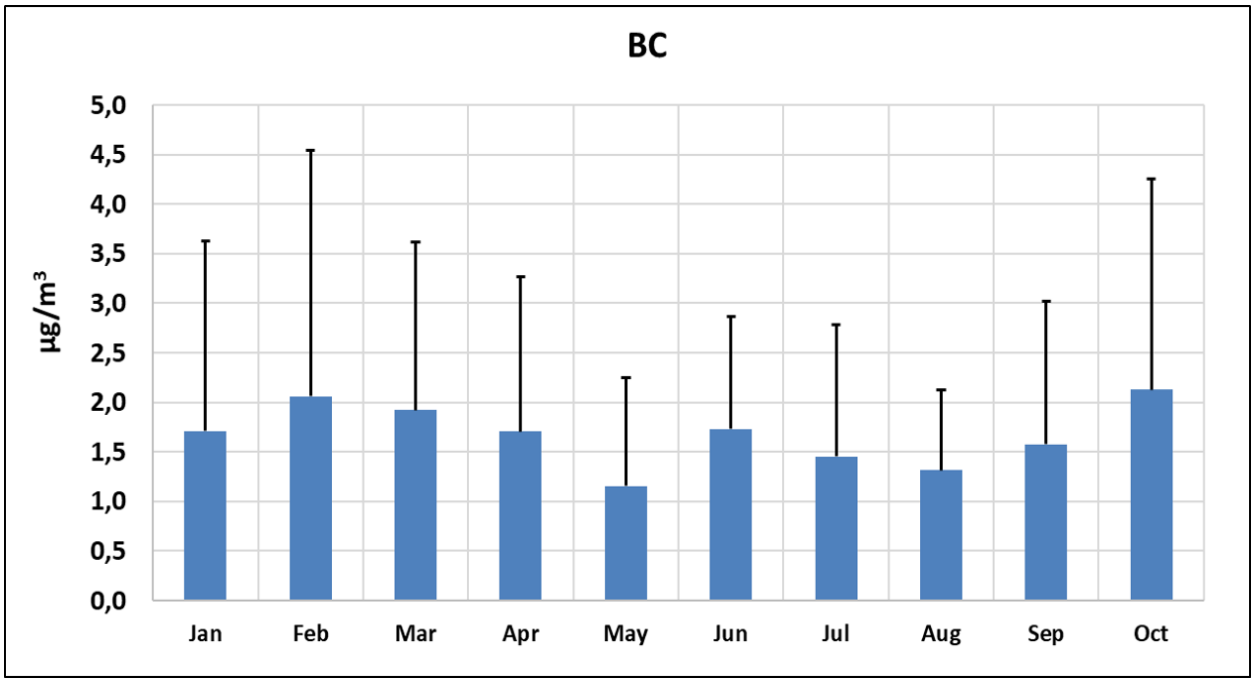

Figure 4.25: Monthly average values of BC

Black carbon indicates approximately the same monthly variability as potassium (Figure 4.18). During the winter and autumn months the average values are higher. This can be attributed to the combustion of fossil fuel for heating. From winter to spring months the concentration decreases as the heating of the buildings gradually decreases. Also, the high values during June and July are indicated probably due to combustion of biomass from fires [223].

4.5 Seasonal Variation

4.5.1 Seasonal Variation of the Cations and Black Carbon

4.5.1.1 Seasonal Variation of Sodium

In the following Figure 4.22 are presented the average concentrations of sodium for every season.

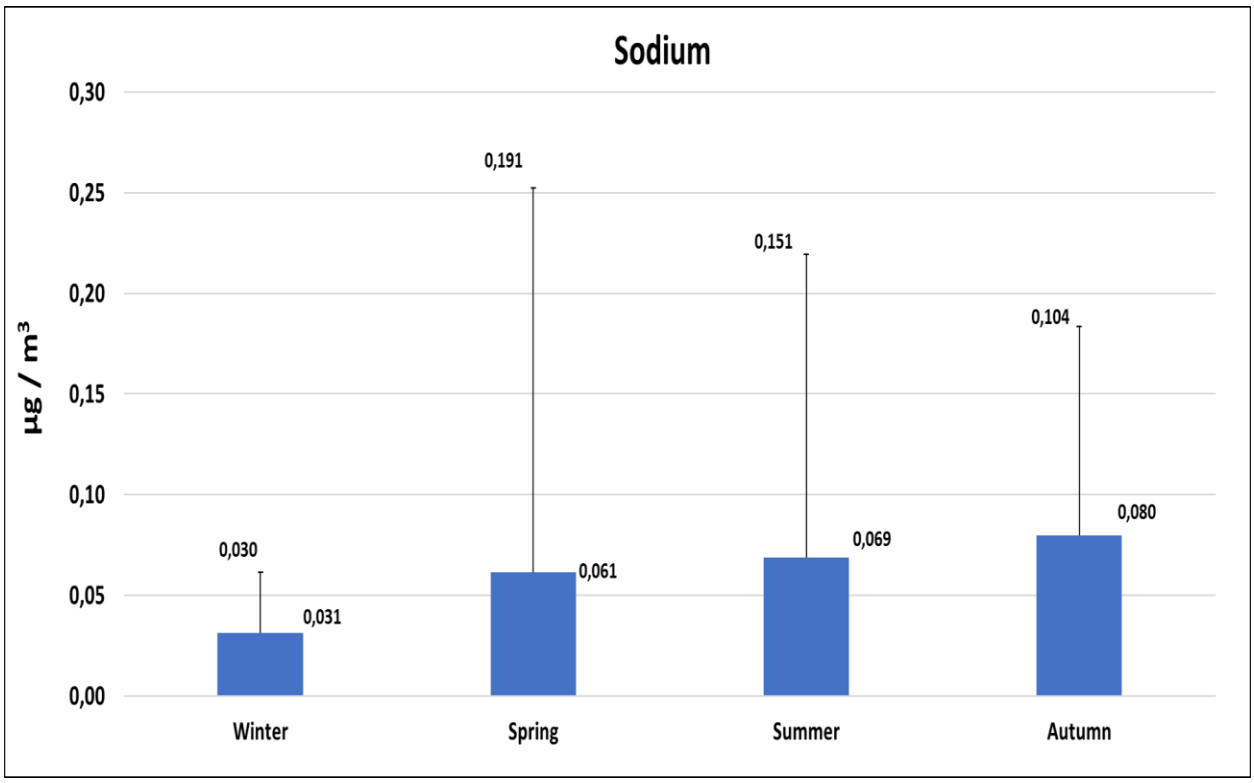

Figure 4.26: Average seasonal concentrations of sodium

The higher concentration is indicated during autumn and the lowest during winter. The concentration is gradually increasing from winter to autumn. This increase can probably be attributed to winds mainly originated from sea [266, 270]. Also, it has to be indicated that the standard deviation is high in all seasons compared to the average value. This means that the data appear to have wide dispersion.

4.5.1.2 Seasonal Variation of Ammonium

In the following Figure 4.23 of the average concentrations of ammonium, is indicated that the highest concentrations are indicated during spring and summer.

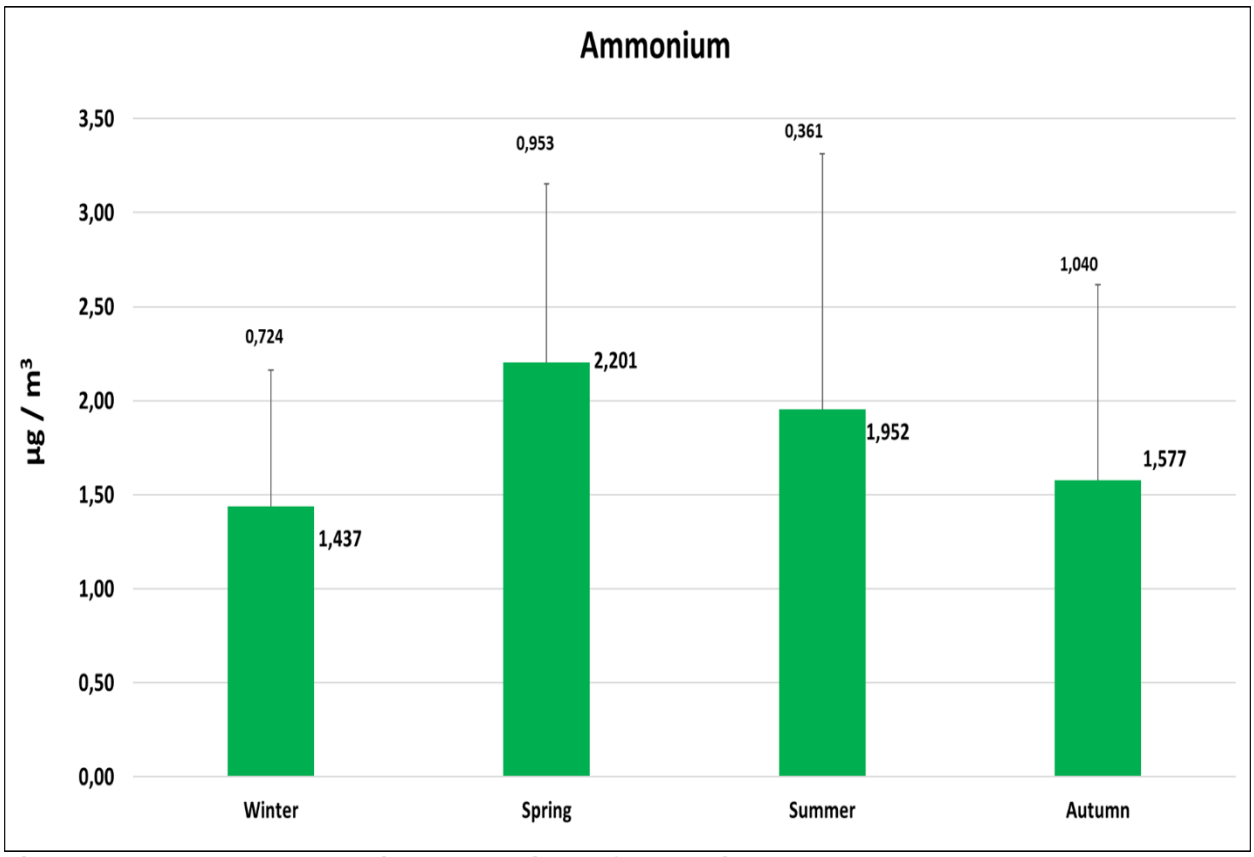

Figure 4.27: Average seasonal concentrations of ammonium

This observation can be attributed to the secondary photochemistry of ammonium as the solar radiation is more intense during spring and summer [219, 220, 273, 274, 277].

The high ammonium concentration during high temperature period is likely to exist because ammonium nitrate is semi-volatile and so it is difficult to condensate [273, 274]. Consequently, high ammonium concentration may indicate that the possibility of forming ammonium nitrate during this period should be very low [261].

Additionally, this can be explained from the formation of NH_4^+ in the particulate matter if it is formed from NH_3. The bidirectional reaction is the following:

$$NH_{3(aq)} + H_2O_{(aq)} \leftrightarrow NH^+_{4(aq)} + OH^-_{(aq)} \quad (1)$$

This reaction has a $\Delta H^0_{(T_0)}/(R*T_0)$= -1.50 mol/kg and $\Delta c^0_p/R$ = 26.92 mol/kg (2) [283-285] :

-$\Delta H^0_{(T_0)}$ is the entalphy at T_0 = 25°C or 298.15^{0}K (normal conditions),

-R=0.008314 J/mol* ^{0}K and

-Δc^0_p is the change of molar capacity of products minus reactants.

At 298.15^{0}K the reaction is endothermic. If we increase the temperature the equilibrum of the reaction will shift to the left and the concentration of NH_4^+ will increase.

At the same time from the equation: $\Delta H^0(T) = \Delta H^0(T_0) + \Delta c^0_p\ (T-T_0)$ (3) (The equation (3) applies for a small temperature rate) [286] if there is an increase for example at 40^0C or 313.15^0K then:

-from (1) solving to $\Delta H^0(T_0) = -3.72$ J/kg and

-from (2) solving to $\Delta c^0_p = 0.2238$ J/kg*^{0}K, then the equation (3) provides $\Delta H^0(T) = -3.72$ J/kg + 0.2238 J/kg*^{0}K (313.15^0K-298.15^0K) = -0.363 J/kg.

In conclusion, with an increase of 15^0C the reaction is still endothermic ($\Delta H^0(T) = -0.363$ J/kg) and the reaction's equilibrum will shift to the left which leads to an increase of the concentration of NH_4^+.

Also, during the warm period there is formation of the following salts:

- NH_4NO_3 from the reaction of NH_3 with HNO_3 (which is formed from reactions of NO_X in troposphere).

$$NH_4NO_{3(s)} \leftrightarrow NH_{3(g)} + HNO_{3(g)} \quad (2)$$

$\Delta H^0(T_0) = -185.34$ J/kg (normal conditions)

- $(NH_4)_2HSO_4$ from the reaction of NH_4^+ with HSO_4^- (which is formed from reactions of SO_2 in troposphere)

$$NH_4HSO_{4(s)} \leftrightarrow NH^+_{4(aq)} + HSO^-_{4(aq)} \quad (3)$$

$\Delta H^0(T_0) = -7.12$ J/kg (normal conditions)

- $(NH_4)_3H(SO_4)_2$ from the reaction of NH_4^+ with HSO_4^- and SO_4^{-2} (which are formed from reactions of SO_2 in troposphere).

$$(NH_4)_3\,H\,(SO_4)_{2(s)} \leftrightarrow 3NH^+_{4(aq)} + HSO^-_{4(aq)} + SO^{2-}_{4(aq)} \quad (4)$$

$\Delta H^0(T_0) = -12.87$ J/kg (normal conditions)

- $(NH_4)_2SO_4$ from the reaction of NH_4^+ with SO_4^{-2} (which is formed from reactions of SO_2 in troposphere)

$$(NH_4)_2\,SO_{4(s)} \leftrightarrow 2NH^+_{4(aq)} + SO^{2-}_{4(aq)} \quad (5)$$

$\Delta H^0(T_0) = -6.57$ J/kg (normal conditions) [238-285, 287]

With an increase of temperature the Deliquescence Relative Humidity (DRH) decreases for all the above salts (Figure 4.24).

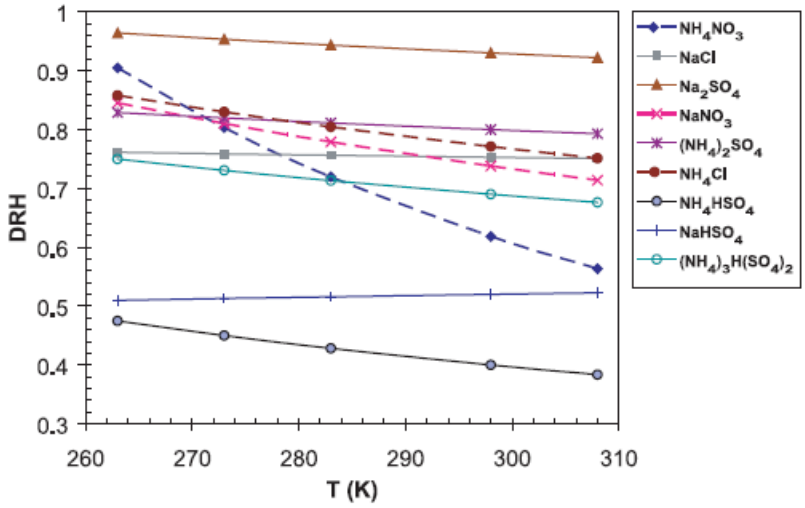

Figure 4.28: DRH as a function of temperature for salts [287].

Above this humidity rate determined by DRH the transition phase from solid to saturated aqueous solution occurs. This leads to the fact that with a decrease of DRH resulted from the increase of temperature then the salts can dissolve in the atmosphere. As a result, from the above reactions (2), (3), (4) and (5) the salts are unstable and the equilibrium will shift to the left which leads to the increase of the concentration of NH_3 from reaction (2) and NH_4^+ from reactions (3), (4) and (5).

In the same way, because the $\Delta H^0(T_0)$ of all the above reactions is negative, which means that they are endothermic reactions, when there is an increase in temperature in specific range (according to equation 3) the equlibrium will again shift to the left (the same concept that we desrcibed for reaction 1). This leads to the production of NH_3 or/and NH_4^+ .

4.5.1.3 Seasonal Variation of Potassium

In the following Figure 4.25 the seasonal variation of potassium is presented. The concentration is high during winter and spring. The high winter concentration can be attributed to combustion sources since potassium is a major cation emitted through this procedure [248, 276].

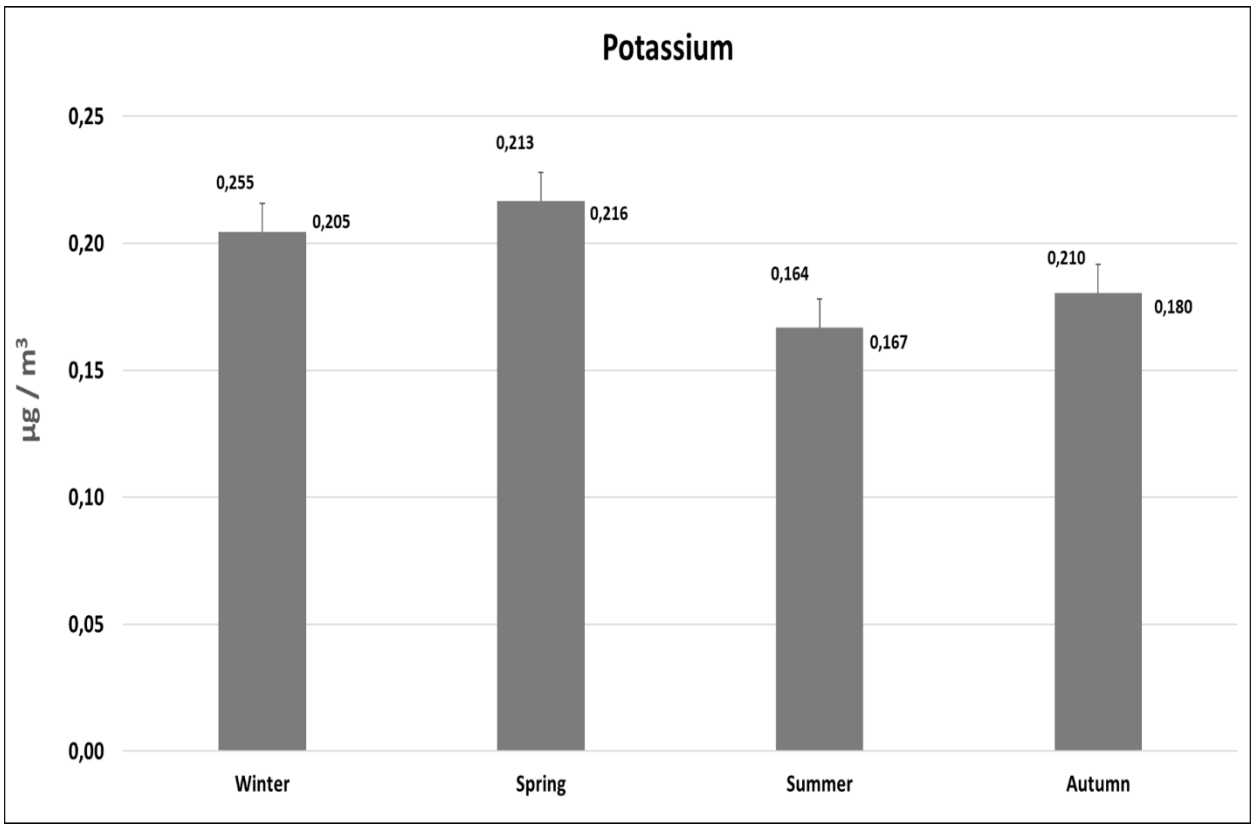

Figure 4.29: Average seasonal concentrations of potassium

Also, the concentration during spring, which is the highest, can be originated from a combination of sea and combustion sources. Moreover, it has to be indicated that the standard deviation is high in all seasons compared to the average value. This means that the data appear to have wide dispersion.

4.5.1.4 Seasonal variation of Magnesium

From the Figure 4.26 of the average concentrations of magnesium for every season is indicated that the highest concentration is during summer.

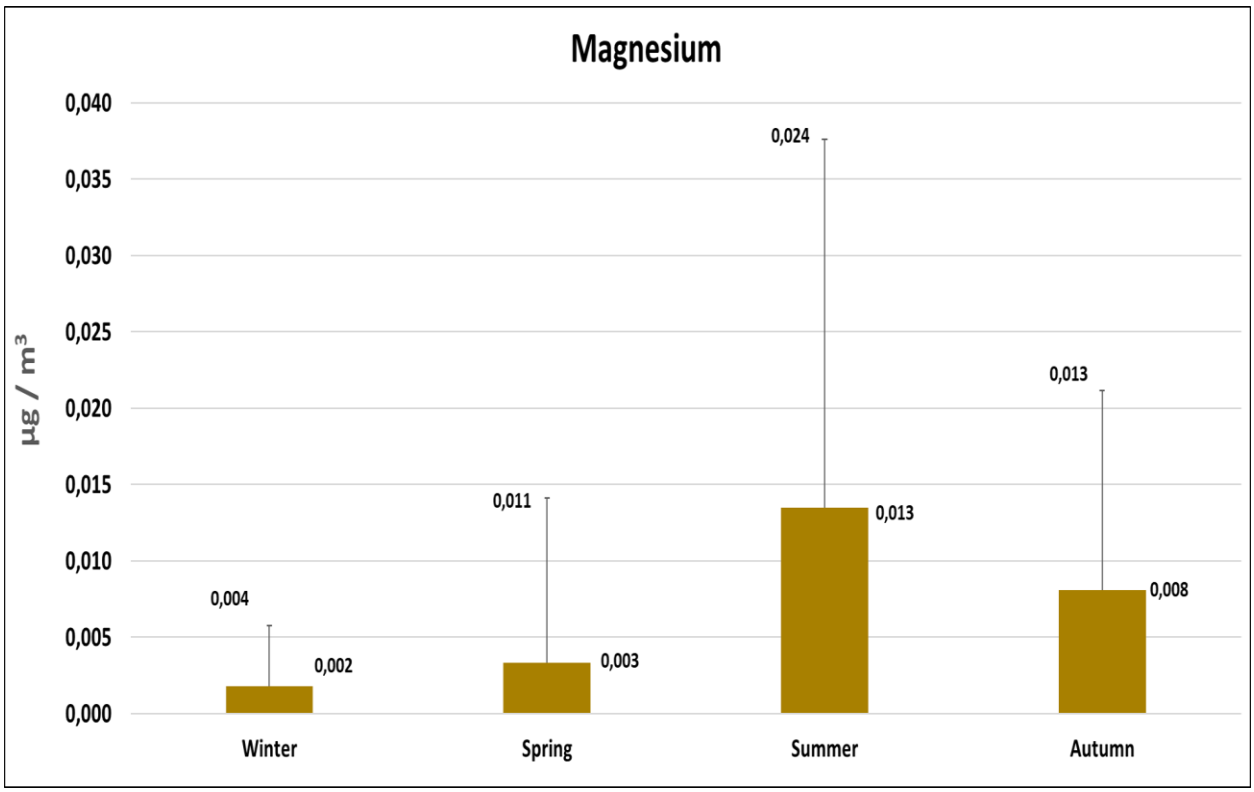

Figure 4.30: Average seasonal concentrations of magnesium

High magnesium average concentration during summer and autumn can be attributed to Sahara dust transportation [278-282]. Additionally, it has to be indicated that the standard deviation is high in all seasons compared to the average value. This means that the data appear to have wide dispersion

4.5.1.5 Seasonal variation of Calcium

In the following Figure 4.27 the average seasonal concentrations of calcium are presented.

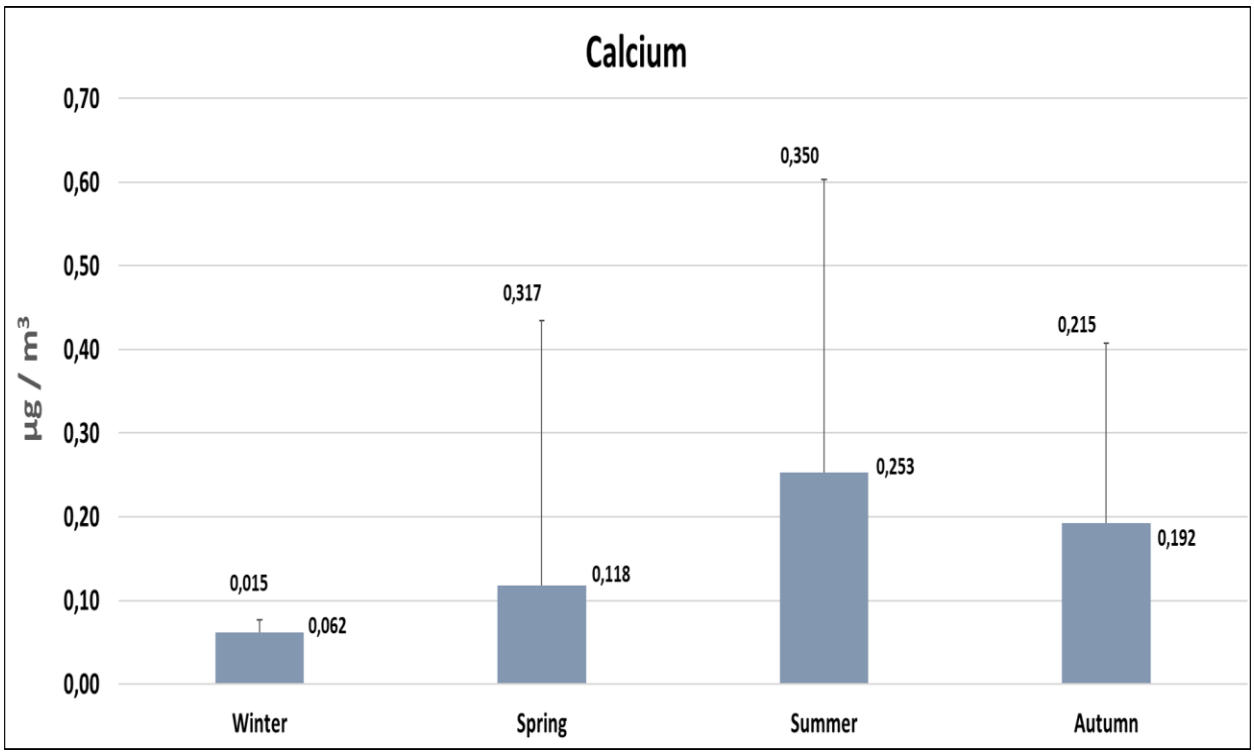

Figure 4.31: Average seasonal concentrations of calcium

The distribution is the same as magnesium's (Figure 4.26). Calcium's high summer and autumn concentrations can be attributed to Sahara dust transportation as magnesium's[278-282]. Moreover, it has to be indicated that the standard deviation is high in all seasons compared to the average value. This means that the data appear to have wide dispersion.

4.5.1.6 Seasonal Variation of Black Carbon

In the following Figure 4.28 the average seasonal concentrations of Black Carbon are displayed.

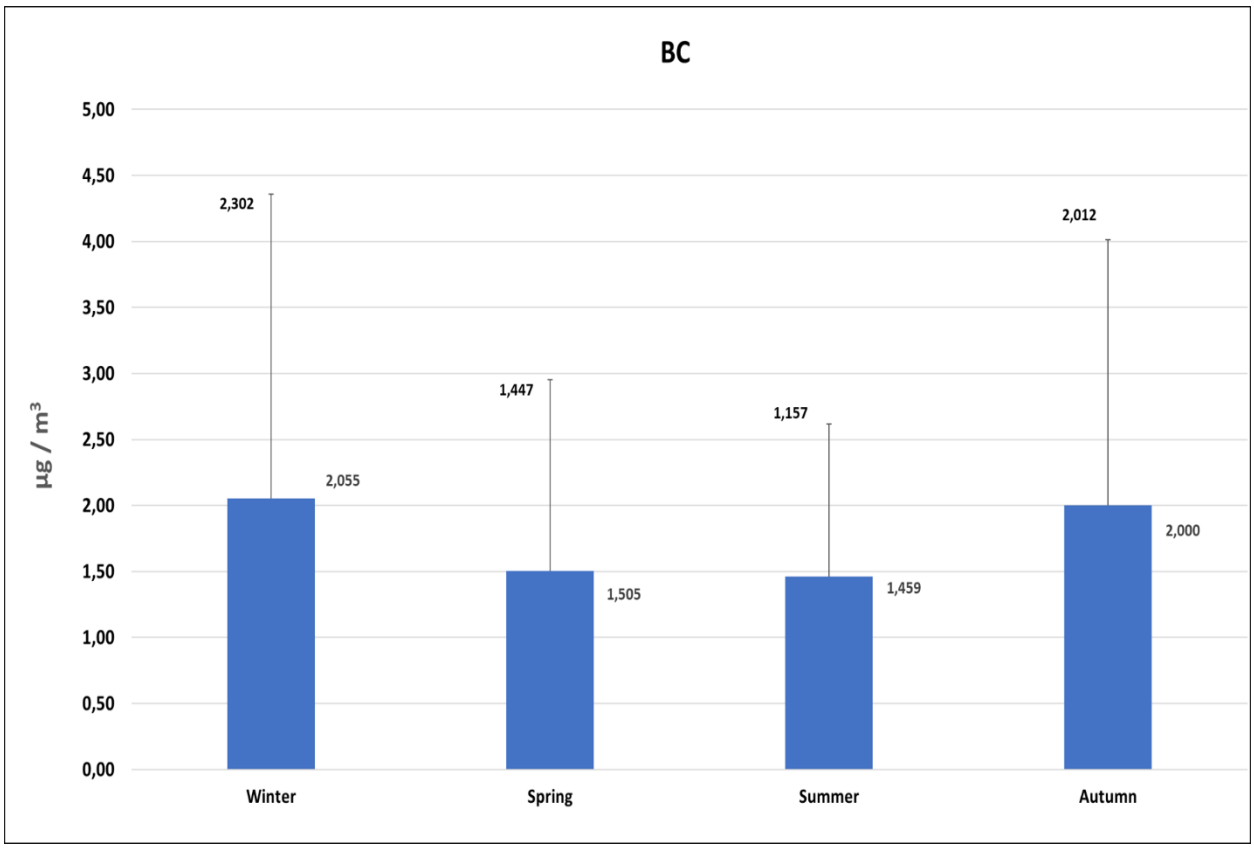

Figure 4.32: Average seasonal concentrations of BC

From the Figure 4.28 is derived the conclusion that during winter and autumn the concentration is higher due to combustion of fossil fuel for heating in the studied area [223]. The seasonal variaton of BC is approximately the same as potassium's (Figure 4.25) Also, during these seasons the standard deviation is high compared to the average value. This means that the data appear to have wide dispersion.

4.5.2 Seasonal Correlations and Diurnal Variation of the Chemical Substances

4.5.2.1 Correlations during Winter

In the following Table 4.3 the statistical analysis of the correlations of the chemical substances during winter is presented.

Table 4.3: Statistical analysis of the correlations which can provide information for the sources of PM_1 during winter.

Statistical analysis ↓	Correlations during winter					
	Correlations that indicate crustal sources			Correlations that indicate marine sources		Correlation that indicates combustion sources
	Mg^{+2} - Ca^{+2}	Mg^{+2} - K^{+}	Ca^{+2} - K^{+}	Mg^{+2} - Na^{+}	Ca^{+2} - Na^{+}	K^{+} - BC
R^2	0,89	0,00	0,01	0,00	0,00	0,50
R	0,11	0,02	0,32	0,03	0,03	1,59
P	0	0,03	8,3E-12	0,0497	5,04E-05	1,33E-115
n	3.117	3.106	3.116	3.115	3.117	762

From the Table 4.3 is indicated that all the correlations are statistically significant as P<0,05. The correlation of K^{+} with BC has the lowest number of samples (n) compared to the other correlations because the measurements of BC are held on an hourly basis.

The highest correlation coefficient is indicated at the correlation of Mg^{+2} with Ca^{+2} (R^2=0,89). Furthermore, during the winter period, it is derived that they have the same sources which are mainly crustal and these sources provide a high portion of PM_1. In the following Figure 4.29 this correlation is presented.

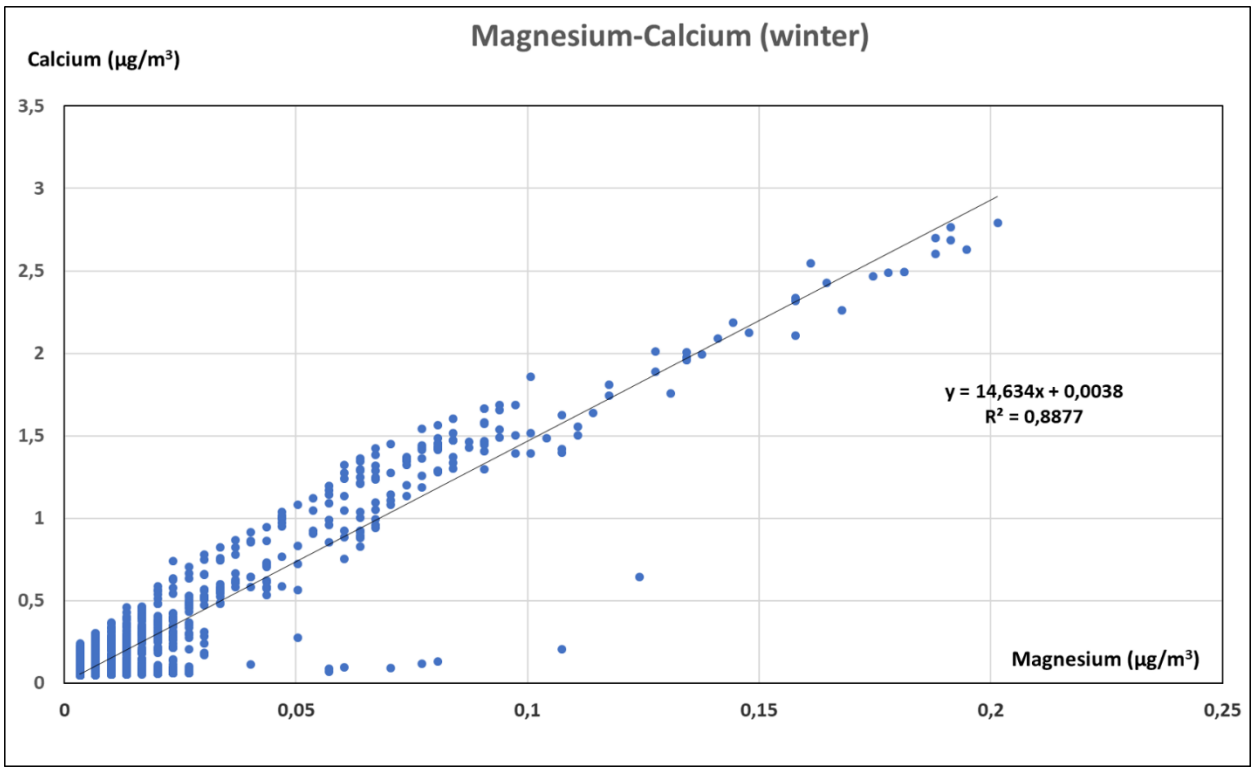

Figure 4.33: Correlation of magnesium with calcium during winter

Also, K^+ with BC indicate a correlation coefficient of R^2=0,50 with a standard deviation R=1,59 (Table 4.3). This standard deviation is the highest of all the correlations that were studied during winter. The correlation coefficient indicates moderate influence of these two substances in the chemical background of PM_1 and are mainly emitted from fossil fuel combustion for heating and it is displayed in the following Figure 4.30.

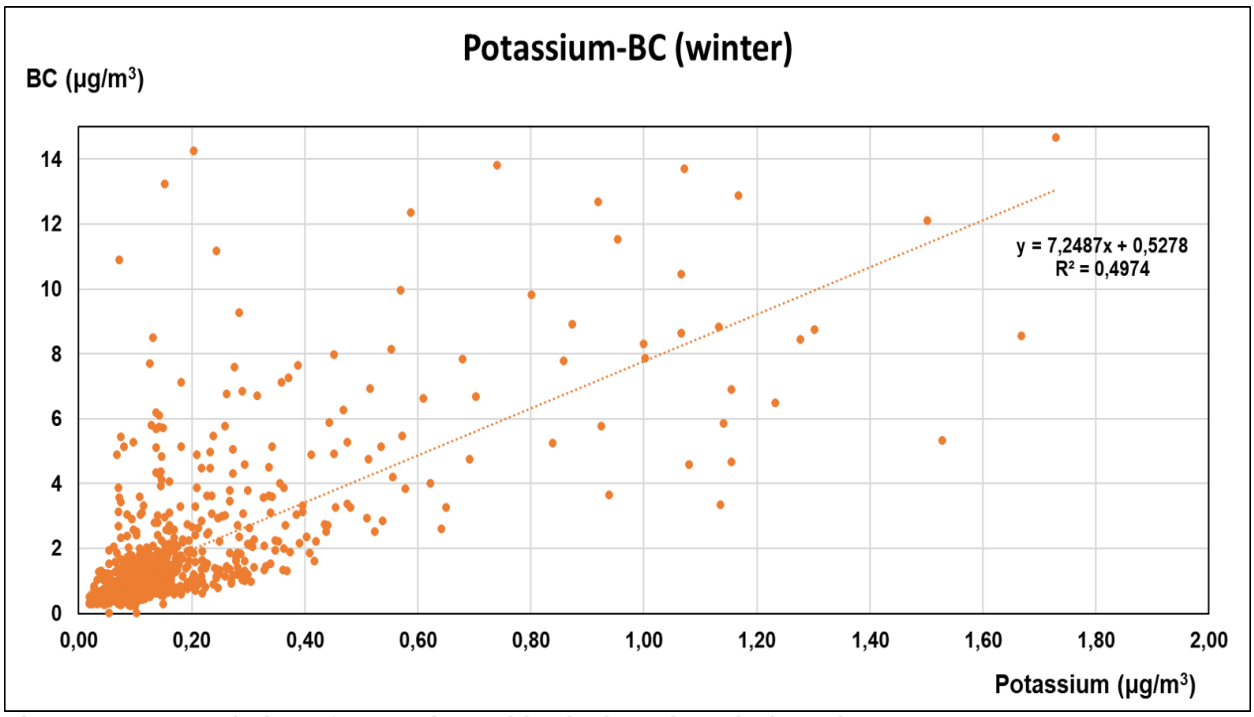

Figure 4.34: Correlation of Potassium with Black Carbon during winter

In the following Figure 4.31 the correlation of sodium with calcium during the winter months is presented. From this Figure 4.31 is derived the conclusion that the sodium of this correlation is probably originated from marine sources, despite the fact that the correlation coefficient is very low (R^2=0,0049).

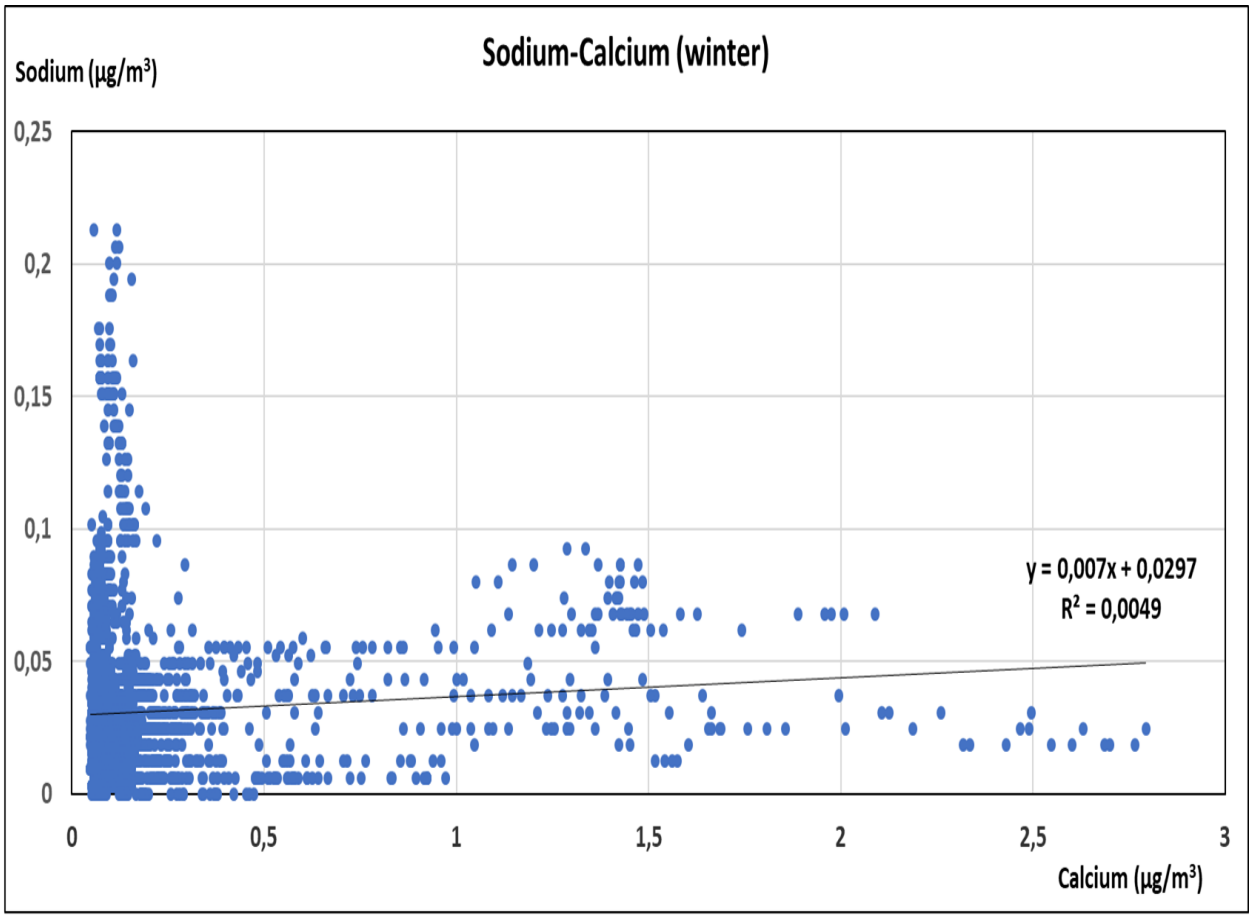

Figure 4.35: Correlation of Sodium with Calcium during winter

4.5.2.2 Diurnal Variations during Winter

4.5.2.2.1 Diurnal Variation of Potassium with Black Carbon during Winter

In the following Figure 4.32 the diurnal variation of potassium with Black Carbon during winter is displayed. It has to be outlined that for all the diurnal seasonal variations the median values are used. Black carbon which is a component of combustion indicates an increase from 15:00 until 00:00. This increase if probably due to the use of heating. During the same hours potassium also displays an increase which can be attributed to heating too.

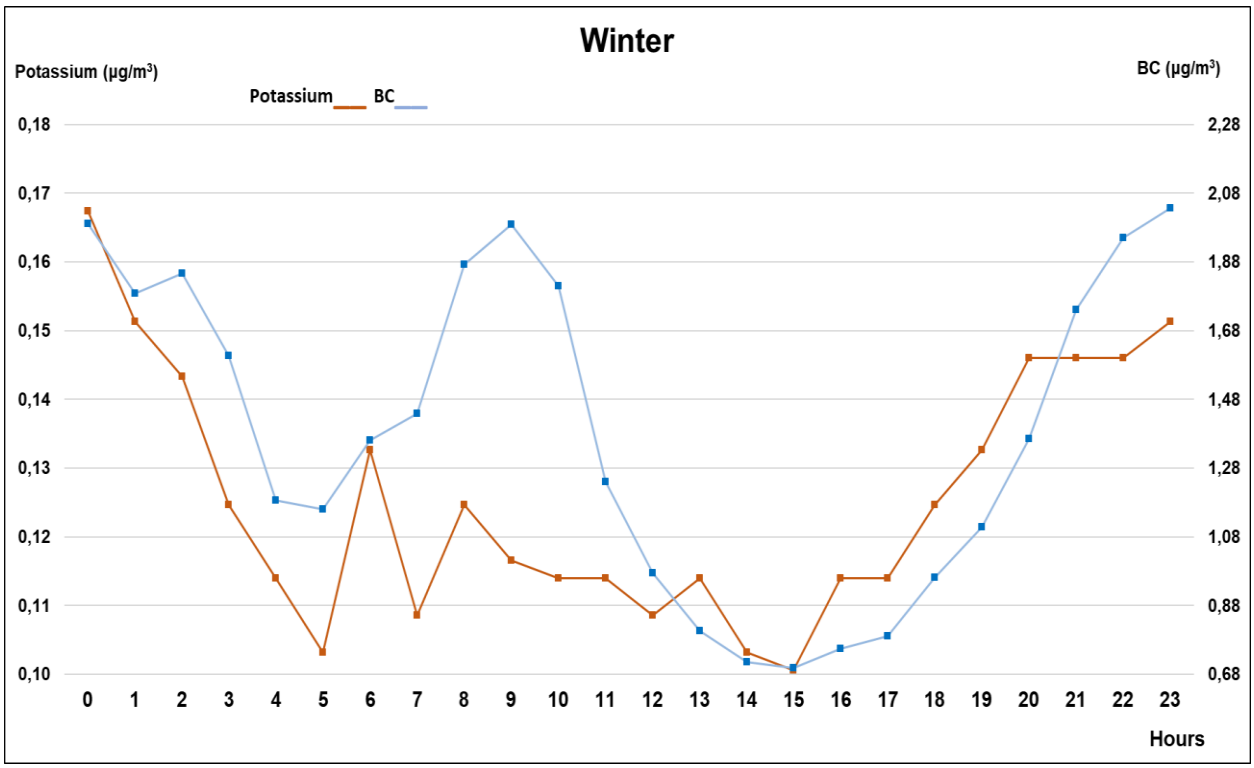

Figure 4.36: Diurnal variation of potassium with black carbon during winter

4.5.2.2.2 Diurnal Variation of Ammonium during Winter

In the following Figure 4.33 the diurnal variation of ammonium during winter is displayed.

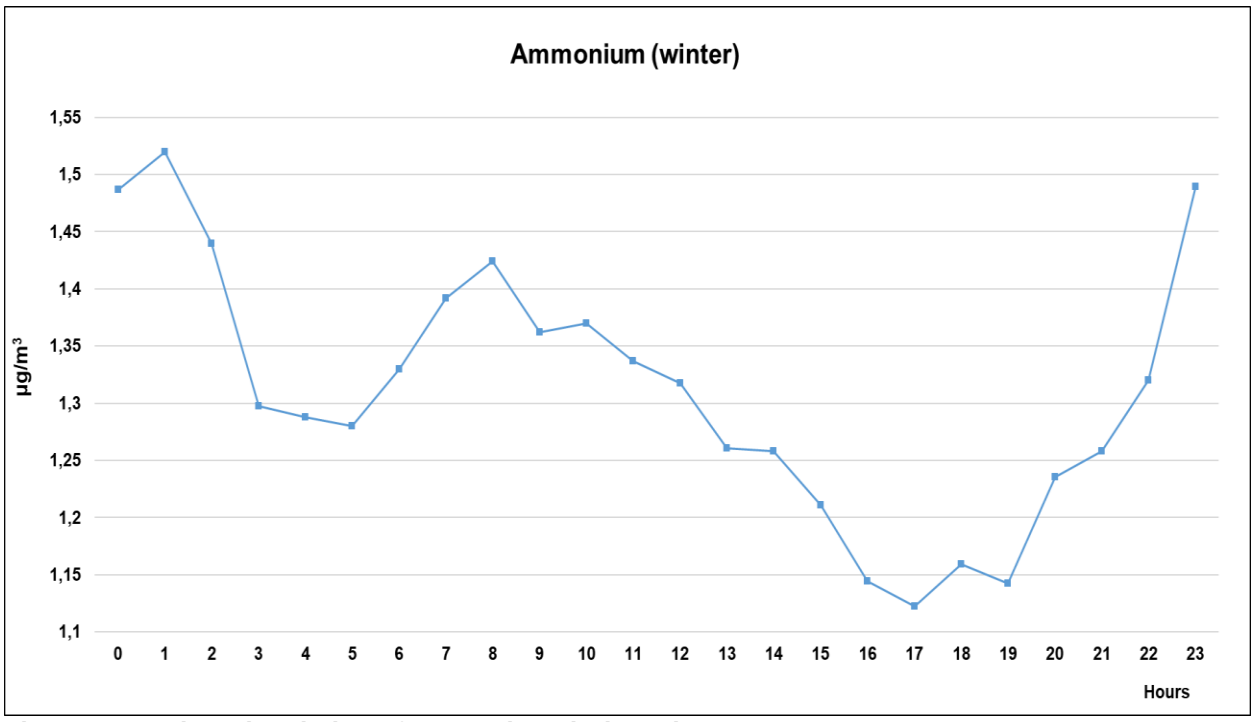

Figure 4.37: Diurnal variation of ammonium during winter

Ammonium, as mentioned in chapter 4.4.1.2, indicates secondary photochemistry. This means that intense solar radiation increases its productivity. During the winter months the intensity of the solar radiation is not so high, and there are not observed significantly higher concentrations during the day hours compared to the night. The increase of the concentration from 19:00 until 00:00 (night hours) can be explained from the reasoning of the chapter 4.5.3 Diurnal variation of Ammonium.

4.5.2.3 Correlations during Spring

In the following Table 4.4 the statistical analysis of the correlations of the chemical substances during spring is presented.

Table 4.4: Statistical analysis of the correlations which can provide information for the sources of PM_1 during spring.

Statistical analysis ↓	Correlations during spring					
	Correlations that indicate crustal sources			Correlations that indicate marine sources		Correlation that indicates combustion sources
	Mg^{+2} - Ca^{+2}	Mg^{+2} - K^{+}	Ca^{+2} - K^{+}	Mg^{+2} - Na^{+}	Ca^{+2} - Na^{+}	K^{+} - BC
R^2	0,86	0,00	0,00	0,31	0,52	0,41
R	0,06	0,01	0,14	0,01	0,11	1,05
P	0	1,06E-09	0	0	0	5,3E-210
n	6.732	6.763	6.733	6.743	7.055	1.787

From the Table 4.4 it is indicated that all the correlations are statistically significant as $P<0,001$.

The highest correlation coefficient is presented in the correlation of Mg^{+2} with Ca^{+2} ($R^2=0,86$). This indicates that the crustal sources contribute at a high portion in the chemical composition of PM_1. In the following Figure 4.34 this correlation is displayed.

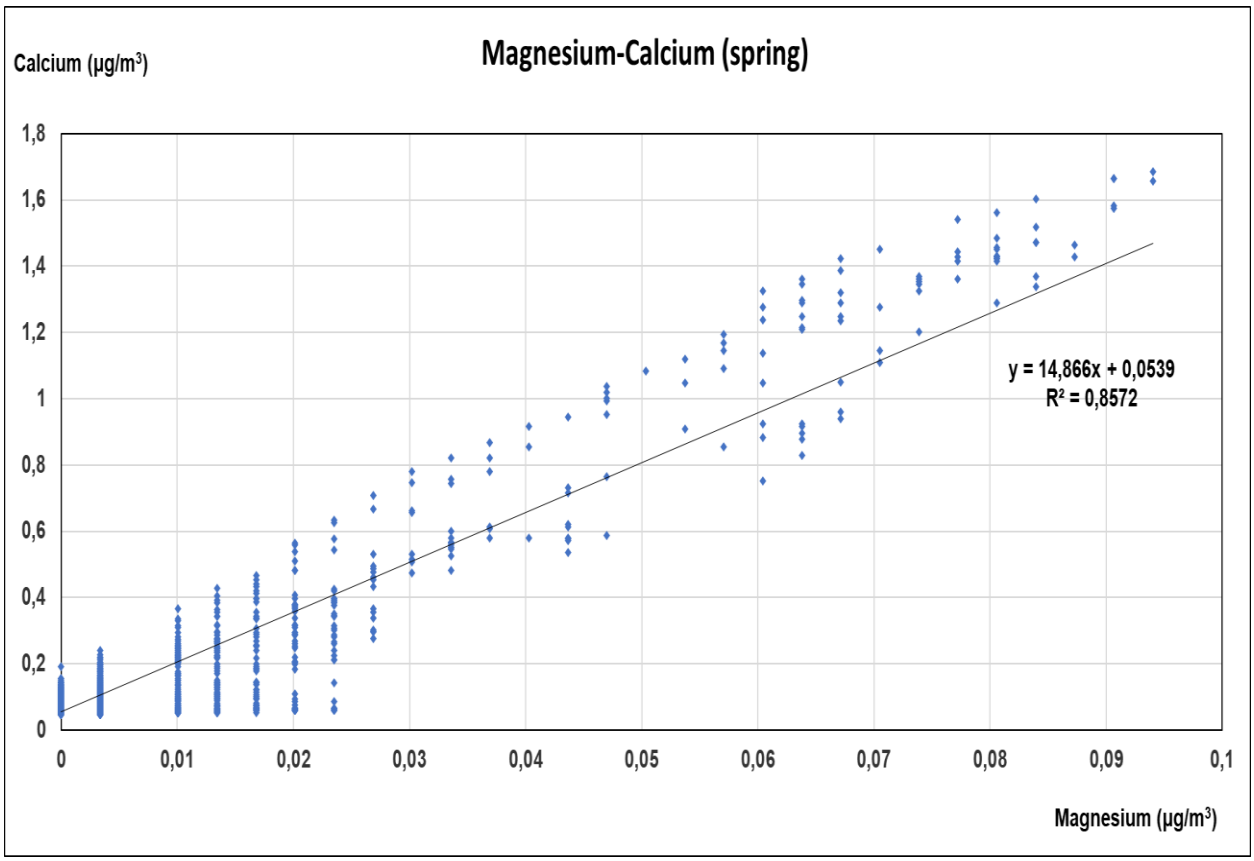

Figure 4.38: Correlation of Magnesium with Calcium during spring

Moreover, the contribution of the marine sources is also significant as the correlations of Mg^{+2} with Na^{+} and Ca^{+2} with Na^{+} indicate correlation coefficients of R^2=0,31 and R^2=0,52 respectively.

Furthermore, the contribution of combustion sources is significant during this season as the correlation coefficient of BC with K^{+} is R^2=0,41.

In the following Figure 4.35 the correlation between potassium and calcium during spring is presented.

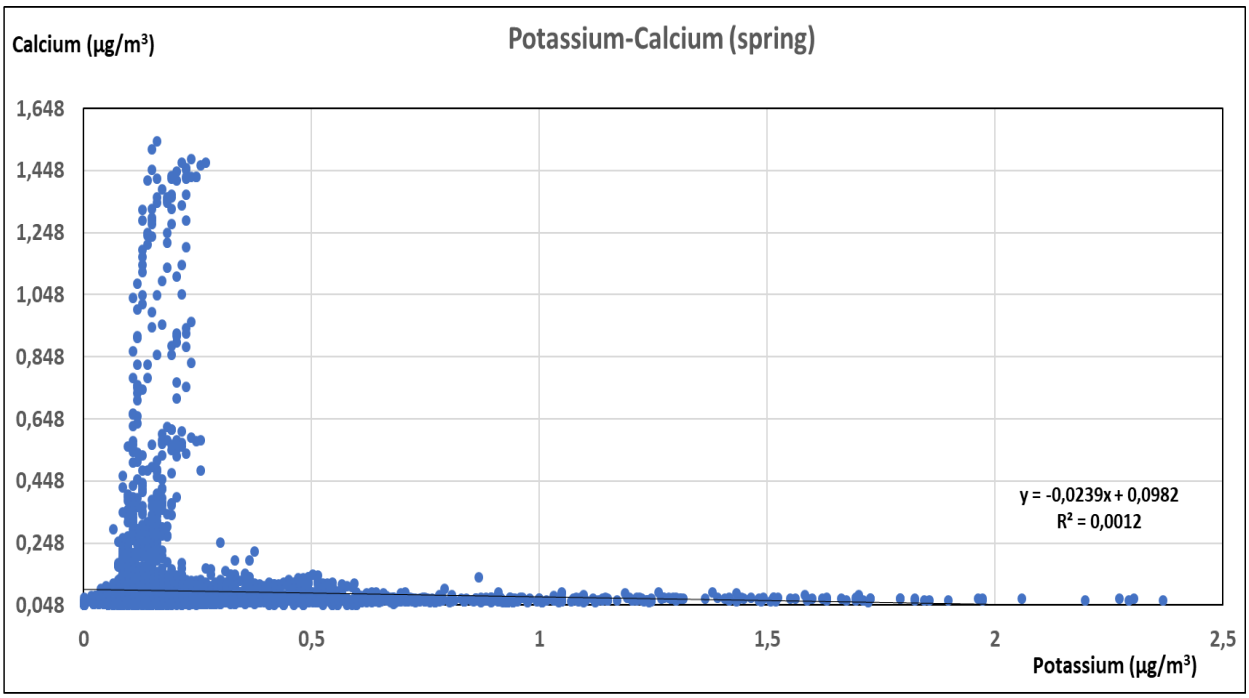

Figure 4.39: Correlation of Potassium with Calcium during spring

From the Figure 4.35 the high concentrations of calcium can be attributed to dust sources and events during the spring period although they are not actually correlated ($R^2 \approx 0$) (Table 4.4).

4.5.2.4 Diurnal Variations during Spring

4.5.2.4.1 Diurnal Variation of Sodium with Calcium during Spring

In the following Figure 4.36 the diurnal variation of sodium with calcium during spring is displayed.

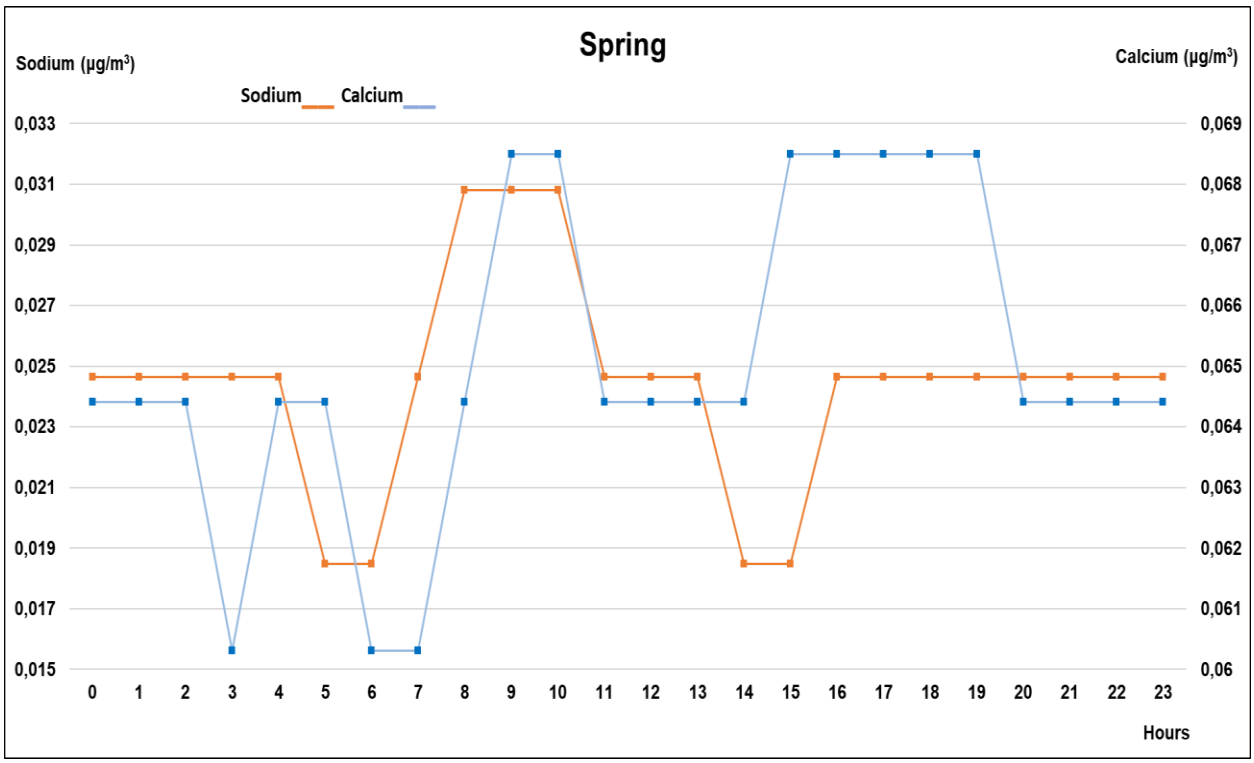

Figure 4.40: Diurnal variation of calcium with sodium during spring

From the Figure 4.36 it is indicated that the two cations present approximately the same hourly variability.

4.5.2.4.2 Diurnal Variation of Ammonium during Spring

In the next Figure 4.37 the diurnal variation of ammonium during the spring months is presented.

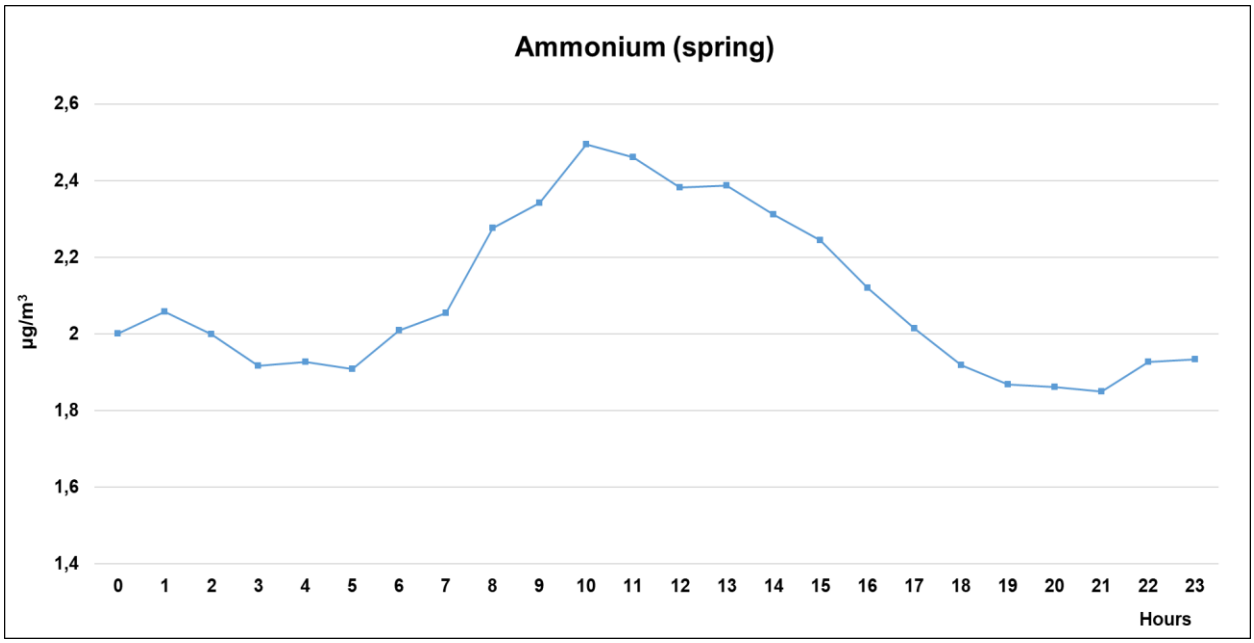

Figure 4.41: Diurnal variation of ammonium during spring

From the Figure 4.37 above it is indicated an increase of ammonium's concentration during the day hours. This increase is not so high but it still displays the secondary photochemical behaviour of ammonium. Moreover, the increase of the concentration from 21:00 until 02:00 (night hours) can be explained from the reasoning of the chapter 4.5.3 Diurnal variation of Ammonium.

4.5.2.5 Correlations during Summer

In the following Table 4.5 the statistical analysis of the correlations of the chemical substances during summer is presented.

Table 4.5: Statistical analysis of the correlations which can provide information for the sources of PM_1 during summer

Statistical analysis ↓	Correlations during summer					
	Correlations that indicate crustal sources			Correlations that indicate marine sources		Correlation that indicates combustion sources
	Mg^{+2} - Ca^{+2}	Mg^{+2} - K^{+}	Ca^{+2} - K^{+}	Mg^{+2} - Na^{+}	Ca^{+2} - Na^{+}	K^{+} - BC
R^2	0,88	0,18	0,17	0,62	0,44	0,10
R	0,12	0,02	0,31	0,05	0,26	0,63
P	0	2,2E-282	5,1E-276	0	0	1,6E-28
n	6.639	6.460	6.594	6.499	6.639	1.219

From the Table 4.5 it is indicated that all the correlations are statistically significant as P<0,001.

The highest correlation coefficient is again indicated for the correlation of magnesium with calcium (R^2=0,88). These two cations are mainly originated from crustal sources and their correlation is displayed in the following Figure 4.38.

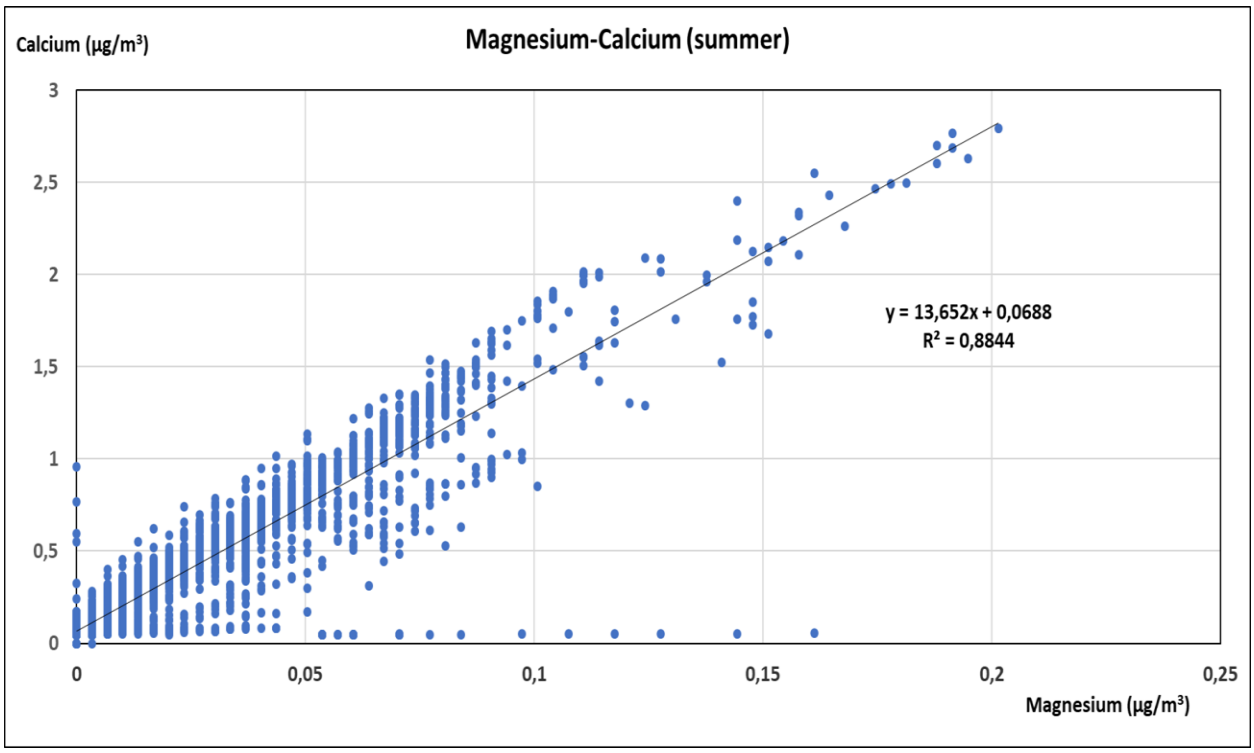

Figure 4.42: Correlation of Magnesium with Calcium during summer

Additionally, the correlation of sodium with magnesium indicates a correlation coefficient of R^2=0,62 and is displayed in the following Figure.

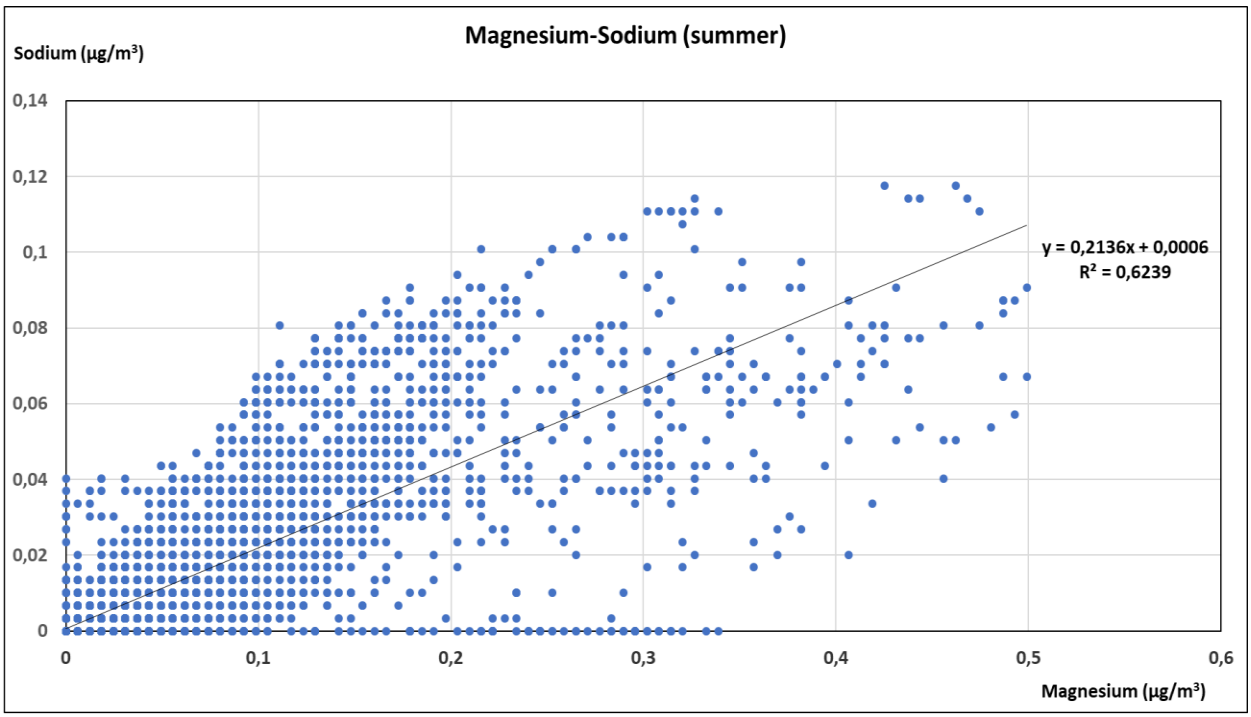

Figure 4.43: Correlation of Magnesium with Sodium during summer

These two cations are mainly originated from sea salt and during summer they contribute significantly in the chemical composition of the fine particulate matter. The same outcome

is derived from the correlation of calcium with sodium which indicate a correlation coefficient of R^2=0,44 and their correlation is presented in the following Figure 4.40.

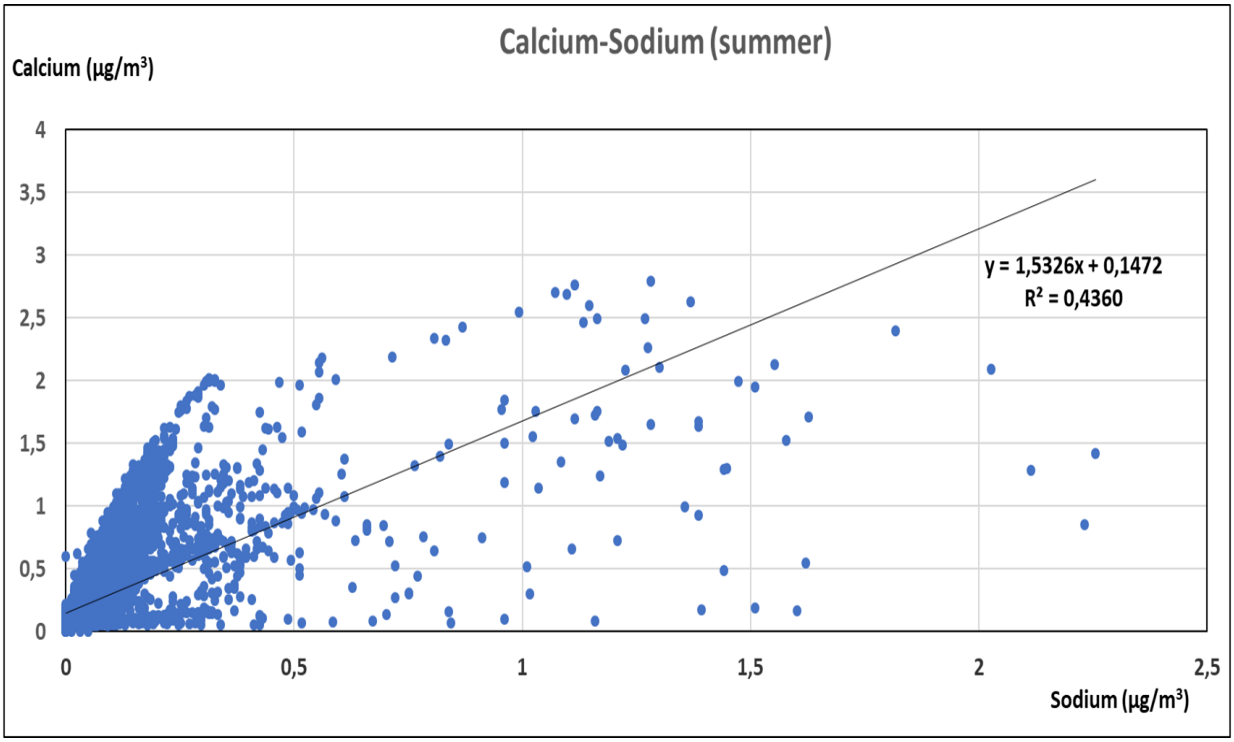

Figure 4.44: Correlation of Calcium with Sodium during summer

4.5.2.6 Diurnal Variations during Summer

4.5.2.6.1 Diurnal Variation of Magnesium with Calcium during Summer

Magnesium and calcium's diurnal variability during summer is presented in the next Figure 4.41.

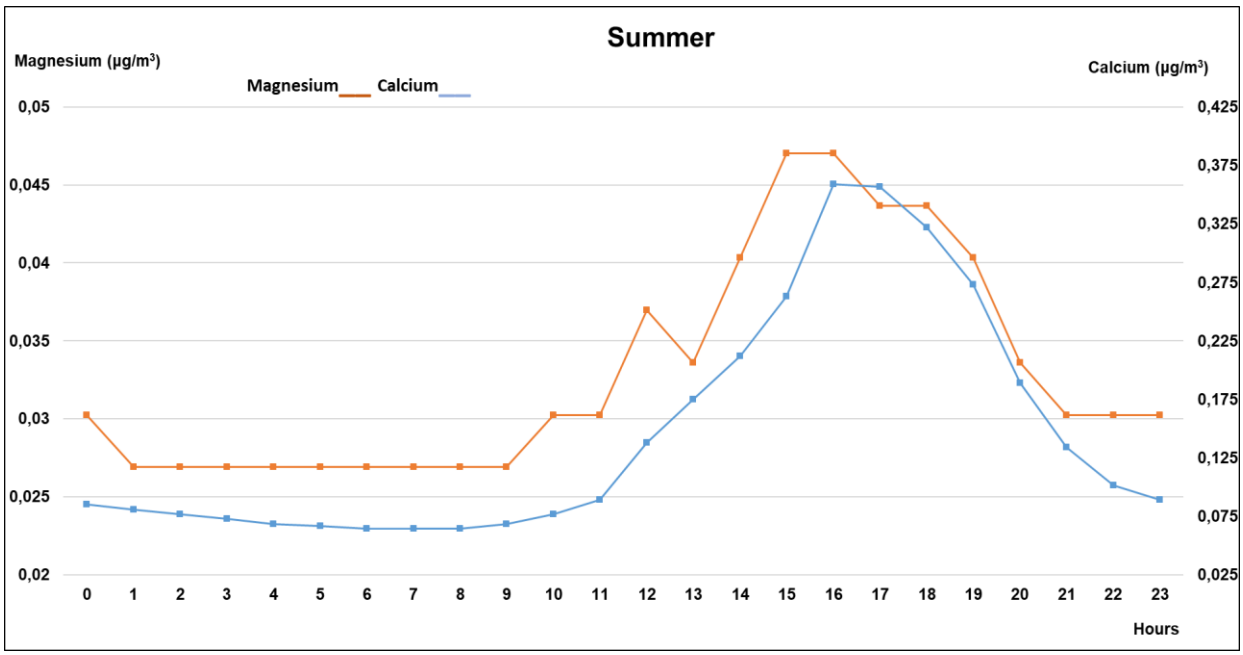

Figure 4.45: Diurnal variation of magnesium with calcium during summer

These two cations indicate approximately the same hourly variability during this season (Figure 4.41). The highest probability is that these two cations are emitted from crustal sources as they are main components of earth's crust. Also, during summer in the Greater Area of Athens the winds that have direction from the Sahara desert mainly prevail[278-282].

4.5.2.6.2 Diurnal Variation of Magnesium with Sodium during Summer

In the following Figure 4.42 the hourly variation of magnesium with sodium during summer is presented.

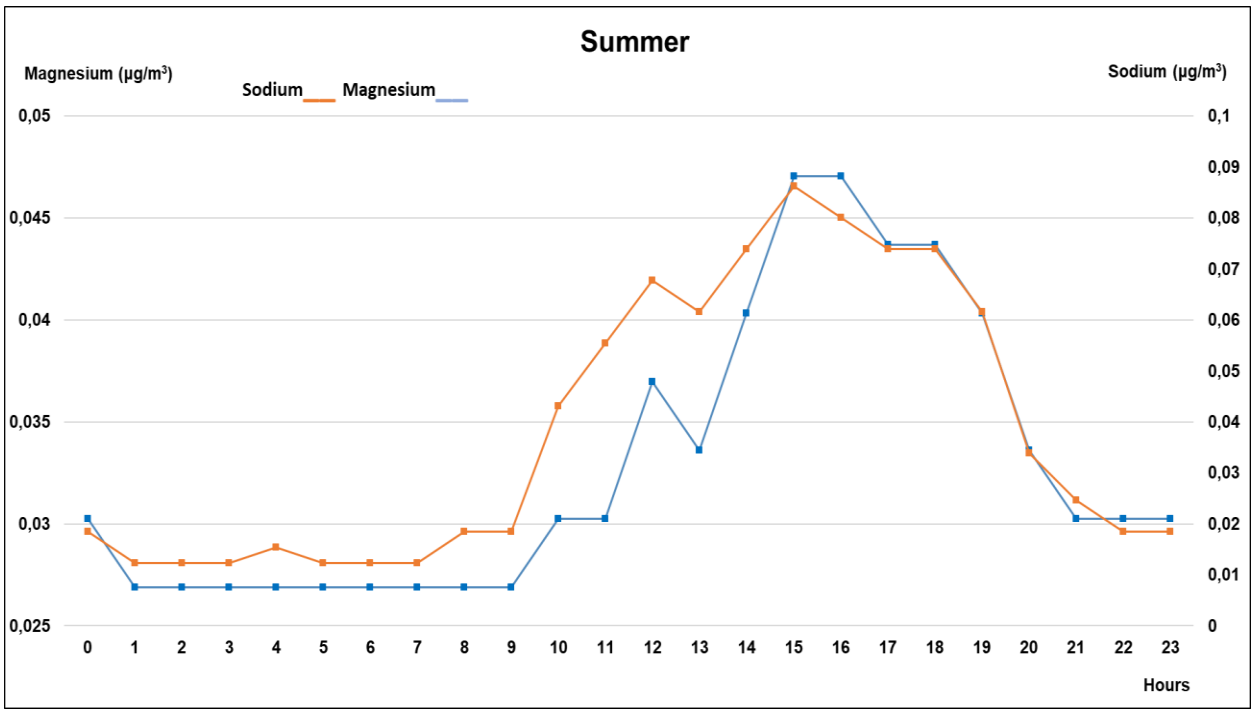

Figure 4.46: Diurnal variation of magnesium with sodium during summer

From Figure 4.41 above it is indicated that the two cations display approximately the same hourly variability and are emitted probably from marine sources [276].

4.5.2.6.3 Diurnal Variation of Calcium with Sodium during Summer

The diurnal variation of sodium with calcium for the summer period is displayed in the following Figure 4.43. The two cations indicate approximately the same hourly variability during this period and are probably emitted from marine sources [276].

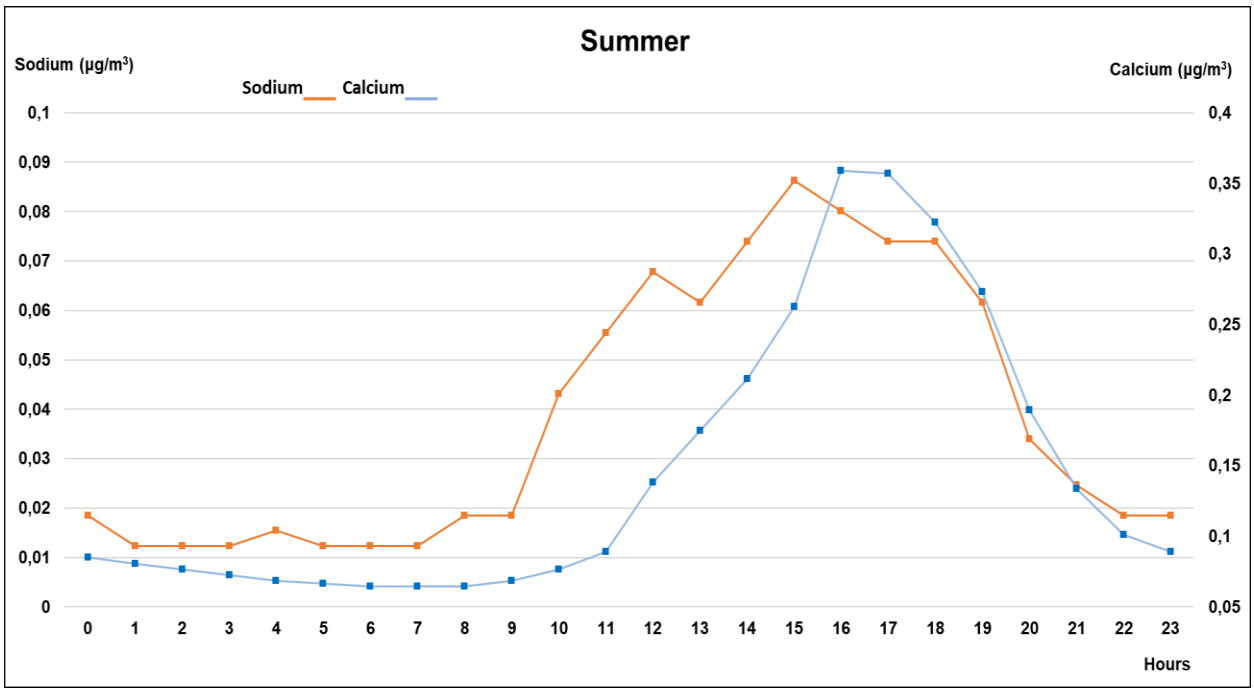

Figure 4.47: Diurnal variation of calcium with sodium during summer

4.5.2.6.4 Diurnal Variation of Ammonium during Summer

In the next Figure 4.44 the hourly variability of ammonium during summer is presented.

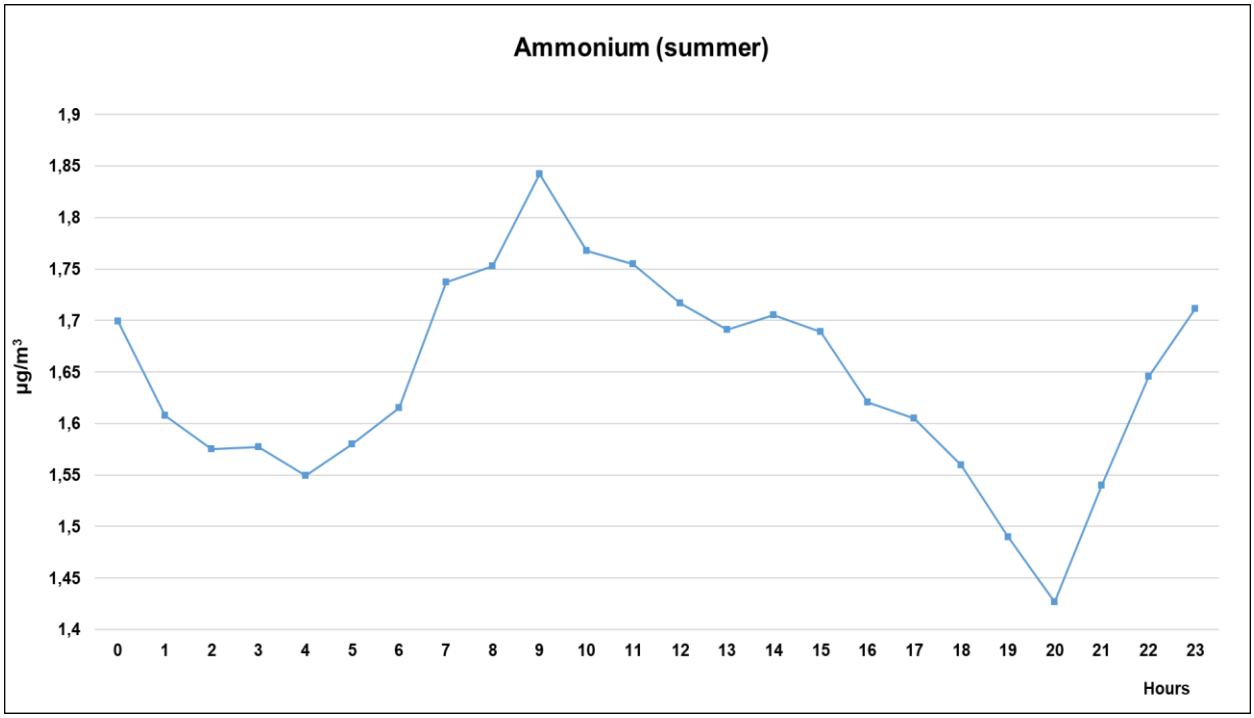

Figure 4.48: Diurnal variation of ammonium during summer

It is displayed from the Figure 4.44 that the concentration of ammonium is increased during the day hours. Again, this chemical performance of ammonium is observed due to

its secondary photochemical behaviour. This performance is approximately the same compared to the diurnal variation of the spring period and is interpreted by the same reasoning as the one presented in the chapter 4.4.2.4.2 Diurnal Variation of Ammonium during Spring. Furthermore, the increase of the concentration from 20:00 until 00:00 (night hours) can be explained from the reasoning of the chapter 4.5.3 Diurnal variation of Ammonium.

4.5.2.7 Correlations during Autumn

In the following Table 4.6 the statistical analysis of the correlations of the chemical substances during autumn is presented.

Table 4.6 : Statistical analysis of the correlations which can provide information for the sources of PM_1 during autumn

Statistical analysis ↓	Correlations during autumn					
	Correlations that indicate crustal sources			Correlations that indicate marine sources		Correlation that indicates combustion sources
	Mg^{+2} - Ca^{+2}	Mg^{+2} - K^{+}	Ca^{+2} - K^{+}	Mg^{+2} - Na^{+}	Ca^{+2} - Na^{+}	K^{+} - BC
R^2	0,84	0,01	0,00	0,66	0,48	0,40
R	0,08	0,25	0,19	0,04	0,05	1,26
P	0	3,85E-10	0	0	0	8,5E-124
n	2.912	2.912	2.912	2.912	2.901	1.088

From the Table 4.6 it is indicated that all the correlations are statistically significant as P<0,001.

The highest correlation coefficient is again indicated for the correlation of magnesium with calcium (R^2=0,8387). These two cations are mainly originated from crustal sources and their correlation is displayed in the following Figure 4.45.

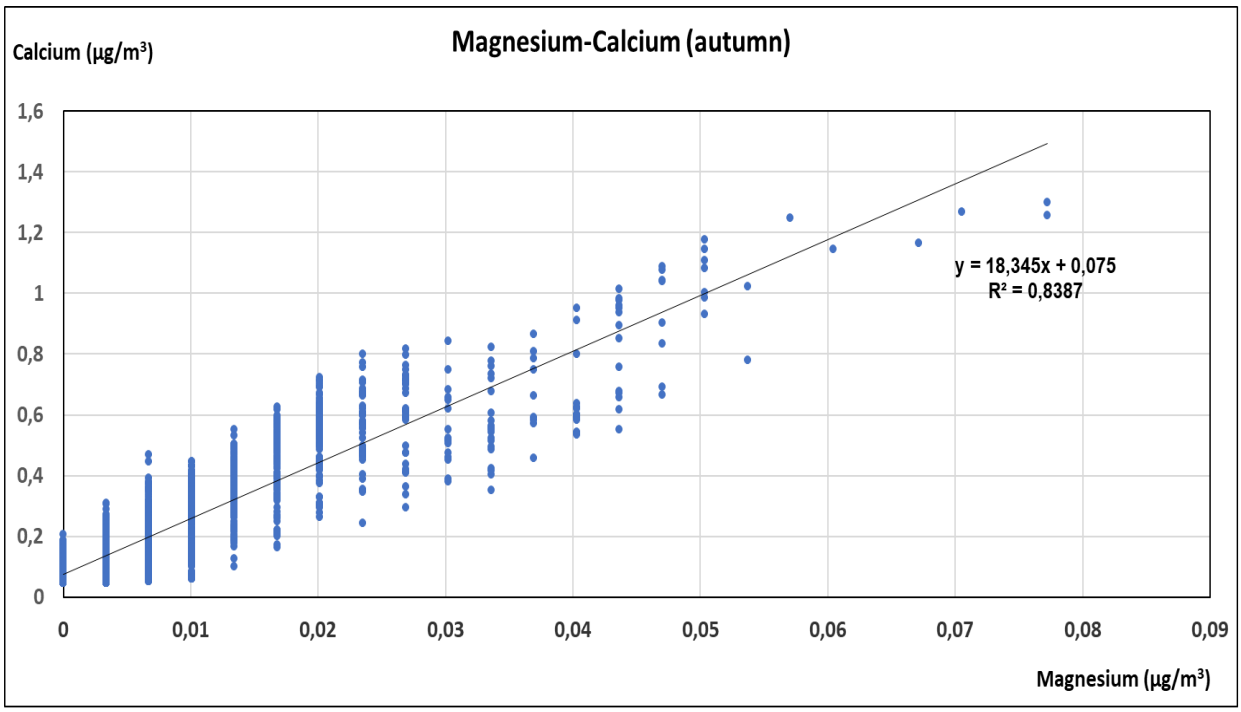

Figure 4.49: Correlation of Calcium with Magnesium during autumn

Also, the correlation of magnesium with sodium indicate a correlation coefficient of R^2=0,66. These two substances are main components of sea salt and during autumn they contribute significantly to the chemical composition of PM_1. The correlation is displayed in the next Figure 4.46.

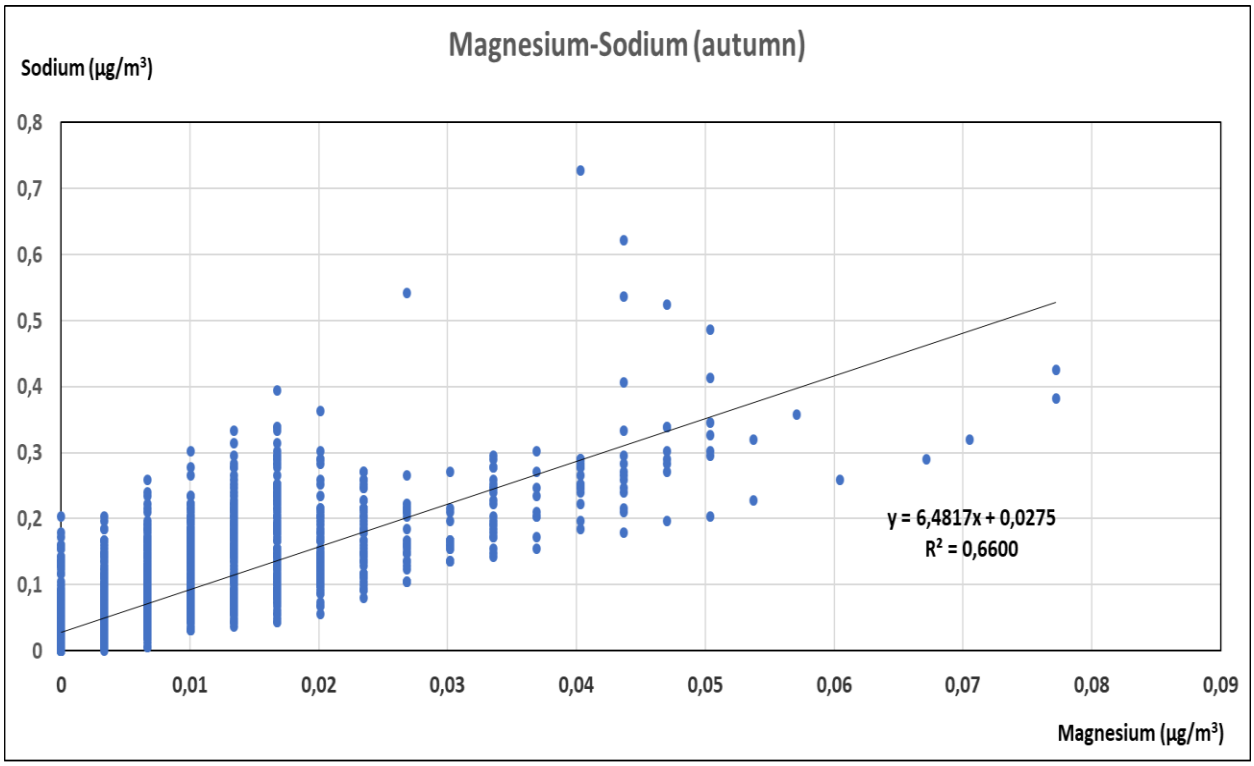

Figure 4.50: Correlation of Magnesium with Sodium during autumn

The same outcome is derived from the correlation of calcium with sodium. They indicate a correlation coefficient of R^2=0,48 during autumn (Table 4.6) and they contribute to the chemical composition of fine particulate matter as components of sea sources. Their correlation is presented in the following Figure 4.47.

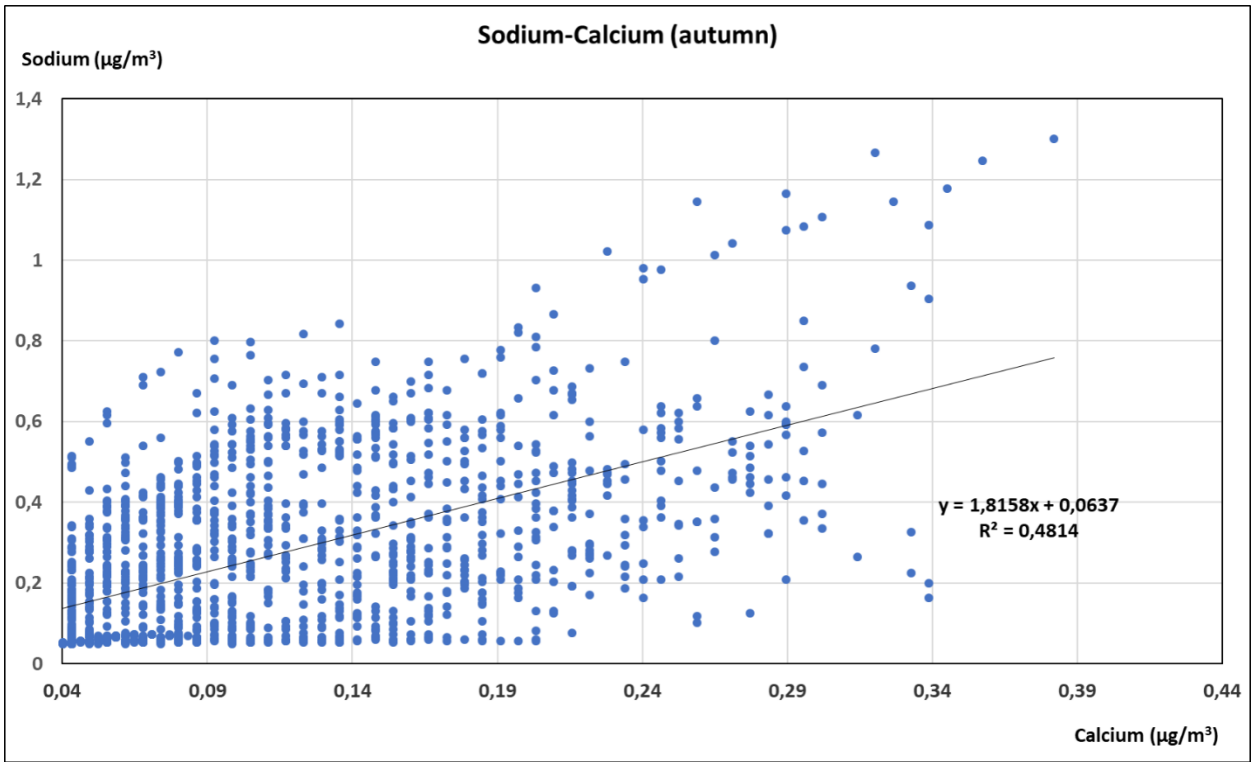

Figure 4.51: Correlation of Sodium with Calcium during autumn

In the following Figure 4.48 the correlation of BC with potassium during autumn is presented. This correlation indicates the presence of PM_1 from combustion of fossil fuel. During autumn they indicate a correlation coefficient of R^2=0,40 and contribute significantly to the chemical composition of fine particulate matter as components of combustion.

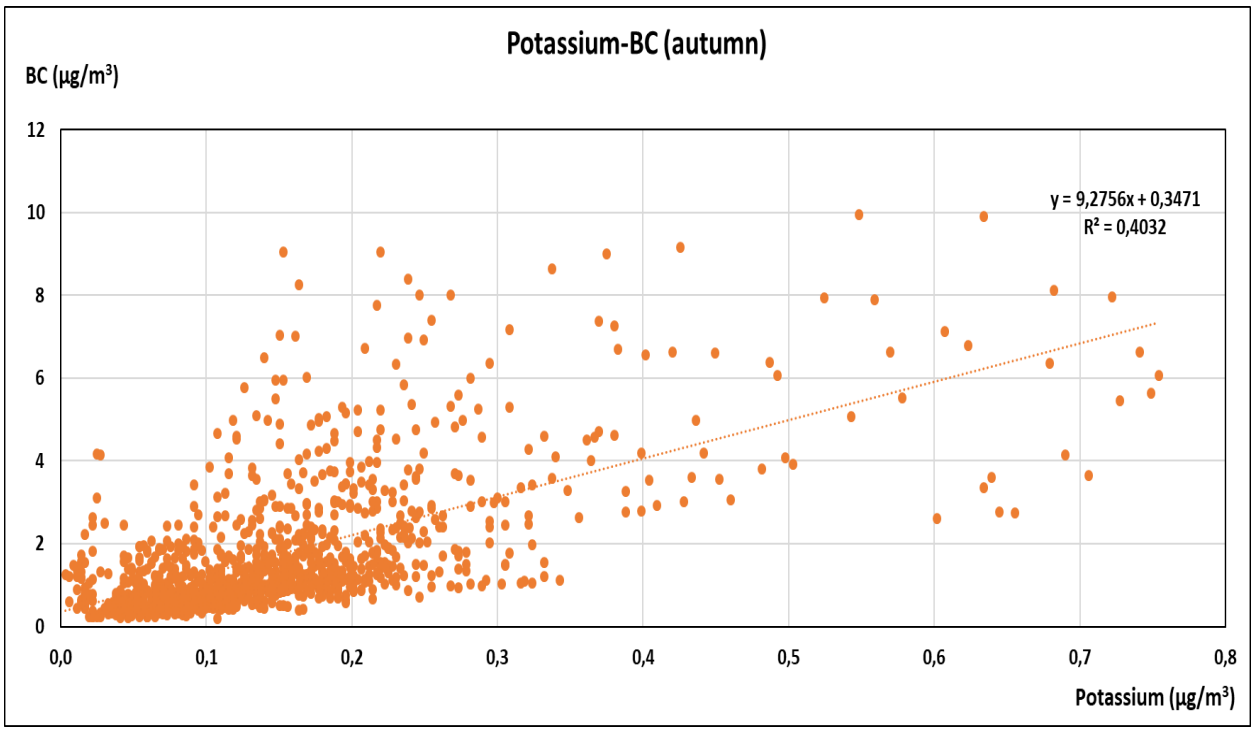

Figure 4.52: Correlation of Potassium with BC during autumn

In the next Figure 4.49 the correlation of calcium with potassium during autumn is presented. These two cations although they are not actually correlated, as $R^2 \approx 0$, from the Figure 4.48 it can be derived the conclusion that the high concentrations of calcium are probably due to dust events.

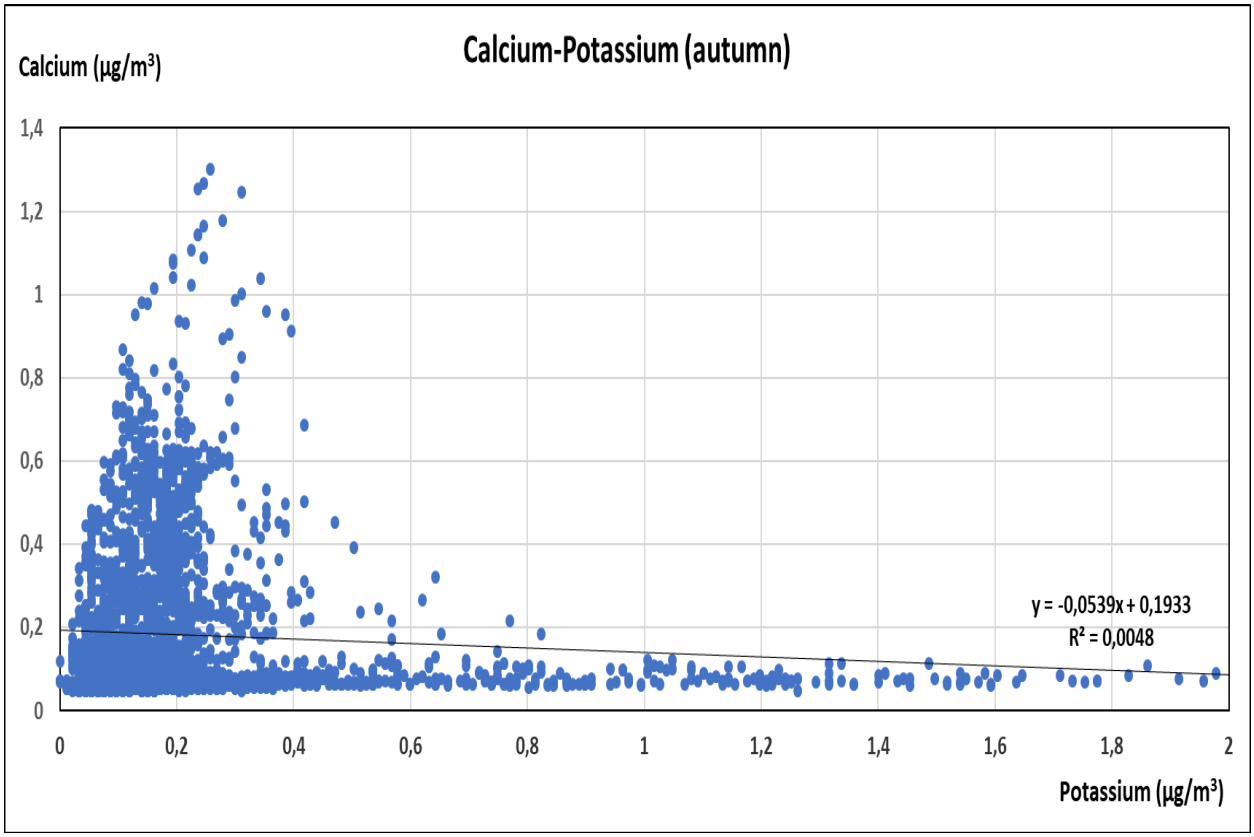

Figure 4.53: Correlation of Potassium with Calcium during autumn

4.5.2.8 Diurnal Variations during Autumn

4.5.2.8.1 Diurnal Variation of Magnesium with Calcium during Autumn

The hourly variability of magnesium with calcium is displayed in the following Figure 4.50. The two cations indicate approximately the same hourly variability during autumn.

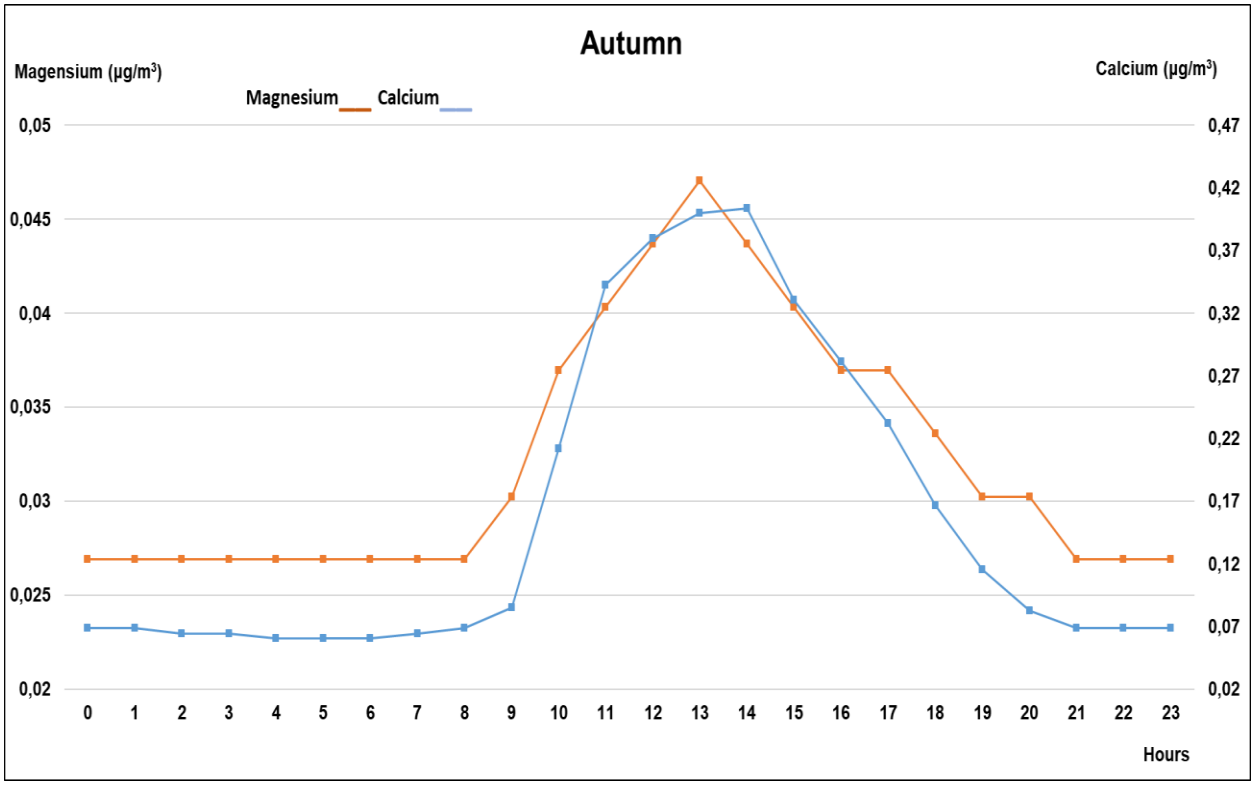

Figure 4.54: Diurnal variation of magnesium with calcium during autumn

4.5.2.8.2 Diurnal Variation of Magnesium with Sodium during Autumn

In the following Figure 4.51 the diurnal variation of magnesium with sodium during autumn is presented. The two cations indicate approximately the same variability during this season.

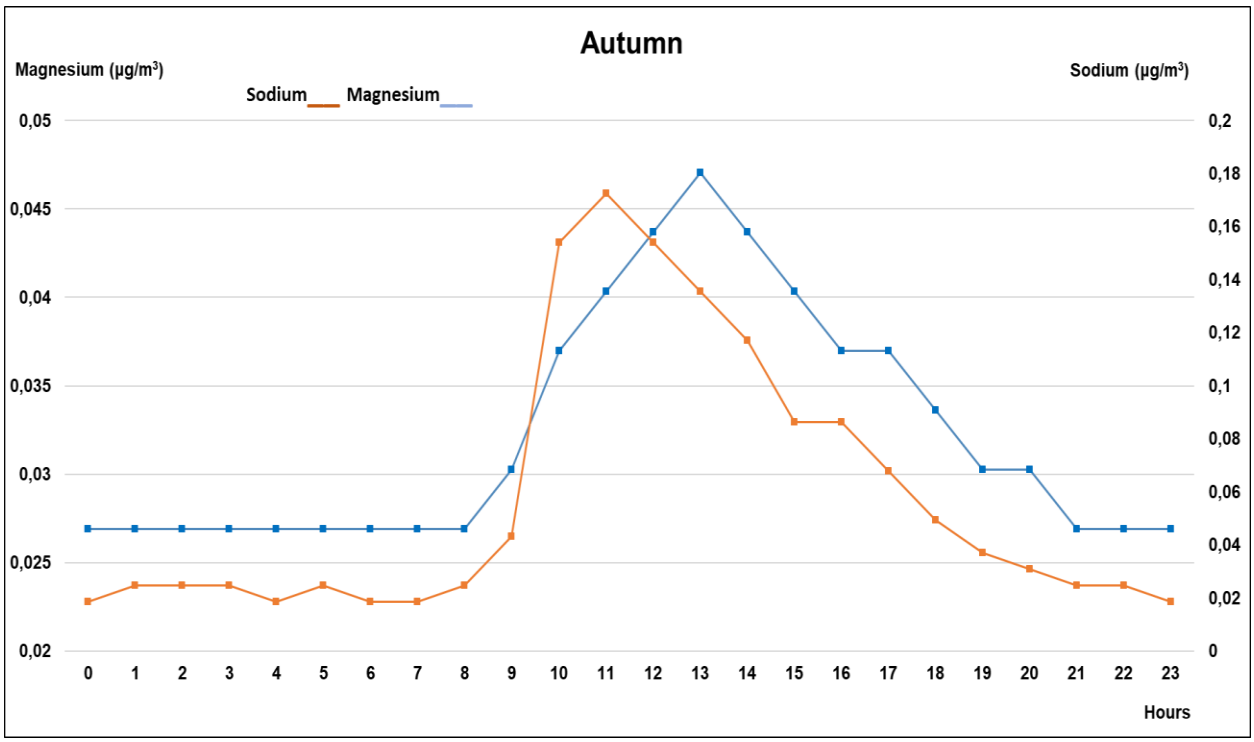

Figure 4.55: Diurnal variation of magnesium with sodium during autumn

4.5.2.8.3 Diurnal Variation of Calcium with Sodium during Autumn

In the following Figure 4.52 the diurnal variation of calcium with sodium during autumn is presented. The two cations indicate approximately the same hourly variation.

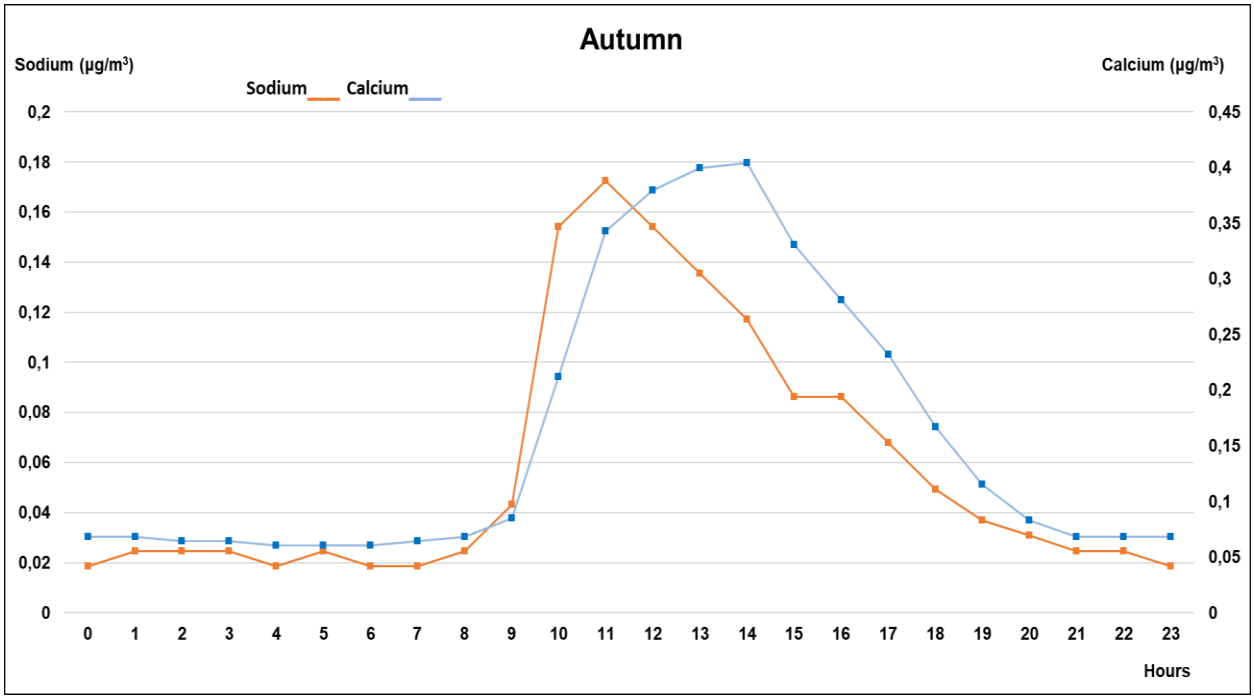

Figure 4.56: Diurnal variation of calcium with sodium during autumn

4.5.2.8.4 Diurnal Variation of Ammonium during Autumn

The diurnal variation of ammonium during the months of autumn is displayed in the next Figure 4.53.

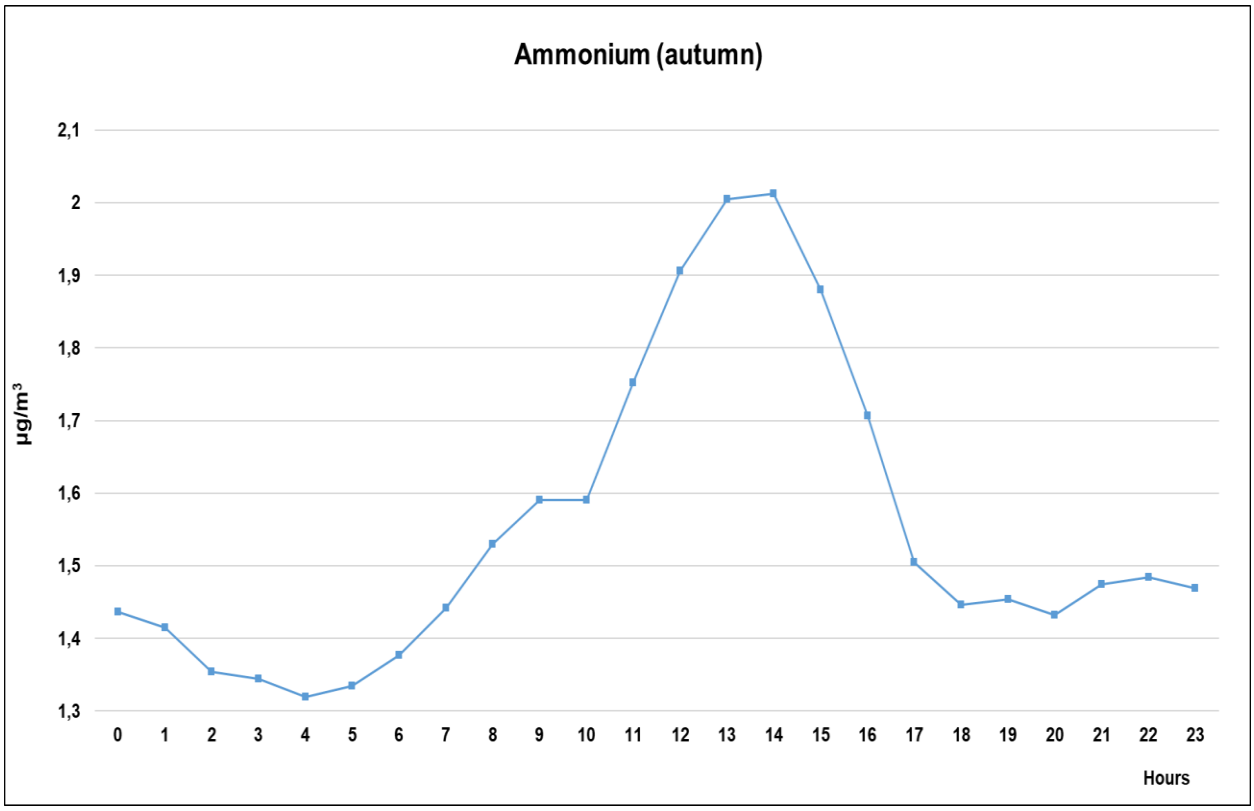

Figure 4.57: Diurnal variation of ammonium during autumn

From the Figure 4.53 it is indicated that the concentration of ammonium is increasing during the daytime hours. Similar performance is presented during summer and spring. This performance is a result of ammonium's secondary photochemical behavior as explained in the chapter 4.4.2.2.7 Diurnal Variation of Ammonium during Spring. Moreover, the increase of the concentration from 20:00 until 00:00 can be explained from the reasoning of the chapter 4.5.3 Diurnal variation of Ammonium.

5 CONCLUSIONS

A new analytical technique has been developed for the measurement of fine particulate matter in the urban area of Athens. PILS sampler coupled with IC provided information for the concentration of the cations in the atmosphere approximately for 10 months. This technique is reliable, indicates high resolution, provides results in real time, is fast and affordable. The chemical characterization of PM_1 which consequently highlights the possible pollution sources can lead to protection measures.

The average concentrations for the whole sampling period, except of Mg^{+2}, are comparable with previous studies in the greater area, which used filters as a sampling method. The correlations of the cations and with Black Carbon are all statistically significant for the whole sampling period and for the four seasons separately. During the whole sampling period there was a high influence of crustal sources in the chemical composition of PM_1.

More specifically, for **Na^+** the high concentrations during May and September are sea salt transportation.

For **Ca^{+2}** the high concentrations during May and August are attributed to a combination of marine and crustal sources. Also, the high concentrations in the end of the summer are due to dust recirculation and low precipitation.

Moreover, **Mg^{+2}** indicates similar variability with Ca^{+2} and the high concentrations during May, August and September, are also attributed to a combination of marine and crustal sources. Like Ca^+, the high concentrations in the end of the summer are due to dust recirculation and low precipitation.

Furthermore, **K^+** displays high concentrations from February until April and during August. This increase is a result of fossil fuel and biomass combustion.

Additionally, **BC** indicates similar monthly variability with K^+. The high concentration during the cold months is attributed to combustion of fossil fuel for heating. Also, the high concentrations during June and July are a result of biomass combustion from fires.

As for **NH_4^+** which is a secondary produced particulate matter through photochemical reactions, indicates higher concentrations during the warm months. Also, the increase during the night hours in all the seasons can be explained from the dissociation of NH_4NO_4 and/or $(NH_4)_2SO_4$ which happens at low temperatures and at Relative Humidity (RH) above the deliquescence. However, this reasoning has to be confirmed with meteorological conditions and with the concentrations of NO_4^- and SO_4^{-2}.

The correlation of the studied cations and BC during every season provides more specific results for the origin of PM_1. During the **winter** months BC and K^+ indicate the highest R^2 of all seasons. Moreover, they display similar hourly variability. As they are both components of combustion this leads to the fact that during winter their production is mainly through fossil fuel combustion for heating and secondarily for transportation.

Furthermore, during **spring** is indicated also high R^2 for BC with K^+ and this can be explained from the use of heating approximately until the first days of April. Also, the correlations that indicate possible marine sources (Mg^{+2} - Na^+ and Ca^{+2} - Na^+) during this season are relatively high. This can be explained from the sea breezes that prevail during these months. Additionally, great influence of crustal sources is displayed through the high R^2 of Ca^{+2} with Mg^{+2}.

During **summer**, the correlations that indicate marine sources (Mg^{+2} - Na^+ and Ca^{+2} - Na^+) display high R^2. The same outcome is derived for the correlations that indicate crustal sources (Mg^{+2} - Ca^{+2}, Mg^{+2} - K^+ and Ca^{+2} - K^+). Also, Mg^{+2} with Na^+ and Ca^{+2} with Na^+ indicate similar hourly variability. Simultaneously, similar hourly variability is displayed for Mg^{+2} with Ca^{+2} which are mainly emitted from crustal sources. Moreover, NH_4^+ indicates high concentrations due to intense solar radiation.

Additionally, during **autumn** BC with K^+ indicate high R^2 probably due to the use of heating. Also, the correlations that indicate sea salt transportation (Mg^{+2} - Na^+ and Ca^{+2} - Na^+) display the highest R^2 of all seasons and similar diurnal variability. Furthermore, Mg^{+2} with Ca^{+2} indicate similar hourly variability. The correlation of Ca^{+2} with K^+ (correlation that indicated crustal sources) although it displays very low R^2, it reveals the influence of dust events as the concentration of Ca^{+2} is relatively high.

The results of this research need to be further investigated with meteorological conditions. Also, measurements with the specific technique at a suburban or remote area could contribute to the understanding of anthropogenic influence in the fraction of fine particulate matter.

Bibliography

1. Environmental Protection Agency, Greenhouse Gas Emissions & Sinks Glossary,2004;
https://ofmpub.epa.gov/sor_internet/registry/termreg/searchandretrieve/glossariesandkeywordlists/search.do?details=&glossaryName=Greenhouse%20Emissions%20Glossary

2. P. Brimblecombe, Interest in Air Pollution among Early Fellows of the Royal Society, Notes and Records of the Royal Society, 1978; 32:123-129.
3. M. Pabst and F. Hofer, Deposits of different origin in the lungs of the 5,300-year-old Tyrolean Iceman, American Journal of Physical Anthropology, 1998; 107(1):1-12.
4. Y. Mamane, Air Pollution Control in Israel during the First and Second Century, Atmospheric Environment, 1987; 21:1861-1863.
5. H. Heimann, Effects of Air Pollution on Human Health, World Health Organization, 1961.
6. M. Katz, Some Aspects of the Physical and Chemical Nature of Air Pollution, World Health Organization, 1961.
7. World Health Organization, Burden of disease from Ambient Air Pollution for 2012-Summary of results, 2014;
http://www.who.int/phe/health_topics/outdoorair/databases/AAP_BoD_results_March2014.pdf

8. International Agency for Research on Cancer, Outdoor air pollution a leading environmental cause of cancer deaths, 2013;
http://www.iarc.fr/en/media-centre/iarcnews/pdf/pr221_E.pdf

9. G. Batta, J. Firket, and E. Leclerc, Les problemes de pollution de l'atmosphere, Georges Thone, 1933.
10. R. D. Fletcher, The Donora Smog Disaster-A problem in Atmospheric Pollution, Weatherwise, 1949; 2:56-60.
11. C. A. Mills, Donora Smog Disaster, Hygeia, 1949a; 27:684.
12. C. A. Mills, The Donora disaster, Journal of the American Medical Association, 1949b; 140:556.
13. H. H. Schrenk, H. Heimann, G. D. Clayton, W. M. Gafafer and H. Wexler, Air pollution in Donora, Pennsylvania, Washington, Public Health Service Bulletin, 1949; 306.
14. J. Shilen, The Donor Disaster, Industrial Medicine and Surgery, 1949; 18(2):70.
15. J. Shilen, J. F. Mellor, A. M. Stang, J. S. Sharrah and C. D. Robson, The Donora smog disaster, Pennsylvania Department of Health, 1949.
16. C. A. Mills, The Donora Episode, Science, 1950; 111:67.
17. B. Roueche, The Fog, The New Yorker, 1950; 26(31):33.
18. L. C. McCabe (ed.), Air pollution. Proceedings of the United States Technical Conference on Air Pollution, McGraw-Hill, 1952.
19. W. P. D. Logan, Mortality in the London Fog Incident, 1952. Lancet, (1953); 1(6,755):336.
20. L. C. McCabe, XIIth International Congress Atmospheric Pollution, Industrial and Engineering Chemistry, 1951; 43(10):135A-138A.
21. L. C. McCabe and G. D. Clayton, American Medical Association Archives of Industrial Hygiene and Occupational Medicine, 1952; 6(3):199-213.

22. T. Wilkins, Air Pollution and the London Fog of December 1952, Journal of the Royal Sanitary Institute, 1954; 74:1-21.
23. S. S. Pinto, S. J. Petronella, D. R. John, and M. F. Arnold, Arsine Poisoning. A Study of Thirteen Cases, Archive of Industrial Hygiene and Occupational Medicine, 1950; 1(4):437.
24. M. Steel and D. V. G. Feltham, Arsine Poisoning in Industry. Report of a Case, Lancet, 1950; 1:108.
25. European Commission, Commission Staff Working Document Accompanying the Communication on a revised EU Strategy on Air Pollution Proposal for a revision of Directive 2001/81/EC on national emission ceilings for certain atmospheric pollutants. Proposal for a legislative instrument on control of emissions from Medium Combustion Plants-Impact Assessment, 2013;
http://ec.europa.eu/environment/archives/air/pdf/Impact_assessment_en.pdf
26. European Environment Agency, Air quality in Europe-2015 report, 2015;
https://www.eea.europa.eu/publications/air-quality-in-europe-2015

27. E. J. Catcott, Effects of Air Pollution on Animals, World Health Organization, 1961.
28. British Medical Journal, 1953; 1:321.
29. H. Joules, A preventive approach to common diseases of the lung, British Medical Journal, 1954; 2:1259-1264.
30. R. A. Solberg and D. F. Adams, Histological Responses of Some Plant Leaves to Hydrogen Fluoride and Sulfur Dioxide, American Journal of Botany, 1956; 43:755.
31. M. D. Thomas and R. H. Hendricks, Effects of Air Pollution on Plants. Air Pollution Handbook, McGraw-Hill, 1956.
32. J. Haagen-Smit, Chemistry and Physiology of Los Angeles Smog, Industrial and Engineering Chemistry, 1952; 44(6):1342-1346.
33. J. T. Middleton, J. B. Kendrick Jr. and D. F. Darley, In: Proceedings of the third national air pollution symposium, Stanford Research Institute, 1955;pp.191.
34. B. L. Richards, J. T. Middleton, & W.B. Hewett, Air pollution with relation to agronomic crops. V.Oxidant stipple of grape, Agronomy Journal, 1958; 50:559.
35. Layfield-Acid Rain Effects On Plants Picture Gallery 2018;
http://www.avril-paradise.com/acid-rain-effects-on-plants/picture-of-wits-end-ecopornography-acid-rain-effects-on-plants/

36. D. Woodfall, Norway spruce trees affected by acid rain, National Geographic/Getty Images, 2009;
https://www.nationalgeographic.com/environment/global-warming/acid-rain/

37. J. T. Middleton, D. F. Darley and R. F. Brewer, Damage to vegetation from polluted atmospheres, Journal of the Air Pollution Control Association, 1958;8(1):9-15.
38. M. D. Thomas, R. H. Hendricks and G. R. Hill, Some impurities in the air and their effect on plants. In L. C. McCabe (ed.), Air pollution. Proceedings of the United States Technical Conference on Air Pollution, McGraw-Hill, 1952.
39. D.P. Kaiser and Y. Qian, Decreasing Trends in Sunshine Duration over China for 1954-1998: Indication of Increased Haze Pollution?, Geophysical Research Letters, 2002; 29:2042-2045.
40. Y. Quian and F. Giorgi, Regional Climatic Effects of Anthropogenic Aerosols? The Case of Southwestern China, Geophysical Research Letters, 2000; 27:3521-3524.
41. S. Menon, J. E. Hansen, L. Nazarenko and Y. Luo, Climate Effects of Black Carbon Aerosols in China and India, Science, 2002; 297(5590):2250-2252.

42. D. Rosenfeld, Suppression of Rain and Snow by Urban and Industrial Air Pollution, Science, 2000; 287:1793-1796.
43. J. M. Molina and T. L. Molina, Megacities and Atmospheric Pollution. Journal of the Air & Waste Management Association, 2004; 54(6):644-680.
44. United Nations Environment Program, Northeast Asian dust and sand storms growing in scale and intensity, 2004;
http://www.unep.org/Documents.Multilingual/Default.Print.asp?DocumentID_389&ArticleID_4401&1_en.

45. British Broadcasting Corporation, China sandstorm leaves Beijing shrouded in orange dust, 2010;
http://news.bbc.co.uk/2/hi/asia-pacific/8577806.stm

46. E. Leclerc, Economic and social aspects of air pollution. World Health Organization, 1961.
47. United Nations Population Division. World Urbanization Prospects: The 2003 Revision, 2004;
http://www.un.org/esa/population/publications/wup2003/2003WUPHighlights.pdf

48. National Research Council, Global Air Quality: An Imperative for Long-Term Observational Strategies, National Academy Press, 2001.
49. P. Kassomenos, N. A. Skouloudis, S. Lykoudis and A. H. Flocas, ‘‘Air-quality indicators’’ for uniform indexing of atmospheric pollution over large metropolitan areas. Atmospheric Environment, 1999; 33:1861-1879.
50. E. T. Wilkins, Air Pollution and the London Fog of December 1952, Journal of the Royal Sanitary Institute, 1954; 74:1-21.
51. J. T. Middleton, J. B.. Kendrick Jr. and H. W. Schwalm, Injury to Herbaceous Plants by Smog or Air Pollution, United States Department of Agriculture-Plant Disease Report, 1950; 34:245-252.
52. A. J. Haagen-Smit, Chemistry and Physiology of Los Angeles Smog, Industrial & Engineering Chemistry, 1952; 44:1342-1346.
53. A. J. Haagen-Smit, E. F. Darley, M. Zaitlin, H. Hull, and W. Noble, Investigation on Injury to Plants from Air Pollution in the Los Angeles Area, Plant Physiology, 1952; 27:18-34.
54. A. J. Haagen-Smit, C. E. Bradley and M. M. Fox, Ozone Formation in Photochemical Oxidation of Organic Substances, Industrial & Engineering Chemistry, 1953; 45:2086-2089.
55. A. J. Haagen-Smit and M. M. Fox, Photochemical Ozone Formation with Hydrocarbons and Automobile Exhaust, Air Repair, 1954; 4:108-136.
56. A. J. Haagen-Smit and M. M. Fox, Automobile Exhaust and Ozone Formation, SAE Transactions, 1955; 63:575-580.
57. A. J. Haagen-Smit, and M. M. Fox, Ozone Formation in Photochemical Oxidation of Organic Substances, Industrial & Engineering Chemistry, 1956; 48:1484-1487.
58. Hulton Getty, Piccadilly Circus, London in the smog: On the weekend that began on Friday December 5 1952, 2018;
https://www.telegraph.co.uk/news/weather/11980339/Weather-Watch-a-foggy-spell-in-London-town.html

59. Daily News, Los Angeles in smog, 2012;
https://www.newscientist.com/article/dn22209-los-angeles-smog-thins-but-remains-a-threat/

60. J. B. Finlayson-Pitts and J. N. Pitts Jr., Chemistry of the Upper and Lower Atmosphere Theory, Experiments, and Applications. Academic Press, 2000.
61. P. Mavroidis and D. Palmeter, Dictionary of Environmental Engineering and Wastewater Treatment, Springer, 1995.
62. Bahadori and S. T. Smith, Dictionary of Environmental Engineering and Wastewater Treatment, Springer 2016.
63. J. Speight, Environmental Inorganic Chemistry for Engineers, Butterworth Heinemann, 2017.
64. Australian Government Department of the Environment and Energy, Air pollutants, 2018;
http://www.environment.gov.au/protection/air-quality/air-pollutants

65. Environmental Protection Agency, What are Hazardous Air Pollutants?M 2018a;
https://www.epa.gov/haps/what-are-hazardous-air-pollutants

66. The Department of the Environment and Heritage, Living Cities-Air toxic Program, Australian Government, 2002.
67. J. Douwes, P. Thorne, N. Pearce and D. Heederik, Bioaerosol Health Effects and Exposure Assessment: Progress and Prospects, The Annals of Occupational Hygiene, 2003; 47(3):187-200.
68. Environmental Protection Agency, Biological Pollutants Impact on Indoor Air Quality, 2018b;
https://www.epa.gov/indoor-air-quality-iaq/biological-pollutants-impact-indoor-air-quality

69. Y. Wang, C. Wang and K. Hsu, Size and seasonal distributions of airborne bioaerosols in commuting trains, Atmospheric Environment, 2010;44:4331-4338.
70. X. Briottet, Radiometry in the Optical Domain, Optical Remote Sensing of Land Surface. Techniques and Methods, Elsevier Ltd., 2017.
71. R. Kahn, Satellites and Satellite Remote Sensing, Aerosol Measurements, Encyclopedia of Atmospheric Sciences (Second Edition), Elsevier Science Ltd, 2015.
72. J. Haywood, Climate Change. Observed Impacts on Planet Earth (Second Edition), Elsevier Science Ltd. 2015.
73. A. Tsuda, F. Henry. and J. Butler, Particle transport and deposition: basic physics of particle kinetics, Comprehensive Physiology, 2013; 3(4):1437-1471.
74. J. L. Goodwin, Aerosol Physics and Particle Control, 2018;
https://slideplayer.com/slide/7454706/

75. W.C. Hinds, Aerosol Technology, John Wiley, 1983.
76. P. Buseck and P. Chere, Variety of aerosol shapes, United States Geological Survey, University of Maryland Baltimore County and Arizona State University,2018;
https://www.nasa.gov/centers/langley/news/factsheets/Aerosols.html

77. L. Silverman, C.E. Billings and M.W. First, Particle size analysis in industrial hygiene, Academic Press, 1971.
78. International Union of Pure and Applied Chemistry, Compendium of Chemical Terminology 2nd ed. (the "Gold Book"), Blackwell Scientific Publications, 1997.
79. Atmospheric Chemistry Division National Center for Atmospheric Research, Glossary of Atmospheric Chemistry Terms, International Union of Pure and Applied Chemistry, 1990.

80. S. Karthika, T. K. Radhakrishnan and P. Kalaichelvi. A Review of Classical and Non Classical Nucleation Theories, Crystal Growth and Design, 2016;16 (11):6663-6681.
81. A.J. Hickey and T.B. Martonen, Behavior of hygroscopic pharmaceutical aerosols and the influence of hydrophobic additives, Pharmaceutical Research, 1993; 10(1):1-7.
82. E. Wilson, Fine and coarse particles: chemical and physical properties important for the standard-setting process, National Center for Environmental Assessment, Environmental Protection Agency, 1999.
83. T. Sandström, D. Nowak and L. van Bree, Health effects of coarse particles in ambient air: messages for research and decision-making, European Respiratory Journal, 2005; 26:187-188.
84. C. Vignal, M. Pichavant, L. Alleman, M. Djouina, F. Dingreville, E. Perdrix, C. Waxin, A. Alami, C. Gower-Rousseau, P. Desreumaux and M. Body-Malapel, Effects of urban coarse particles inhalation on oxidative and inflammatory parameters in the mouse lung and colon, Particle and Fibre Toxicology, 2017; 14:46.
85. S. C. Lee, Y. Cheng, K. F. Ho, J. J. Cao, P. K.-K. Louie, J. C. Chow and J. G. Watson, PM1.0 and PM2.5 Characteristics in the Roadside Environment of Hong Kong, Aerosol Science and Technology, 2006;40:157–165.
86. R. Zhang, J. Jing, J. Tao, S.-C. Hsu, G. Wang, J. Cao, C. S. L. Lee, L. Zhu, Z. Chen, Y. Zhao, and Z. Shen, Chemical characterization and source apportionment of PM2.5 in Beijing: seasonal perspective, Atmospheric Chemistry and Physics, 2013; 13:7053-7074.
87. S. Masri, C.M. Kang and P. Koutrakis, Composition and sources of fine and coarse particles collected during 2002–2010 in Boston, Journal of the Air&Waste Management Association 2015; 65(3):287-97.
88. Y. Zhu, W.C. Hinds, K. Seongheon, S. Shen and C. Sioutas, Study of ultrafine particles near a major highway with heavy-duty diesel traffic, Atmospheric Environment, 2002; 36:4323-4335.
89. C. Terzano , F. Di Stefano, V. Conti , E. Graziani and A. Petroianni, Air pollution ultrafine particles: toxicity beyond the lung, European Review for Medical and Pharmacological Sciences. 2010; 14(10):809-821.
90. R. Baldauf, R. Devlin, P. Gehr, R. Giannelli, B.Hassett-Sipple, H. Jung , G. Martini, J. McDonald, J. Sacks and K. Walker, Ultrafine Particle Metrics and Research Considerations: Review of the 2015 UFP Workshop, International Journal of Environmental Research and Public Health, 2016; 13(11):1054.
91. J.P. Shi, D.E. Evans, A.A. Khan and R.M. Harrison, Source and concentration of nanoparticles (<10nm diameter) in the urban environment, Atmospheric Environment 2001; 35(7):1193-1202.
92. M. Methner, L. Hodson and C. Geraci, Nanoparticle Emission Assessment Technique (NEAT) for the Identification and Measurement of Potential Inhalation Exposure to Engineered Nanomaterials-Part A, Journal of Occupational and Environmental Hygiene, 2009; 7(3):127-132.
93. O. V. Karpov, D. M. Balakhanov, E. V. Lesnikov, D. A. Dankin, V. B. Lapshin, A. A. Paliy, A. V. Syroeshkin, V. A. Zagaynov and I. E. Agranovskii, Nanoparticles in Ambient Air. Measurement Methods, Measurement Techniques, 2011, 54(3):269-274.
94. D. Levin, Big Road Blues:Living near a highway can be bad for your health in a million small ways, TuftsNow 2012.
95. M.O. Andreae and D. Rosenfeld, Aerosol-cloud-precipitation interactions. Part 1. The nature and sources of cloud-active aerosols, Earth-Science Reviews, 2008; 89(1-2):13-41.

96. A. Bougiatioti, P. Zarmpas, E. Koulouri, M. Antoniou, C. Theodosi, G.Kouvarakis, S. Saarikoski, T. Mäkelä, R. Hillamo and N. Mihalopoulos,Organic, elemental and water-soluble organic carbon in size segregated aerosols, in the marine boundary layer of the Eastern Mediterranean, Atmospheric Environment , 2013; 64:251-262.
97. J. J. Schauer, W.F. Rogge, L.M. Hildemann, M.A. Mazurek, G.R. Cass and B.R.T. Simoneit, Source apportionment of airborne particulate matter using organic compounds as tracers, Atmospheric Environment, 1996; 30(22):3837-3855.
98. K. F. Boon, L. Kiefert and G. H. Ctainsh, Organic Matter Content of Rural Dust in Australia. Atmospheric Environment, 1998; 32(16):2817-2823.
99. J. H. Seinfeld and S. N. Pandis, Atmospheric chemistry and physics: from air pollution to climate change, Wiley, 2006.
100. M. Kanakidou, K. Tsigaridis, F. J. Dentener and P. J. Crutzen, Human activity enhanced formation of organic aerosols by biogenic hydrocarbon oxidation, Journal of Geophysical Research 2000; 105 (D7):9243-9254.
101. J. De Gouw and J. L. Jimenez, Organic aerosols in the Earth's Atmosphere, Atmospheric Science and Technology, 2009; 43(20):7614-7618.
102. P. Saxena and L. M. Hildemann, Water absorption by organics: Survey of laboratory evidence and evaluation of UNIFAC for estimating water activity, Environmental Science and Technology, 1997; 31(11):3318- 3324.
103. J. P. Putaud, F. Raes, R. Van Dingenen, E., Brüggemann, M. C. Facchini, S. Decesari, S. Fuzzi, R. Gehrig, C. Hüglin, P. Laj, G. Lorbeer, W.Maenhaut, N. Mihalopoulos, K. Müller, X. Querol, S. Rodriguez, J.Schneider, G. Spindler, ten Brink, H, K. Tørseth, and A. Wiedensohler, A European aerosol Phenomenology-2: chemical characteristics of particulate matter at kerbside, urban, rural and background sites in Europe, Atmospheric Environment, 2004; 38 (16):2579-2595.
104. M. Kanakidou, J.H. Seinfeld, S.N. Pandis, I. Barnes, F.J. Dentener, M.C. Facchini, R. Van Dingenen, B. Ervens, A. Nenes, C.J. Nielsen, E. Swietlicki, J.P. Putaud, Y. Balkanski, S. Fuzzi, J. Horth, G.K. Moortgat, R. Winterhalter, C.E.L. Myhre, K. Tsigaridis, E. Vignati, E.G.Stephanou and J. Wilson, Organic aerosol and global climate modeling: a review, Atmospheric Chemistry and Physics, 2005;5(4):1053-1123.
105. R. J. Weber, A.P. Sullivan, R.E. Peltier, A.Russell, B. Yan, M. Zheng, J. de Gouw, C. Warneke, C. Brock, J.S. Holloway, E.L. Atlas and E. Edgerton, A study of secondary organic aerosol formation in the anthropogenic-influenced southeastern United States, Journal of Geophysical Research, 2007; 112(D133).
106. S.-S. Park, J. J. Schauer and S.-Y. Cho, Sources and their contribution to two water-soluble organic carbon fractions at a roadway site, Atmospheric Environment, 2013; 77:348-357.
107. N. M. Donahue, A. L. Robinson and S. N. Pandis, Atmospheric organic particulate matter: from smoke to secondary organic aerosol, Atmospheric Environment, 2009; 43:94-106.
108. M. Dall'Osto, D. C. S. Beddows, R. P. Kinnersley, R. M. Harrison, R.J. Donovan and M.R. Heal, Characterisation of individual airborne particles by using aerosol time-of-flight mass spectrometry at Mace Head, Ireland. Journal of Geophysical Research, 2004; 109(D21302).
109. S.A. Guazzotti, K.R. Coffee and K.A. Prather, Continuous measurements of size-resolved particle chemistry during INDOEX-Intensive Field Phase 99, Journal of Geophysical Research 2001; 106(D22):28607-28628.
110. F. Mirante, P. Salvador, C. Pio, C. Alves, B. Artiñano, A. Caseiro, and Mª A.

Revuelta, Size fractionated aerosol composition at roadside and background environments in the Madrid urban atmosphere, Atmospheric Research, 2014; 138:278-292.
111. L. B. Lave and E. P. Seskin, Air pollution and human health, Science, 1970;169:723-733.
112. R. Mendelsohn and G. Orcutt, An empirical analysis of air pollution dose response curves, Journal of Environmental Economics and Management, 1979; 6:85-106.
113. J.S. Evans, T. Tosteson and P. L. Kinney, Cross-sectional mortality studies and air pollution risk assessment, Environment International, 1984; 10:55-83.
114. F.W. Lipfert, Air pollution and mortality: specification searches using SMSA-based data, Journal of Environmental Economics and Management, 1984; 11: 208-243.
115. H. Ozkaynak and G.D. Thurston, Associations between 1980 U.S. mortality rates and alternate measures of airborne particle concentrations, Risk Analysis, 1987; 7:449-461.
116. F. W. Lipfert, R. G. Malone, M. L. Daum, N. R. Mendell and C. C. Yang, A statistical study of the macroepidemiology of air pollution and total mortality, No. BNL-52122. Brookhaven National Lab. Upton, N.Y. (USA), 1988.
117. C. A. Pope III, Epidemiology of Fine Particulate Air Pollution and Human Health: Biologic Mechanisms and Who's at Risk?, Environmental Health Perspectives, 2000; 108(4): 713-723.
118. World Health Organization, Ambient (outdoor) air quality and health, 2018; http://www.who.int/news-room/fact-sheets/detail/ambient(outdoor)-air-quality-and-health.

119. T. Schikowski, D. Sugiri, U. Ranft, U. Gehring, J. Heinrich, H-E. Wichmann and U Krämer, Long-term air pollution exposure and living close to busy roads are associated with COPD in women. Respiratory Research. 2005;6(1):152.
120. G. Viegi, S. Maio, F. Pistelli, S. Baldacci and L. Carrozzi, Epidemiology of chronic obstructive pulmonary disease: health effects of air pollution, Respirology,2006; 11(5):523-532.
121. S. Liu, Y. Zhou, X. Wang, D. Wang, J. Lu , J. Zheng , N. Zhong and P. Ran, Biomass fuels are the probable risk factor for chronic obstructive pulmonary disease in rural South China, Thorax, 2007; 62(10):889-897.
122. S. H. Ling and S. F. van Eeden, Particulate matter air pollution exposure:role in the development and exacerbation of chronic obstructive pulmonary disease, International Journal of Chronic Obstructive Pulmonary Disease, 2009; 4: 233-243.
123. J. Wang, Z. Hu, Y. Chen, Z. Chen and S. Xu, Contamination characteristics and possible sources of PM10 and PM2.5 in different functional areas of Shanghai, China, Atmospheric Environment, 2013;68:221-229.
124. G.- C. Fang, C.- N. Chang, Y.- S. Wu, N.- P. Wang, V. Wang, P.P.-C. Fu and S.C. Chen, Comparison of particulate mass, chemical species for urban, suburban and rural areas in central Taiwan, Taichung, Chemosphere, 2000;41(9):1349-1359.
125. M. Hu, L.- Y. He, Y.- H. Zhang, M. Wang, Y. P. Kim and K. C. Moon, Seasonal variation of ionic species in fine particles at Qingdao, China, Atmospheric Environment, 2002; 36(38):5853-5859.
126. J. J. Lin, Characterization of water-soluble ion species in urban ambient particles, Environment International, 2002; 28(1-2):55-61.
127. F. K. Duan, K. B. He, Y. L. Ma, F. M. Yang, X. C. Yu, S. H. Cadle, T. Chan and P. A. Mulawa, Concentration and chemical characteristics of $PM_{2.5}$ in Beijing, China: 2001-2002, Science of the Total Environment, 2006; 355 (1-3):264-275.
128. N.T. K. Oanh, N. Upadhyaya, Y.- H. Zhuang , Z. - P. Hao , D.V.S. Murthy , P. Lestari , J. T. Villarin , K. Chengchua , H. X. Co , N.T. Dung and E. S. Lindgren,

Particulate air pollution in six Asian cities: Spatial and temporal distributions, and associated sources, Atmospheric Environment, 2006; 40(18):3367-3380.
129. E. Terzi, G. Argyropoulos, A. Bougatioti, N. Mihalopoulos, K. Nikolaou and C. Samara, Chemical composition and mass closure of ambient PM_{10} at urban sites, Atmospheric Environment, 2010; 44(18):2231-2239.
130. J. Ma, X. Xu, C. Zhao and P. Yan, A review of atmospheric chemistry research in China: photochemical smog, haze pollution, and gas-aerosol interactions, Advances in Atmospheric Sciences, 2012; 29:1006-1026.
131. Y. Sun, Q. Jiang, Z. Wang, P. Fu, J. Li, T. Yang and Y. Yin, Investigation of the sources and evolution processes of severe haze pollution in Beijing in January 2013, Journal of Geophysical Research: Atmospheres, 2014; 19:4380-4398.
132. T. Yang, A. Gbaguidi, P. Yan., W. Zhang, L. Zhu, X. Yao, Z. Wang and H. Chen, Model elucidating the sources and formation mechanisms of severe haze pollution over Northeast mega-city cluster in China, Environmental Pollution, 2017;230:692-700.
133. Y. Wang, L. Yao, L. Wang, Z. Liu, D. Ji, G. Tang, J. Zhang, Y. Sun, B. Hu and J. Xin, Mechanism for the formation of the January 2013 heavy haze pollution episode over central and eastern China, Science China Earth Sciences,2014;57 (1):14-25.
134. M. H. Bergin, Aerosol Radiative Properties and Their Impacts, School of Civil and Environmental Engineering and School of Earth and Atmospheric Sciences, Georgia Institute of Technology, 2004.
135. N. A. Marley, J. S. Gaffney, and M. M. Cunningham, Aqueous Greenhouse Species in Clouds, Fogs, and Aerosols, Environmental Science and Technology, 1993; 27:2864-2869.
136. J. S. Gaffney and N. A. Marley, Uncertainties of Aerosol Effects in Global Climate Models, Atmospheric Environment, 1998; 32:2873-2874.
137. J. E. Penner, R. J. Charlson, J. M. Hales, N. S. Laulainen, R. Leifer, T. Novakov, J. Ogren, L. F. Radke, S. E. Schwartz and L. Travis, Quantifying and minimizing uncertainty of climate forcing by anthropogenic aerosols, Bulletin of the American Meteorological Society, 1994; 75:pp. 375-400
138. I. Tegen, P. Hollrig, M. Chin, I. Fung, D. Jacob and J. Penner, Contribution of Different Aerosol Species to the Global Aerosol Extinction Optical Thickness: Estimates from Model Results, Journal of Geophysical Research, 1997; 102(D20):23,895-23,915.
139. H. Wang and D. Shooter, Coarse – fine and day–night differences of water soluble ions in atmospheric collected in Christchurch and Auckland, New Zealand, Atmospheric Environment, 2002; 36(21):3,519-3,529.
140. E. Manoli, D. Voutsa and C. Samara, Chemical characterization and source identification/apportionment of fine and coarse air particles in Thessaloniki, Greece, Atmospheric Environment, 2002; 36(6):949-961.
141. A. Vasilakos, S. Pateraki , D. Veros, T. Maggos, J. Michopoulos, D. Saraga and C.G. Helmis, 2006, Temporal determination of heavy metals in $PM_{2.5}$ aerosols in a suburban site of Athens, Greece. Journal of Atmospheric Chemistry, 2007; 57(1):1-17.
142. M. R. Harrison and J. Yin, 2000, Particulate matter in the atmosphere: which particle properties are important for its effects on health? Science of The Total Environment, 2000; 249(1-3):85-101.
143. S. Fuzzi, U. Baltensperger, K. Carslaw, S. Decesari, H. Denier van der Gon, M. C. Facchini, D. Fowler, I. Koren, B. Langford, U. Lohmann, E. Nemitz, S. Pandis, I. Riipinen, Y. Rudich, M. Schaap, J. G. Slowik, D. V. Spracklen, E. Vignati, M.

Wild, M. Williams, and S. Gilardoni, Particulate matter, air quality and climate: lessons learned and future needs, Atmospheric Chemistry and Physics, 2015; 15(14):8,217-8,299.
144. V. A. Lanz, A. S. H. Prévôt, M. R. Alfarra, S. Weimer, C. Mohr, P. F. DeCarlo, M. F. D. Gianini, C. Hueglin, J. Schneider, O. Favez, B. D'Anna, C. George and U. Baltensperger, Characterization of aerosol chemical composition with aerosol mass spectrometry in Central Europe: an overview, Atmospheric Chemistry and Physics, 2010; 10(21):10,453-10,471.
145. M. Crippa, P. F. DeCarlo, J. G. Slowik, C. Mohr, M. F. Heringa, R.Chirico, L. Poulain, F. Freutel, J. Sciare,J. Cozic, C. F. Di Marco, M. Elsasser, J. B. Nicolas, N. Marchand, E. Abidi, A. Wiedensohler, F. Drewnick, J. Schneider, S. Borrmann, E. Nemitz, R. Zimmermann, J.- L. Jaffrezo, A. S. H. Prévôt, and U. Baltensperger, Wintertime aerosol chemical composition and source apportionment of the organic fraction in the metropolitan area of Paris, Atmospheric Chemistry and Physics,2013a; 13(2):961-981.
146. M. Crippa, F. Canonaco, J. G. Slowik, I. El Haddad, P. F. Decarlo, C. Mohr, M. F. Heringa, R. Chirico, N. Marchand, B. Temime-Roussel, E. Abidi, L. Poulain, A. Wiedensohler, U. Baltensperger, and A. S. H. Prévôt, Primary and secondary organic aerosol origin by combined gas-particle phase source apportionment, Atmospheric Chemistry and Physics, 2013b; 13(16):8,411-8,426.
147. M. Crippa, F. Canonaco, V. A. Lanz, M. Äijälä, J. D. Allan, S. Carbone, G. Capes, D. Ceburnis, M. Dall' Osto, D. A. Day, P. F. DeCarlo, M. Ehn, A. Eriksson, E. Freney, L. Hildebrandt Ruiz, R. Hillamo, J. L. Jimenez, H. Junninen, A. Kiendler-Scharr, A.- M. Kortelainen, M. Kulmala, A. Laaksonen, A. A. Mensah, C. Mohr, E. Nemitz, C. O'Dowd, J. Ovadnevaite, S. N. Pandis, T. Petäjä, L. Poulain, S. Saarikoski, K.Sellegri, E. Swietlicki, P. Tiitta,D. R. Worsnop, U. Baltensperger and A.S. H. Prévôt, Organic aerosol components derived from 25 AMS data sets across Europe using a consistent ME-2 based source apportionment approach, Atmospheric Chemistry and Physics, 2014; 14(2):6,159-6,176.
148. L. M. Hildemann, G. R. Markowski, M. C. Jones and G. R. Cass, Submicrometer aerosol mass distributions of emissions from boilers, fireplaces, automobiles, diesel trucks, and meat-cooking operations, Aerosol Science and Technology, 1991; 14(1):138-152.
149. J.J. Schauer, W. Rogge, L.M. Hildemann, M.A Mazurek, G.R Cass and B.R.T. Simoneit, Source apportionment of airborne particulate matter using organic compounds as tracers, Atmospheric Environment , 1996:30 (22):3,837-3,855.
150. M.J. Kleeman and G. R. Cass, Source contributions to the size and composition distribution of urban particulate air pollution, Atmospheric Environment, 1998; 32(16):2,803-2,816.
151. M. R. Perrone, S. Becagli, J. A. García-Orza, R. Vecchi, A. Dinoi, R. Udisti and M. Cabello, The impact of long-range-transport on PM_1 and $PM_{2.5}$ at a Central Mediterranean site, Atmospheric Environment, 2013; 71:176-186.
152. G. Titos, H. Lyamani, M. Pandolfi, A. Alastuey and L. Alados-Arboledas, Identification of fine (PM_1) and coarse (PM_{10-1}) sources of particulate matter in an urban environment, Atmospheric Environment, 2014; 89:593-602.
153. N. Furuta, A. Iijima, A. Kambe, K. Sakai and K. Sato, Concentrations, enrichment and predominant sources of Sb and other trace elements in size classified airborne particulate matter collected in Tokyo from 1995 to 2004, Journal of Environmental Monitoring, 2005; 7(12):1155-1161.
154. U. Makkonen, H. Hellén, P. Anttila, M. Ferm, Size distribution and chemical

composition of airborne particles in south-eastern Finland during different seasons and wildfire episodes in 2006, Science of the Total Environment, 2010; 408(3):644-651.
155. J. Malilay, A review of factors affecting the human health impacts, of air pollutants from forest fires, Heath Guidelines for Vegetation Fire Events-Background Papers, 1999; 255-270.
156. D. W. Dockery, P. C. Arden, X. P. Xu, J. D. Spengler, J. H. Ware, M. E. Fay, B. G. Ferris, and F. E. Speizer, An Association between Air Pollution and Mortality in Six U.S. Cities, The New England Journal of Medicine, 1993;329(24):1,753-1,759.
157. J. Schwartz, D. W. Dockery, and L. M. Neas, Is Daily Mortality Associated Specifically with Fine Particles?, Journal of the Air & Waste Management Association, 1996; 46(10):927-939.
158. K. Katsouyanni, G. Touloumi, E. Samoli, A. Gryparis, A. Le Tertre, Y. Monopolis, G. Rossi, D. Zmirou, F. Ballester, A. Boumghar, H. Ross Anderson, B. Wojtyniak, A. Paldy, R. Braunstein, J. Pekkanen, C. Schindler and J. Schwartz, Confounding and Effect Modification in the Short-Term Effects of Ambient Particles on Total Mortality: Results from 29 European Cities within the APHEA2 Project, Epidemiology, 2001, 12(5):521-531.
159. J. M. Lim, J. H. Lee, J. H. Moon, Y. S. Chung and K. H. Kim, Source apportionment of PM_{10} at a small industrial area using positive matrix factorization, Atmospheric Research, 2010; 95(1):88-100.
160. C. A. Pope III, R. Burnett, M. Thum, E. Eugenia, D. Krewski, K. Ito and G. Thurston, Lung Cancer, Cardiopulmonary Mortality and Long Term Exposure to Fine Particulate Air Pollution, Jama, 2002; 287(9):1,132-1,141.
161. J.J. Lin and L.- C. Lee, Characterization of the concentration and distribution of urban submicron (PM_1) aerosol particles. Atmospheric Environment,2004;38(3): 469-475.
162. C. B. Mason and B. Moore, Principles of Geochemistry, Wiley, 1982.
163. W. Johnson and S. E. Lindberg, Atmospheric Deposition and Forest Nutrient Cycling, Springler-Verlag, 1992.
164. Steemit, The positives and negatives of the Sahara dust, 2018; https://steemit.com/desert/@africaunited/the-positives-and-negatives-of-the-sahara-dust-by-dcrypto-1532547990

165. G. Lövblad, L. Tarrason and K. Tørseth and S. Dutchak, The European Monitoring and Evaluation Programme Assessment Part I European Perspective, Norwegian Meteorological Institute, 2004.
166. D.W. Cole and M. Rapp, Elemental cycling in forest ecosystems. In D.E. Reichle (ed.), Dynamic principles of forest ecosystems, Cambridge University Press, 1981.
167. E. R. Lewis and S. E. Schwartz, Sea Salt Aerosol Production: Mechanisms, Methods, Measurements and Models-A Critical Review American Geophysical Union, 2004.
168. Colorado State University, Salty sea spray affects the lifetimes of clouds, researchers find, 2015; https://phys.org/news/2015-12-salty-sea-affects-lifetimes-clouds.html

169. C. O'Dowd and M. Smith, Physicochemical properties of aerosols over the northeast Atlantic: Evidence for wind speed related submicron sea salt aerosol production, Journal of Geophysical Research:Atmospheres, 1993;98(D1):1,123-1,135.

170. R. A. Duce, R. Arimoto, B. J. Ray, C. K. Unni, and P. J. Harder, Atmospheric trace elements at Enewetak Atoll: 1. Concentrations, sources, and temporal variability, Journal of geophysical research, 1983; 88(C9):5,321-5,342.
171. P. K. Quinn and D. J. Coffman, Local closure during the First Aerosol Characterization Experiment (ACE 1): Aerosol mass concentration and scattering and backscattering coefficients, Journal of geophysical research: Atmospheres, 1998; 103(D13):16,575-16,596.
172. P. K. Quinn, T. S. Bates, D. J. Coffman, T. L. Miller, J. E. Johnson, D. S. Covert, J.- P. Putaud, C. Neusüß and T. Novakov, A comparison of aerosol chemical and optical properties from the 1st and 2nd Aerosol Characterization Experiments, Tellus, 2000; 52B, 239-257
173. J. Sardans and J. Peñuelas, Potassium: a neglected nutrient in global change. Global Ecology and Biogeography, 2015; 24(3), 261-275.
174. P. Brimblecombe, Aqueous Phase Chemistry of the Troposphere. In C. N. Hewitt and A. V. Jackson (eds), Handbook of Atmospheric Science: Principles and Applications, Blackwell Science, 2003.
175. D. R. Lide (ed), CRC Handbook of Chemistry and Physics 79th Edition: A Ready-Reference Book of Chemical and Physical Data, CRC Press,1998.
176. Soil Survey Staff, Soil Taxonomy. A Basic System of Soil Classification for Making and Interpreting Soil Surveys. 2nd edition, US Government Printing Office, 1999.
177. R.G. Hoe ft, E.D. Nafziger, R.R. Johnson and S.R. Aldrich, Modern Corn and Soybean Production (MCSP), MCSP Publications, 2000.
178. Food and Agriculture Organization of the United Nations, Current world fertilizer trends and outlook to 2014, 2008.
179. United States Geological Survey, Potash. Mineral commodity summaries, 2009; http://minerals.er.usgs.gov/minerals/pubs/mcs.

180. R. Pawlowicz, Key physical variables in ocean: temperature, salinity, and density, Nature Education Knowledge, 2013; 4(4):13.
181. V. Chow, D. Maidment and L. Mays, Hidrología Aplicada, Nomos S.A., 2000.
182. G. A. Cole, Textbook of Limnology. 3rd Ed., The C.V. Mosby Co., 1983.
183. V. A. Silva, G. Marchi, L.R. Guimaraes Guilherme, J.M. de Lima, F. Dias Nogueira and P.T. Gontijo Guimaraes, Kinetics of K release from soils of Brazilian coffee regions: effect of organic acids, Revista Brasileira de Ciência do Solo, 2008; 32(2):533-540.
184. G. Marchi, V. A. Silva, L. R. Guimaraes Guilherme, J. M. Lima, F.D. Nogueira, & P. T. G. Guimaraes, Potassium extractability from soils of Brazilian coffee regions, Bioscience Journal, 2012; 28(6):913-919.
185. T. Vegas-Vilarrúbia, F. Baritto, P. López, G. Meléan, M. E. Ponce, L. Mora and O. Gómez, Tropical Histosols of the lower Orinoco Delta, features and preliminary quantification of their carbon storage, Geoderma, 2010; 155(3-4): 280-288.
186. I. R. Da Silva, A. E. Furtini Neto, L. A. Fernandes, N. Curi and F.B. Do Vale, Formas, relaçao quantidade/intensidade e biodisponibilidade de potassio em diferentes Latossolos, Pesquisa Agropecuária Brasileira, 2000; 35:2065-2073.
187. B.W. Eakins and G.F. Sharman, Volumes of the World's Oceans from ETOPO1, National Oceanic and Atmospheric Administration-National Geophysical Data Center, Boulder, CO, 2010; 7.
188. Canada's National Observer, Fossil Fuel Burning, 2017; https://www.nationalobserver.com/2017/07/13/analysis/these-missing-charts-may-change-way-you-think-about-fossil-fuel-addiction

189. National Aeronautics and Space Administration Earth Observatory, Biomass burning, 2001;
https://earthobservatory.nasa.gov/Features/BiomassBurning

190. M. O. Andreae, Soot Carbon and Excess Fine Potassium:Long-Range Transport of Combustion-Derived Aerosols, Science, 1983; 220(4,602):1,148-1,151.
191. D. Lindberg, R. Backman and P. Chartrand, Thermodynamic evaluation and optimization of the (Na_2SO_4 + K_2SO_4 + $Na_2S_2O_7$ + $K_2S_2O_7$) system. Journal of Chemical Thermodynamics, 2006; 38(12):1,568-1,583.
192. T. Allgurèn, Chemical Interactions between Potassium, Nitrogen, Sulfur and Carbon Monoxide in Suspension-Fired Systems, Thesis for the Degree of Doctor of Philosophy, Energy Technology Department of Space, Earth and Environment, Chalmers University of Technology, 2017.
193. D. L. Savoie, J. M. Prospero and R. T. Nees, Nitrate, non-sea-salt sulfate, and mineral aerosol over the northwestern Indian Ocean, Journal of Geophysical Research: Atmospheres 1987; 92(D1):933-942.
194. C.-U. Ro, H. Hwang , H. Kim , Y. Chun and R. Van Grieken , Single- particle characterization of four "Asian Dust" samples collected in Korea, using low-Z particle electron probe X-ray microanalysis, Environmental Science and Technology, 2005; 39(6):1,409-1,419.
195. Sellegri, J. Gourdeau, J. P. Putaud and S. Despiau. Chemical composition of marine aerosol in a Mediterranean coastal zone during the FETCH experiment, Journal of Geophysical Research:Atmospheres, 2001;106(D19):12,023-12,037.
196. H. Sievering, B. Lerner, J. Slavich, J. Anderson, M. Posfai and J. Cainey, O_3 oxidation of SO_2 in sea-salt aerosol water: size distribution of non-sea salt sulfate during the first aerosol characterization experiment (ACE1), Journal of Geophysical Research:Atmospheres, 1999; 104(D17):21,707- 21,717.
197. U. Krischke, R. Staubes, T. Brauers, M. Gautrois, J. Burkert, D. Stöbener and W. Jaeschke, Removal of SO_2 from the marine boundary layer over the Atlantic Ocean: a case study on the kinetics of the heterogeneous S(IV) oxidation on marine aerosols, Journal of Geophysical Research:Atmospheres, 2000;105 (D11):14,413-14,422.
198. B. Allen, Atmospheric Aerosols: What Are They, and Why Are They So Important?, National Aeronautics and Space Administration, 2015; 6.
199. A. Ooki, M. Uematsu, K. Miura and S. Nakae, Sources of sodium in atmospheric fine particles, Atmospheric Environment, 2002; 36(27):4,367-4,374.
200. L. Granat, On the relation between pH and the chemical composition in atmospheric precipitation, Tellus, 1972; 24(6):550-560.
201. E. J. Hoffman, G. L. Hoffman, and R. A. Duce, Chemical fractionation of alkali and alkaline earth metals in atmospheric particulate matter over the North Atlantic, Journal de Recherches Atmospheriques, 1974; 8:675-688.
202. B. Bonsang, B.C. Nguyen, A. Gaudry and G. Lambert, Sulfate enrichment in marine aerosols owing to biogenic gaseous sulfur compounds, Journal of Geophysical Research: Oceans, 1980; 85(C12):7,410-7,416.
203. J. N. Galloway and A. Gaudry, The composition of precipitation on Amsterdam Island, Indian Ocean, Atmospheric Environment (1967), 1984;18(12):2,649-2,656.
204. M. Patel, C.L., Azanza Ricardo, P. Scardi, P.B. Aswath, Morphology, structure and chemistry of extracted diesel sootdPart I: Transmission electron microscopy, Raman spectroscopy, X-ray photoelectron spectroscopy and synchrotron X-ray diffraction study, Tribology International, 2012; 52:29-39.
205. B. Yousaf, G. Liu, R. Wang, M. Zia-ur-Rehman, M.S. Rizwan, M. Imtiaz, G.

Murtaza and A. Shakoor, Investigating the potential influence of biochar and traditional organic amendments on the bioavailability and transfer of Cd in the soil-plant system. Environmental Earth Sciences,2016; 75(5):375
206. D.S. Lee, S.E. Espenhahn and S. Baker, Evidence for long-term changes in base cations in the atmospheric aerosol, Journal of Geophysical Research: Atmospheres, 1998; 103(D17):21,955-21,966.
207. F.W. Clarke and H.S. Washington, The composition of the Earth's crust, US Government Printing Office, 1924.
208. R. Arimoto, R. A. Duce, B. J. Ray, W. G. Ellis Jr., J. D. Cullen and J. T. Merrill, Trace elements in the atmosphere over the North Atlantic, Journal of Geophysical Research, 1995; 100(D1):1199-1213.
209. D. S. Lee, R. D. Kingdon, J. M. Pacyna, A.F. Bouwman and I. Tegen, Modelling base cations in Europe-sources, transport and deposition of calcium, Atmospheric Environment, 1999; 33:2,241-2,256.
210. W. C. Keene, A. A. P. Pszenny, J. N. Galloway and M. E. Hawley, Sea salt corrections and interpretation of constituent ratios in marine precipitation, Journal of Geophysical Research, 1986; 91(D6):6,647-6,658.
211. D. A. Gillette, G. J. Stensland, A. L. Williams, W. Branard, D. F. Gatz, P.C. Sinclair and T. C. Johnson, Emissions of alkaline elements calcium, magnesium, potassium and sodium from open sources in the contiguous United States, Global Biogeochemical Cycles, 1992; 6(4)437-457.
212. D. W. Raper and D. S. Lee, Wet deposition at the sub-20 km scale in a rural upland area of England, Atmospheric Environment, 1996;30(8):1193-1207.
213. D. F. Gatz, Urban precipitation chemistry: a review and synthesis, Atmospheric Environment. Part B. Urban Atmosphere, 1991; 25(1):1-15.
214. D.S. Lee, Spatial variability of urban precipitation chemistry and deposition: statistical associations between constituents and potential removal processes of precursor species, Atmospheric Environment. Part B. Urban Atmosphere, 1993; 27(3):321-337.
215. O. Hedin, L. Granat, G. E. Likens, T. A. Buishand, J. N. Galloway, T. J. Butler and H. Rodhe, Steep declines in atmospheric base cations in regions of Europe and North America, Nature, 1994; 367(6,461):351-354.
216. D. S. Lee and J. M. Pacyna, An industrial emissions inventory of calcium for Europe. Atmospheric Environment, 1998; 33(11): 1,687-1,697.
217. A. Semb, J. E. Hanssen, F. Francois, W. Maenhaut and J. M. Pacyna, Long range transport and deposition of mineral matter as a source for base cations, Water, Air, and Soil Pollution, 1995; 85(4):1,933-1,940.
218. D. W. Cole and M. Rapp, Elemental cycling in forest ecosystems. In: D.E. Reichle (ed) Dynamic properties of forest ecosystems. Cambridge University Press, Cambridge, 1981.
219. S. K. Friedlander, A Note on New Particle Formation in the Presence of Aerosol, Journal of Colloid and Interface Science, 1978; 67:387-388.
220. S. K. Friedlander, Future Aerosols of the Southwest: Implications for Fundamental Aerosol Research, Annals of the New York Academy of Sciences, 1980; 338(1):588-598.
221. F. Paulot and D. J. Jacob, Hidden Cost of U.S. Agricultural Exports:Particulate Matter from Ammonia Emissions, Environmental Science and Technology, 2014b; 48(2):903-908.
222. F. Paulot, D. J. Jacob, R. W. Pinder, J. O. Bash, K. Travis and D. K. Henze, Ammonia emissions in the United States, European Union, and China derived by high-resolution inversion of ammonium wet deposition data: Interpretation with a

new agricultural emissions inventory (MASAGE NH_3), Journal of Geophysical Research: Atmospheres, 2014a;119(7):4343-4364.
223. R. Zhang, H. Wang, Y. Qian, P. J. Rasch, R. C. Easter, P.- L. Ma, B. Singh, J. Huang, and Q. Fu, Quantifying sources, transport, deposition and radiative forcing of black carbon over the Himalayas and Tibetan Plateau, Atmospheric Chemistry and Physics, 2015; 15:6,205-6,223.
224. C. Zhan, J. Zhang, J. Cao, Y. Han, P. Wang, J. Zheng, R. Yao, H. Liu, H. Li and W. Xiao, Characteristics and Sources of Black Carbon in Atmospheric Dustfall Particles from Huangshi, China, Aerosol and Air Research, 2016; 16:2,096-2,106.
225. T. Hussein, T. Glytsos, J. Ondráček, P. Dohányosová, V. Ždímal, K.Hämeri, M. Lazaridis, J. Smolík and M. Kulmala, 2006. Particle size characterization and emission rates during indoor activities in a house. Atmospheric Environment, 2006; 40(23):4285-4307.
226. M. U. Ali, A. Rashid, B. Yousuf and A. Kamal, Health outcomes of road traffic pollution among exposed roadside-workers in the Rawalpindi City Pakistan. 2017b, Human and Ecological Risk Assessment: An International Journal, 2017; 23(6):1,330-1,339.
227. B. Glaser, A. Dreyer, M. Bock, S. Fiedler, M. Mehring and T. Heitmann, Source apportionment of organic pollutants of a highway-traffic-influenced urban area in Bayreuth (Germany) using biomarker and stable carbon isotope signatures, Environmental Science and Technology, 2005; 39(11):3,911-3,917.
228. K. S. Johnson, B. Zuberi,, L. T. Molina, M. J. Molina, M. J. Iedema, J. P. Cowin, D. J. Gaspar, C.Wang, and A. Laskin, Processing of soot in an urban environment: case study from the Mexico City Metropolitan Area, Atmospheric Chemistrya and Physics, 2005; 5:3,033-3,043.
229. J. Niu, P. Rasmussen, N. Hassan and R . Vincent, Concentration Distribution and Bioaccessibility of Trace Elements in Nano and Fine Urban Airborne Particulate Matter: Influence of Particle Size. Water Air and Soil Pollution, 2010, 213:211-225.
230. E. Gramsch, F. Reyes, P. Oyola, M. A. Rubio, G. López, P. Pérez and R. Martínez, Particle size distribution and its relationship to black carbon in two urban and one rural site in Santiago de Chile, Journal of the Air & Waste Management Association, 2014; 64(7):785-796.
231. O. L. Hadley and T. W. Kirchstetter, Black-carbon reduction of snow albedo, Nature Climate Change, 2012; 2(6):437-440.
232. T. C. Bond, S. J. Doherty, D. W. Fahey, P. M. Forster, T. Berntsen, B.J.DeAngelo, M. G. Flanner, S. Ghan, B. Kärcher, D. Koch, S. Kinne, Y. Kondo, P. K. Quinn, M. C. Sarofim, M. G. Schultz, M. Schulz, C. Venkataraman, H. Zhang, S. Zhang, N. Bellouin, S. K. Guttikunda, P. K. Hopke, M. Z. Jacobson, J. W. Kaiser, Z. Klimont, U. Lohmann, J. P. Schwarz, D. Shindell, T. Storelvmo, S. G. Warren and C. S. Zender, Bounding the role of black carbon in the climate system: A scientific assessment, Journal of Geophysical Research:Atmospheres, 2013; 118(11):5,380-5,552.
233. S. G. Warren and W. J. Wiscombe, A model for the spectral albedo of snow. II: Snow containing atmospheric aerosols, Journal of the Atmospheric Sciences, 1980; 37(12):2,734-2,745.
234. S. G. Warren and W. J. Wiscombe, Dirty snow after nuclear war, Nature, 1985; 313(6,002):469.
235. H. Conway, A. Gades, and C. F. Raymond, Albedo of dirty snow during conditions of melt, Water resources research , 1996; 32(6):1,713-1,718.
236. J. Hansen and L. Nazarenko: Soot climate forcing via snow and ice albedos, Proceedings of the National Academy of Sciences, 2004; 101(2)423-428.
237. M. Z. Jacobson, Climate response of fossil fuel and biofuel soot, accounting for

soot's feedback to snow and sea ice albedo and emissivity, Journal of Geophysical Research:Atmospheres, 2004; 109(D21).
238. J. Hansen, M. Sato, R. Ruedy, L. Nazarenko, A. Lacis, G. A. Schmidt, G. Russell, I. Aleinov, M. Bauer, S. Bauer, N.Bell, B. Cairns, V. Canuto, M. Chandler, Y. Cheng, A.Del Genio, G. Faluvegi, E. Fleming, A. Friend, T. Hall, C. Jackman, M. Kelley, N. Kiang, D. Koch, J. Lean, J. Lerner, K. Lo, S.Menon, R. Miller, P. Minnis, T. Novakov, V. Oinas, Ja.Perlwitz, Ju. Perlwitz, D. Rind, A. Romanou, D. Shindell, P. Stone, S. Sun, N. Tausnev, D. Thresher, B. Wielicki, T. Wong, M. Yao And S. Zhang, Efficacy of climate forcings, Journal of Geophysical Research, 2005; 110(D18104).
239. M. G. Flanner, C. S. Zender, P. G. Hess, N. M. Mahowald, T. H., Painter, V., Ramanathan, and P. J. Rasch, Springtime warming and reduced snow cover from carbonaceous particles, Atmospheric Chemistry and Physics, 2009; 9(7):2,481-2,497.
240. Y. Qian, M. G. Flanner, L. R. Leung, and W. Wang, Sensitivity studies on the impacts of Tibetan Plateau snowpack pollution on the Asian hydrological cycle and monsoon climate, Atmospheric Chemistry and Physics, 2011; 11(5):1,929-1,948.
241. H. Ye, R. Zhang, J. Shi, J. Huang, S. G., Warren, and Q. Fu, Black carbon in seasonal snow across northern Xinjiang in northwestern, China, Environmental Research Letters, 2012; 7(4):044002.
242. S. J. Doherty, C. Dang, D. A. Hegg, R. Zhang, and S. G. Warren, Black carbon and other light-absorbing particles in snow of central North America, Journal of Geophysical Research:Atmospheres, 2014; 119(22):12,807-12,831.
243. M. Ostrander, Black carbon decreases snow's and ice's albedo, 2017; https://ensia.com/features/black-carbon/

244. S. Fuzzi, U. Baltensperger, K. Carslaw, S. Decesari, H. Denier van der Gon, M. C. Facchini, D. Fowler, I. Koren, B. Langford, U. Lohmann, E. Nemitz, S. Pandis, I. Riipinen, Y. Rudich, M. Schaap, J. G. Slowik, D. V. Spracklen, E. Vignati, M. Wild, M. Williams, and S. Gilardoni, Particulate matter, air quality and climate: lessons learned and future needs, Atmospheric Chemistry and Physics, 2015; 15(14):8,217-8,299.
245. T. Ackerman and O. Toon, Absorption of visible radiation in atmosphere containing mixtures of absorbing and non-absorbing particles, Applied Optics, 1981; 20(20):3,661-3,668.
246. D. Koch and A. D. Del Genio, Black carbon semi-direct effects on cloud cover: review and synthesis, Atmospheric Chemistry and Physics, 2010; 10(16):7,685-7,696.
247. G. Grivas, A. Chaloulakou and P. Kassomenos. An overview of the PM_{10} pollution problem, in the Metropolitan Area of Athens, Greece. Assessment of controlling factors and potential impact of long range transport. Science of Total Environment, 2008; 389(1):165-177.
248. S. Pateraki, V. D. Assimakopoulos, A. Bougiatioti, G. Kouvarakis, N. Mihalopoulos and C. Vasilakos, Carbonaceous and ionic compositional patterns of fine particles over an urban Mediterranean area, Science of the Total Environment, 2012; 424:251-263.
249. S. Pateraki, T. Maggos, J. Michopoulos, H.A. Flocas, D.N. Asimakopoulos and C. Vasilakos, Ions species size distribution in particulate matter associated with VOCs and meteorological conditions over an urban region, Chemosphere, 2008; 72:496-503.
250. H. Flocas, A. Kelessis, C. Helmis, M. Petrakakis, N. Zoumakis and K. Pappas,

Synoptic and local scale atmospheric circulation associated with air pollution episodes in an urban Mediterranean area, Theoretical and Applied Climatology, 2009; 95:265-77.
251. M. Kanakidou, N. Mihalopoulos, T. Kindap , U. Im , M. Vrekoussis, E. Gerasopoulos , E. Dermitzaki , A. Unal , M. Koçak , K. Markakis, D. Melas, G. Kouvarakis , A. F. Youssef , A. Richter , N. Hatzianastassiou, A. Hilboll,F. Ebojie, F. Wittrock , C. von Savigny , J. P. Burrows, A. Ladstaetter-Weissenmayer and H. Moubasher, Megacities as hot spots of air pollution in the East Mediterranean. Atmospheric Environment, 2011; 45:1223-235.
252. M. Vrekoussis, A. Richter, A. Hilboll, J. P. Burrows, E. Gerasopoulos, J. Lelieveld, L. Barrie, C. Zerefos and N. Mihalopoulos,. Economic crisis detected from space: air quality observations over Athens/Greece. Geophysical Research Letters, 2013; 40:458-463.
253. L. Fourtziou, E. Liakakou, I. Stavroulas, C. Theodosi, P. Zarmpas, B. Psiloglou, J. Sciare, T. Maggos, K. Bairachtari, A. Bougiatioti, E. Gerasopoulos, R. Sarda-Estéve, N. Bonnaire, N. Mihalopoulos Multi-tracer approach to characterize domestic wood burning in Athens (Greece) during wintertime. Atmospheric Environment, 2017; 148:89-101.
254. B.R.T. Simoneit, Biomass burning - a review of organic tracers for smoke from incomplete combustion, Applied Geochemistry, 2002; 17(3):129-162.
255. M.A. Bari, G. Baumbach, B. Kuch and G. Scheffknecht, Wood smoke as a source of particle-phase organic compounds in residential areas. Atmospheric Environment 2009; 43(31):4722-4732.
256. D. A. Sarigiannis, S. P. Karakitsios, M. Kermenidou, S. Nikolaki, D.Zikopoulos, S. Semelidis, A. Papagiannakis, R. Tzimou, Lung cancer risk from PAHs emitted from biomass combustion, 2015. Environmental Research, 137:147-156.
257. K. Saarnio, M. Aurela, H. Timonen, S. Saarikoski, K. Teinilä, T. Mäkelä, M. Sofiev, J. Koskinen, A. A. Aalto, M. Kulmala, J. Kukkonen and R. Hillamo, Chemical composition of fine particles in fresh smoke plumes from boreal wild-land fires in Europe, Science of Total Environment, 2010; 408(12):2527-2542.
258. C. Reche, M. Viana, F. Amato, A. Alastuey, T. Moreno, R. Hillamo, K. Teinilä, K. Saarnio, R. Seco, J. Peñuelas, C. Mohr, A.S.H. Prévôt, X. Querol, Biomass burning contributions to urban aerosols in a coastal Mediterranean City, Science of The Total Environment, 2012; (427-428): 175-190.
259. D. Paraskevopoulou, E. Liakakou, E. Gerasopoulos, C. Theodosi and N. Mihalopoulos, Long-term characterization of organic and elemental carbon in the $PM_{2.5}$ fraction: the case of Athens Greece. Atmospheric Chemistry and Physics, 2014; 14:13,313-13,325.
260. S. Pateraki, D. N. Asimakopoulos, A. Bougiatioti, T. Maggos, C. Vasilakos and N. Mihalopoulos,. Assessment of $PM_{2.5}$ and PM_1 chemical profile in a multiple-impacted Mediterranean urban area: origin, sources and meteorological dependence. Science of The Total Environment. 2014; 479-480:210-220.
261. D. Paraskevopoulou, E. Liakakou, E. Gerasopoulos and N. Mihalopoulos, Sources of atmospheric aerosol from long-term measurements (5 years) of chemical composition in Athens, Greece. Science of the Total Environment, 2015; 527-528:165-178.
262. One Stop Map, Map of the Mediterranean, 2018; https://www.onestopmap.com/product/map-of-the-mediterranean-political-with-shaded-relief-644/
263. Athena Info, Map of Thissio, 2018;

http://www.athinainfo.gr/index.html

264. J. Wood (Alamy Stock Photo), National Observatory of Athens, 2018; https://www.alamy.com/stock-photo-national-observatory-of-athens-1610920.html

265. T. Kindap, U. U. Turuncoglu, S.- H. Chen, A. Unal and M. Karaca, Potential threats from a likely nuclear power plant accident: a climatological trajectory analysis and tracer study, Water, Air & Soil Pollution, 2009; 198: 1-4.
266. D. Melas, I. C. Ziomas and C. Zerefos, Boundary layer dynamics in an urban coastal environment under sea breeze conditions, Atmospheric Environment, 1995; 29(24):3,605-3,617.
267. Sailing Issues, Monsoon circulation of the Eastern Mediterranean, 2018; http://www.sailingissues.com/meltemi.html

268. Weather Online (United Kingdom), Wind of the World: Etesian Winds, 2018; https://www.weatheronline.co.uk/reports/wind/The-Etesian-Winds.htm

269. U. Im, M. Tayanç and O. Yenigün, Analysis of major photochemical pollutants with meteorological factors for high ozone days in Istanbul,Turkey, Water, Air &Soil Pollution, 2006; 175(1-4):335-359.
270. G. Kallos, P. Kassomenos and R. A. Pielke, Synoptic and mesoscale weather conditions during air pollution episodes in Athens, Greece. In H. Kaplan, N. Dinar, A. Lacser and Y. Alexander (eds), Transport and Diffusion in Turbulent Fields, Springer, 1993.
271. D. A. Orsini, Y. Ma, A. Sullivan, B. Sierau and K. Baumann and R. J. Weber, Refinements to the particle-into-liquid sampler (PILS) for ground and airborne measurements of water soluble aerosol composition, Atmospheric Environment, 2003; 37(9-10):1243-1259.
272. J. Sciare, K. Oikonomou, H. Cachier, N. Mihalopoulos, M.O. Andreae, W. Maenhaut, R. Sarda-Esteve, 2005. Aerosol mass closure and reconstruction of the light scattering coefficient over the Eastern Mediterranean Sea during the MINOS campaign, Atmospheric Chemistry and Physics, 2005; 5(8):2,253-2,265.
273. J. Sciare , K. Oikonomou, O. Favez, E. Liakakou, Z. Markaki, H. Cachier and N. Mihalopoulos, Long-term measurements of carbonaceous aerosols in the Eastern Mediterranean: evidence of long-range transport of biomass burning. Atmospheric Chemistry and Physics, 2008; 8(18):5,551-5,563.
274. H. Bardouki, H. Liakakou, C. Economou, J. Sciare, J. Smolík, V. Ždímal, K. Eleftheriadis, M. Lazaridis, C. Dye and N. Mihalopoulos, Chemical composition of size-resolved atmospheric aerosols in the eastern Mediterranean during summer and winter, Atmospheric Environment, 2003; 37(2):195-208.
275. E. Koulouri, S. Saarikoski, C. Theodosi, Z. Markaki, E. Gerasopoulos, G. Kouvarakis a,T Mäkelä, R. Hillamo and N. Mihalopoulos, Chemical composition and sources of fine and coarse aerosol particles in the Eastern Mediterranean, Atmospheric Environment, 2008; 42:6,542-6,550.
276. C. Theodosi, G. Grivas, P. Zarmpas, A. Chaloulakou, and N. Mihalopoulos, Mass and chemical composition of size-segregated aerosols (PM_1, $PM_{2.5}$, PM_{10}) over Athens, Greece: local versus regional sources, Atmospheric Chemistry and Physics, 2011; 11:11,895–11,911.
277. M. Viana, W. Maenhaut, X. Chi, X. Querol and A. Alastuey, Comparative chemical

mass closure of fine and coarse aerosols at two sites in south and west Europe: Implications for EU air pollution policies, Atmospheric Environment, 2007; 41:315-326.
278. C. Moulin, C. E. Lambert, U. Dayan, V . Masson,M . Ramonet,P . Bousquet , M. Legrand, Y. J. Balkanski ,W . Guelle, B. Marticorena G, . Bergametti and F. Dulac, Satellite climatology of African dust transport in the Mediterranean Atmosphere, Journal of Geophysical Research, 1998; 103 (D11):13,137-13,144.
279. S. Rodriquez, X. Querol, A. Alastuey, G. Kallos and O. Kakaliagou, Saharan dust contributions to PM_{10} and TSP levels in Southern and Eastern Spain, Atmospheric Environment, 2001; 35: 2,433-2,447.
280. D. Meloni, A. di Sarra, G. Biavati, J. J. DeLuisi, F. Monteleone, G. Pace, S. Piacentino and D.M. Sferlazzo, Seasonal behavior of Saharan dust events at the Mediterranean island of Lampedusa in the period 1999‐2005, Atmospheric Environment, 2007; 41: 3,041-3,056.
281. P. Kassomenos, A. N. Skouloudis, S. Lykoudis and H. A. Flocas, ‘‘Air-quality indicators’’ for uniform indexing of atmospheric pollution over large metropolitan areas, Atmospheric Environment, 1999; 33:1,861-1,879.
282. M. Lazaridis, Organic Aerosols. In Environmental Chemistry of Aerosols, I.Colbech (ed.), Willey, 2008.
283. Y. P. Kim and J. H. Seinfeld, Atmospheric gas – aerosol equilibrium III. Thermodynamics of crustal elements Ca^{2+}, K^{+}, and Mg^{2+}, Aerosol Science and Technology, 1995; 22:93-110.
284. Y. P. Kim, J. H. Seinfeld and P. Saxena, Atmospheric gas- aerosol equilibrium I. Thermodynamic model, Aerosol Science and Technology, 1993a; 19:157-181.
285. Y. P. Kim, J. H. Seinfeld and P. Saxena, Atmospheric gas-aerosol equilibrium II. Analysis of common approximations and activity coefficient calculation methods, Aerosol Science and Technology, 1993b; 19:182-198.
286. K. Denbigh, The principles of chemical equilibrium, Fourth Edition, Cambridge University Press, 1981.
287. C. Fountoukis and A. Nenes, ISORROPIA II: a computationally efficient thermodynamic equilibrium model for K^{+}- Ca^{2+} - Mg^{2+}- NH^{+4} - Na^{+}- SO_4^{2-}- NO^{-3} - Cl^{-} - H_2O aerosols. Atmospheric Chemistry and Physics, 2007; 7: 4,639-4,659.